UNIVERSITY OF LIVERPOOL

Investigating the Structure-Function Relationships of Heparin By-Products

Thesis submitted in accordance with the requirements of The University of Liverpool for the degree of Doctor of Philosophy

Sarah Louise Taylor

December 2017

Dedicated to my three beautiful girls, love you to the moon and back...

Acknowledgments

Producing this thesis would have been impossible without the support and encouragement from every person in my life, no matter how small the part they played in getting me through this actual thesis.

Firstly, I would like to extend my greatest thanks and gratitude to my supervisors, Prof Jerry Turnbull and Dr Ed Yates. Without your constant support, guidance and encouragement the task of completing this project and probably more so this thesis would have been a far greater task! I would like to thank Ed for stepping up as my supervisor and for all the support with the structural aspects of this thesis, providing an ear (probably somewhat battered now) to listen to my panicking and frustrations. I would also like to thank the members of Lab B, Scott, Chris, Liz and Kirsty, you may be a newbie but you've made my work life far easier with non-work related chats. My biggest shout out goes out to Fi and Sophie, I could not have got through this without your friendship, laughs, dog walks and food/drink related socialness (with some science chats thrown in for good measure!). I also would like to thank Dr Tim Rudd and Dr Igor Barsukov for providing practical help with aspects of this project.

To my family, in particular my sister, Carolyn. Thank you to both you and Phil for taking on and giving a home to that 11 year old girl and letting her believe she could achieve anything in life, no matter what! I wouldn't have done this without your constant support, love and dog sitting. Nadine, Katelyn and Tegan, what can I say, you are all so beautiful and intelligent, I am so proud to be your 'big sister'. I hope that in some small part I can inspire you to do whatever you want and look beyond the obstacles in your way. There is no doubting the thanks I should extend to Karl, for his love and encouragement, no matter how many miles apart, you certainly provided plenty of non-PhD related distraction ☺ To the rest of my family and friends, thank you for your support and giving me a life away from the world of science - drinks will now be gratefully received!!

Finally, any of the people mentioned above will not be surprised that my last acknowledgment, although they will never be able to read it, has to go to my 3 beautiful canine boys, Banjo, Milo and Red. The last 4 years has certainly been made easier with the cuddles, walks and love I have received in bucket loads from you.

Abstract

Heparin (Hp) has been used in hospitals as an anticoagulant for over three decades. The process from porcine intestine to purified Hp requires the removal of many by-products at each stage of the process. It was hypothesised that these by-products could contain an economical, bioactive source of heparan sulfate (HS) / Hp polysaccharides. This project has led to the investigation of 4 by-products, D1, F1, H and M1. After purification, all by-products underwent structural analysis, which showed they have a large diversity in structure and that they were all uniquely different to Hp and each other. Two samples D1 and H were highly sulfated like Hp, ~2.0 sulfates per disaccharide, with the latter showing the most comparable structure to Hp, at the disaccharide level. M1 was not as highly sulfated as the first 2 and F1 was overall more HS-like in its structure, with the lowest level of the tri-sulfated disaccharide (~1.6 sulfates per disaccharide). Following this, sized oligosaccharide libraries were produced by digesting samples with heparinase III, D1 and F1 showed a large range of defined mixtures of oligosaccharides from dp 2-18. These fractions, along with the parental material were used for activation studies in bioassays with three selected growth factors. FGF2 showed a size dependant increase in activity preferentially with highly sulfated H and D1. Size fractionation showed that fractions below ~dp 6 were significantly less active than the parental material. VEGF-A_{165} mediated phosphorylation also preferred H (AKT^{Ser473}), Hp showed the largest phosphorylation response for ERK1/2, with size refinement also showing preference for sulfation; smaller fractions depended on the higher sulfated D1 to induce comparable levels of activity to the parental material. Finally, PDGF-BB showed preference to M1 and H, which interestingly have the highest level of N-sulfation and NA residues, fractionated D1 and F1 show comparable activity to the intact material up to the largest fraction which show a consistent decrease in GF-HS driven proliferation. Encouragingly, all of the by-products show low levels of toxicity, up to concentrations of 1 mg/ml and at lower concentrations appear to actively induce cell survival over normal growth media. Furthermore, all of the by-products have significantly less anticoagulant activity than Hp. Overall, this data suggests that the by-products show significant structural and biological difference to Hp and therefore make possible candidates for therapeutic research. This was investigated in the ability of the by-products to reduce adenylate kinase associated with apoptosis, as a consequence of cells infected by Zika virus. D1 in particular showed significant ability at reducing virally derived apoptosis and is a promising agent for future investigations.

Contents

List of Figures

List of Tables

List of Abbreviations

Δ	Unsaturated double bond
^{1}H	Proton NMR
14mer	Heparan sulfate chain made up of 14 monomers
$^{1}C_{4}$	Chair conformation
$^{2}S^{0}$	Skew boat conformation
aa	Amino acid
AKT^{Ser473}	Protein Kinase B Serine 473
APTT	Activated partial thromboplastin
AT	Antithrombin
BaF3-1c	B-lymphoid cells (with a FGFR1c receptor)
BCA	Bicinchoninic acid assay
BSA	Bovine serum albumin
C13	Carbon 13 NMR
$CaCl_2$	Calcium chloride
$Ca(OAC)_2$	Calcium acetate
CASP-3	Caspase 3
CS	Chondroitin sulfate
CHO	Chinese hamster ovary cells
Da	Dalton
DAG	Diacylglycerol
ddH_2O	Double distilled water
DEAE	Diethylaminoethanol

DMEM	Dulbecco's modified eagle's medium
Dp	Degree of polymerisation
DS	Dermatan sulfate
ECM	Extracellular matrix
E. coli	*Escherichia coli*
EDTA	Ethylenediaminetetraacetic acid
Em	Emission
ERK1/2	Extracellular signal-regulated kinase 1/2
Ex	Excitation
EXT	exostosin glycosyltransferase
FBS	Foetal bovine serum
FDA	Food and drug administration
FGF	Fibroblast growth factor
FGF1/2	Fibroblast growth factor 1 and 2
FGFR	Fibroblast growth factor receptor
FIIa	Factor IIa
FXa	Factor Xa
GAGs	Glycosaminoglycans
GalT	Galactosyltransferase
GlcA	Glucuronic acid
GlcA(2S)	2-O sulfated glucuronic acid
GlcNAc	N-acetyl-D-glucosamine
GlcNAc(6S)	6-O-sulfated-N-acetyl-D-glucosamine

GlcNS	N-acetyl-sulfated-D-glucosamine
GlcNS(6S)	6-O-N-acetyl-sulfated-D-glucosamine
GM	Growth media
GMP	Good manufacturing practice
GRB1/2	Growth factor receptor-bound protein 1/2
HA	Hyaluronan
hASMCs	Human aortic smooth muscle cells
HBS	Heparin binding site
Hp	Heparin
HPLC	High performance liquid chromatography
HRP	Horseradish peroxidase
HS	Heparan sulfate
HS2ST	2-O sulfotransferase
HS3ST	3-O sulfotransferase
HS6ST	6-O-sulfotrasnferase
HSPG	Heparan sulfate proteoglycan
HSQC	Heteronuclear single quantum coherence
HUVEC	Human umbilical vein endothelial cell
I-1	Iduronic acid
IC_{50}	Inhibitory concentration at 50%
IdoA	Iduronic acid
IdoA(2S)	2-O sulfated iduronic acid
IL-3	Interleukin 3

IP_3	Inositol triphosphate
JAK	Janus family tyrosine kinase
LDH	Lactase dehydrogenase
KDa	Kilodalton
KfiA	N-acetyl-D-glucosaminyl transferase of K5 strain of *E. coli*
KS	Keratan sulfate
LDH	Lactate dehydrogenase
LMWH	Low molecular weight heparin
MAPK	Mitogen-activated protein kinase
MEK36	MAPK/ERK kinase 36
$MgCl_2$	Magnesium chloride
mTOR	Mammalian target of rapamycin
MTT	3-(4,5-dimethylthiazol-2-yl)-2,5-diphenyltetrazolium bromide
NA	N-acetylated domain
NaCl	Sodium chloride
NaOAc	Sodium acetate
Nck	Non-catalytic region of tyrosine kinase adaptor protein 1
NDST	N-deacetylase/N-sulfotransferase
NH_4HCO_3	Ammonium bicarbonate
NIH3T3	NIH Swiss mouse embryo 3 day transfer cells
NMR	Nuclear magnetic resonance
NP	Nitrophenol
NS	N-sulfated residue

NOS	Nitrous oxide synthase
p38 MAPK	Mitogen-activated protein kinase 38
PAGE	Polyacrylamide gel electrophoresis
PAPS	Phosphoadenosine 5’ – phosphosulfate
PAX	Paxcillin
PBS	Phosphate buffered saline
PDGF	Platelet derived growth factor
PDGFR	Platelet derived growth factor receptor
PGs	Proteoglycan
PI3K	Phosphoinositide 3-kinase
PIGF	Placental growth factor
PKB	Protein kinase B
PKC	Protein kinase C
PLC_{γ}	Phospholipase C-gamma
PNP	Paranitrophenol
PPM	Parts per million
PT	Partial thromboplastin
RAC	Ras-related C3 botulinum toxin substrate 1
RAF	Rapidly Accelerated Fibrosarcoma
RAS	Ras guanyl nucleotide-releasing protein
RIPA	Radioimmunoprecipitation assay
SAX	Strong Anion Exchange
SEC	Size Exclusion Chromatography

SH2	Src homology 2
SHP-2	Src homology phosphatase 2
SM	Starvation media
SOS	Son of sevenless guanine nucleotide exchange factor
Src	Sarcoma-family kinases
STATs	Signal transducer and activator of transcription
TAE	Tris acetate
TBS	Tris-buffered saline
TBST	Tris-buffered saline with tween
TGF-β	Transforming growth factor beta
Try	Tyrosine
TSP	Trimethylsilylpropanoic acid
UA(2S)	2-O-sulfated uronic Acid
UDP-GlucUA	Uridine diphosphate-glucuronic acid
UFH	Unfractionated heparin
UV	Ultraviolet
VEGF	Vascular endothelial growth factor
VEGFR	Vascular endothelial growth factor receptor
XYLT	Xylosyltransferase

Chapter 1: General Introduction

1.1 General Introduction

1.1.1 Glycosaminoglycans

Glycosaminoglycans (GAGs) are a class of long linear polysaccharides to which heparan sulfate (HS) and heparin (Hp) belong. There are four other members of the group; hyaluronan (HA), chondroitin sulfate (CS), dermatan sulfate (DS) and keratan sulfate (KS).

HA can self-associate and form fibres, which can aggregate on the cell surface forming a pericellular matrix, which has several important roles in cell motility and division. It is important to note that it is also the only homogenous and unsulfated member of the GAG family, made up of repeating glucuronic acid and N-acetyl-D-glucosamine (Evanko *et al*. 2007).

CS, made in the Golgi, has a similar biosynthetic pathway to HS, starting off with the linker region, followed by alternating sugars of D-glucosamine and N-acetyl-D-galactosamine. Like HS, CS chains can be sulfated, however at the 4-O and 6-O position of glucosamine and offer a wide variety biological functions (Mikami and Kitagawa 2013).

DS, like CS contains repeating units of N-acetyl-D-galactosamine and iduronic/glucuronic acid, however, sulfation is usually seen at the 2-O position of the uronic acid. DS is predominately found in the skin and cardiovascular system (Trowbridge and Gallo 2002).

KS, is made up of repeating chains of iduronic acid and galactose, which again can be sulfated to form biologically relevant domains. Unlike Hp/HS, KS can only contain un-sulfated Galβ4GlcNAcβ3, mono-sulfated Galβ4GlcNAc(6S)β3 or di-sulfated Gal(6S0β4GlcNAc(6S) β3 residues (Reviewed by Lindahl *et al.*, 2017). The chains can also be fucosylated and sialylated and are found in collagen abundant tissues, such as cartilage, cornea and the brain (Funderburgh 2002).

These constitute a diverse range of GAG structures which have huge biodiversity. Usually anchored to the cell surface by a protein core, proteoglycans (PGs), as they are termed, present GAGs to available protein ligands where their main role is as a co-ligand to anchor the protein of choice to interact with their receptor.

1.2 Proteoglycans

Many core proteins of PGs anchor GAGs to the membrane of the cell and presents them to potential ligands in the extracellular matrix or at the cell surface, e.g. fibroblast growth factor 2 (FGF2) is usually freely moving in the extracellular matrix to the sites where it is required, upon passing the cell surface, it meets an FGF receptor (FGFR), which is

membrane bound. HS bound to core proteins facilitates this interaction by 'catching' and sequestering the growth factor. Core proteins are tissue specific and can contain different mixtures of GAGs for different roles, e.g. syndecan PGs have been shown to have an essential role in the progression of muscle turnover and muscular dystrophy, where they can contain HS or CS chains (Pisconti *et al.,* 2012). The two most abundant types of cell surface heparan sulfate proteoglycan (HSPG) core proteins are glycosylphosphatidyl inositol-linked glypicans and transmembrane syndecans. These are known to be in high abundance (>10^6 cells) on the cell surface, making HS available for its biological activity (Bernfield *et al*., 1992).

1.3 Heparan Sulfate

1.3.1 Heparan Sulfate Biosynthesis

HS is essential in controlling many biological processes. The GAG chain is abundant on the cell surface, often anchored to a protein core, as well as on secreted HSPGs in the extracellular matrix. Within the cell environment it interacts with high affinity to growth factors, adhesion proteins and cytokines to regulate processes such as cell proliferation, migration and adhesion.

The biosynthesis of HS is a complex, non-template driven process, which involves the inclusion of many enzymes acting in a specific step-wise manner to form a mature HS chain (Table 1.1). There are 4 main steps involved in the production of HS; initiation, elongation, sulfation and post-synthetic modifications. Although they all continue throughout life, the latter may play an important role in normal ageing and disease.

Initiation

Current knowledge of HS biosynthesis suggests that the process of forming a sulfated, bioactive proteoglycan is a sequential enzymatic process. Starting in the Golgi, the non-template driven synthesis begins with one of multiple enzymatic steps in the initiation phase. The first step of the initiation phase occurs when a xylose monosaccharide from UDP-xylose attaches to a serine acceptor amino acid substrate on a core protein via the action of two xylosyltransferases, XYLT-1 and -2. Yamada *et al*. (2002) have shown that phosphorylation of the xylose residue may be crucial in the attachment of the first GlcA residue. Knockout of XYLT leads to the failure of the cells to produce either CS, Hp or HS suggesting that there is no differentiation between them at this stage (Esko *et al*., 1985).

Galactosyltransferases, GalT-1 and -2 complete the initiation phase by adding two D-galactose residues to the protein core. Mutations in GalT-1 have been shown to cause Ehlers-Danlos syndrome, a rare inherited family of diseases, which cause severe connective tissue disorders (Okajima *et al*., 1999).

To this tetrasaccharide in HS/Hp biosynthesis, the enzyme GlcAT-1, adds a D-glucuronic acid residue from uridine diphosphate-glucuronic acid (UDP-GlcA) forming a complete linker region and determining the chain as HS/Hp (Pedersen *et al*., 2000). This region allows HS to be presented on the cell surface for attachment to receptor molecules (Esko and Zhang, 1996).

Elongation

Glycosylation, the sequential addition of single sugar monomers occurs after the production of the protein linker region. Proteoglycans, as they are termed from this point can have a variety of GAG chains built onto the protein core e.g. CS/HS. However, not all protein cores build onto the tetrasaccharide region, some can also serve as part time proteoglycans, where they may not contain sugar chains e.g. Thrombomodulin exists with or without CS chains attached (Nadanaka *et al*., 1998). The reason behind the glycosylation of some proteins and not others is still relatively unknown, although it has been suggested that sulfation of the tetrasaccharide linker region favours the addition of more sugars (Tone *et al*., 2008).

The elongation phase builds the primary chain of HS onto the linker region by two EXT enzymes. EXT-1 and -2 can form hetero-oligomeric complexes in the Golgi and have both been shown to have dual activities in GlcA and GlcNAc glycosyltansferase (Senay *et al.*, 2000). Interference in the action of EXT1 or EXT2 by siRNA have been shown to result in shorter chains of HS, and conversely over-expression results in the formation of longer chains (Bussel *et al*. 2007). Whilst it has been shown that the over-expression of either can elicit more EXT activity, one cannot compensate for the knockout of the other and together they possess significantly more activity. Knockout of EXT-1 showed embryonic lethality prior to E7 in mice embryos, whilst HS deficient CHO cells do not show any abnormality in EXT-2 signalling (Wei *et al*., 2000; Lin *et al*., 2000). This evidence suggests that EXT-1 is the driving force behind the elongation of the GAG chain, but there is a need for equal partnership between the two for elongation of the chain and later activities of the NDST enzymes (McCormick *et al*., 2000; Carlsson *et al*., 2008). 50-200 alternating N-acetyl-α-D-glucosamine and β-D-glucuronic acid residues linked by 1-4 glycosidic bonds, provide the first level of diversity to the HS structure (Figure 1.1).

Sulfation

N-sulfation, followed by epimerisation, of the primary chain is the main reason for the backbone heterogeneity and formation of domain structure seen in natural sources of HS. There are 3 primary sulfation modifications; C2 of L-iduronic/D-glucuronic acid and C2 and C6 of glucosamine. Sulfation of C3 position of D-glucosamine occurs less frequently but does have biological significance, discussed later in this Chapter.

All sulfation modifications occur in the presence of the sulfate donor 3'-phosphoadenosine 5'-phosphosulfate (PAPS). In the absence of PAPS, random N-deacetylation (~40%) occurs along the saccharide chain, compared to ~65% N-sulfation in its presence. Having a substantial increase in N-sulfation of full length chains, has led to the suggestion that the presence of PAPS may also increase activity of the enzyme NDST1 (Carlsson *et al*., 2008).

Both N-deacetylase and N-sulfotransferase action occur by a group of bifunctional NDST enzymes. NDSTs work in the cis-Golgi to modify sections of the initial primary chain by transforming sections of GlcNAc to GlcNS (Lindahl *et al*, 1998). To date there has been a single mammalian gene identified, which produces 4 NDST enzymes. The actions of NDST-1 and -2 have been shown to be similar, although knockout (KO) mice with a deficiency in NDST-1 are embryonic lethal with very low levels of sulfated HS. Whereas in the KO of NDST-2, mice fail to produce Hp but can produce HS and are viable (Ringvall *et al*., 2000). This suggests that NDST-2 plays a more crucial role in the production of Hp and longer chains of N-sulfation, possibly laying the foundation for further O-sulfation (Kusche-Gullberg *et al*., 1998; Carlsson and Kjellen., 2012). NDST -3 and -4 show respective opposing increased deacetylase and sulfotransferase activities (Aikawa *et al*., 2001).

Following N-sulfation, uronyl C5-epimerase converts β-D-GlcA residues to α-L-IdoA in both Hp and HS. A single epimerase enzyme recognises a specific GlcNS residue and acts on the GlcA situated towards the reducing end of the chain (Sheng *et al.*, 2012). Although this is a reversible process, the resulting iduronate residues can be sulfated at the 2-O position by a 2-O- sulfotransferase (HS2ST), this can also occur to GlcA to a lesser extent (Smeds *et al.*, 2010 – Figure 1.2). Mice knockdown models of HS2ST not only show a decrease in 2-O sulfation of HS, but also show a significant reduction in 6-O sulfation of glucosamine on neighbouring unsulfated IdoA residues (Bai and Esko, 1996). Therefore, it could be suggested that the position of 2-O sulfation may be a prerequisite for some sites of 6-O sulfaton. This may be due to the combinatorial action of both sulfation positions in activating growth factors.

Subsequently 6-O sulfation of glucosamine residues occurs by the action of 6-O-sulfotransferases (HS6STs – Figure 1.2). There are three enzymes in this family which are derived from different genes. Although all three enzymes show high levels of homogeneity, HS6ST-1 preferentially sulfates glucosamines adjacent to IdoA residues, HS6ST-2 with GlcA neighbouring residues and -3 shows equal affinity for both IdoA and GlcA neighbouring residues (Habuchi *et al*., 2000).

The rarest of the sulfation modifications is at the C3 position of glucosamine residues (Figure 1.2). Although the least evident in HS/Hp chains in quantitative terms, 3-O sulfation is important in the ability of Hp to interact with high affinity to antithrombin (AT). Interestingly there have been 7 HS3ST enzymes found to date. All isoforms show specificity to glucosamine residues and in part are dependent on their neighbouring sugars, of which 2-O sulfation is a requirement (Maccarana *et al.,* 1996).

Sulfation modification of the backbone continues in a non-template driven manner, increasing the diversity of the resulting saccharides. Significant investigation has been undertaken to elucidate specific sulfation patterns of HS, which are important for interactions between growth factors and their receptors. However, as discussed later in this Chapter, the large variation in the HS structure complicates studies to investigate the selectivity of specific structures (Linhardt *et al*. 1990). Knockout models have shown that abolishing the activity of any of these modifying enzymes can result in unmodified, unsulfated HS and non-viable embryos. This is almost certainly due to the mutant chains inability to interact with proteins essential for development, suggesting that these sulfotransferase enzymes are indispensable for normal development (Fuster and Wang 2010).

Sulfation of the sugar residues increases the hydrodynamic volume of the HS chain and are dispersed between different lengths of unmodified residues along a typical chain (Turnbull and Gallagher, 1990; Esko and Lindahl 2001). Conformational arrangements of these sugars are important to allow sulfate residues to be physically available to interacting proteins. IdoA/2S residues form in chair ($^1C_4$) and skew boat (^2S_O) conformations, which are known to be flexible and promote protein interactions, particularly in growth factors where one HS chain is bound to multiple ligands. In contrast GlcA/2S and GlcN exclusively reside in the ($^4C_1$) chair conformation (Hsieh *et al.*, 2016).

Post Synthetic Modifications

A family of enzymes which are responsible for posttranslational modifications of the HS chain are sulfatase enzymes. The action of these enzymes are more often evident in disease than biosynthesis. Their role is to remove 6-O sulfate groups from the sugar chain by hydrolysing 6-O sulfate esters of glucosamine, which can result in a reduction or loss in the mode of action of the GAG and further progression of a disease (Parenti *et al*., 1997).

Furthermore, HS and Hp can be cleaved by a glycosidase called heparanase. Heparanase is the only known enzyme found in the body which has the ability to cut the HS chain, facilitating internalisation, general turnover and recycling of HS. Some specificity for the action of this enzyme has been described, N-sulfate residues are required for the enzyme to cleave HS but the presence of O-sulfation is not necessary. There is also evidence to suggest that the enzyme only works on chains larger than 10 kDa (Oldberg *et al.*, 1980; Thunberg *et al.*, 1982; LaPierre *et al.*, 1996). It is activated into its mature form by cathepsins, which cleave a 6 kDa linker domain. Under disease states it has the ability to affect composition of the ECM, signalling pathways and has been shown to be connected with inflammation, cell invasion and tumour angiogenesis (Gingis-Veltski *et al*., 2004; Dempsey *et al*., 2000).

1.3.2 Alternative Biosynthetic Routes of HS

An alternative biosynthetic pathway, where substrates from previous steps very much determines where and how the next set of enzymes act has been proposed by Rudd and Yates, 2012. Furthermore, it is suggested that there are 2 branches of the biosynthetic chain, one of which produce the most commonly occurring disaccharides, GlcA-GlcNAc – GlcAGlcNS - IdoA-GlcNAS - IdoA-GlcNS(6S), Ido(2S)GlcNS - IdoA2S-GlcNS(6S), whilst the other produces less common structures but those that still have biological importance; IdoA-GlcNAc – Ido(2S)GlcNAc – IdoA-GlcNAc(6S) – IdoA(2S)GlcNAc(6S).

These branches support the hypothesis that biosynthetic enzymes, such as HS6ST-2 and -3 show preference for substrates already sulfated in the 2-O position and oligosaccharides with more than 2 sulfate groups are more likely to then be 6-O sulfated, with this structure being central in the chain (Merry *et al*., 2001).

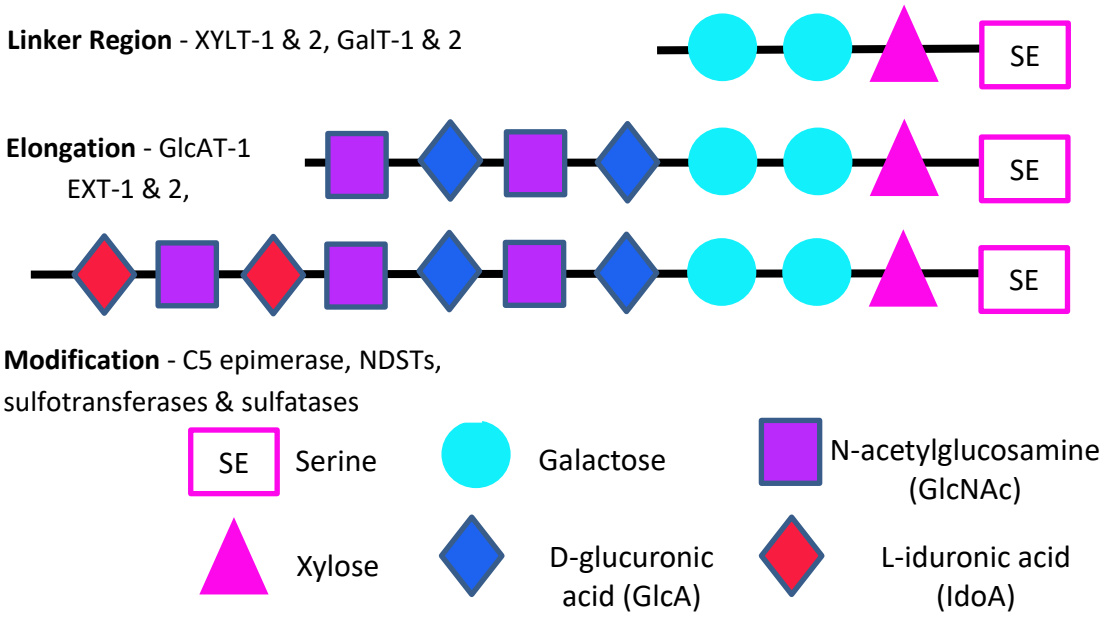

Figure 1.1 - A diagrammatic representation of the building blocks that make up HS chains and the enzymes that catalyse its production.

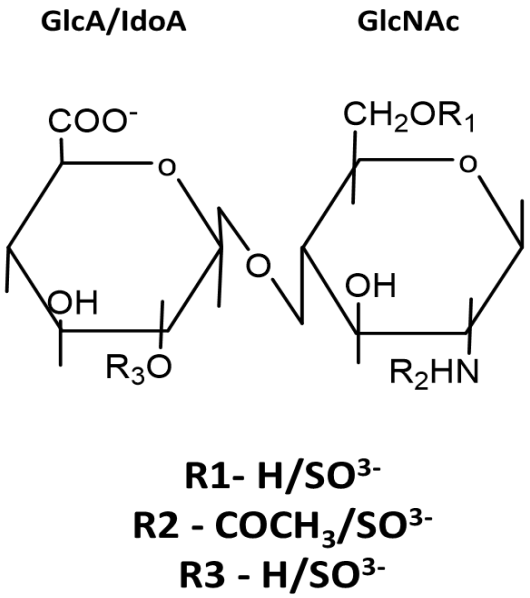

Figure 1.2- A diagrammatic representation of the sulfation positions of D-glucuronic/L-iduronic and N-acetyl-D-glucosamine disaccharides. The disaccharide can be sulfated with 2-O sulfation at carbon 2 of glucuronic/iduronic acid and N- and 6-O sulfation of glucosamine at carbon 2 and 6, respectively (more rarely carbon 3).

Enzyme	Role	Place of action
XYLT-1 and -2	Attaches xylose to serine on protein core	Golgi
GalT-1 and -2	Adds 2 galactose to protein core	Golgi
GlcAT-1	Adds a glucuronic acid to the galactose and xylose on the protein core	Golgi
EXT-1 and -2	Builds chain (dual action adding N-acetylglucosamine and glucuronic acid)	Golgi
NDST	GlcNAc to GlcNS Dual action de-acetylase/N-sulfotransferase	Golgi
C5' epimerase	GlcA to IdoA	Golgi
HS2ST	GlcA/IdoA to GlcA(2S)/IdoA(2S)	Membrane
HS6STs	GlcNAc/NS to GlcNAc(6S)/NS(6S)	Membrane
6-O Sulfatases	Remove 6-O sulfate groups from the chain	Membrane

Table 1.1- Biosynthetic and post-synthetic modification enzymes for the production of HS/Hp. Listed are the major groups of enzymes involved in the production of HS/Hp (reviewed by Kreuger and Kjellén, 2012).

1.3.3 Differences Between Hp and HS

HS and Hp are closely related, as far as we know sharing the same biosynthetic pathway and identical building block monomers that in full length Hp/HS only differ in the ratios of sulfation and Ido/GlcA along their chain. Manufacturing processes which extract and digest the oligosaccharide chains make distinguishing Hp from HS substantially harder when characterising them.

By convention, the two are distinguished broadly by their make-up and the cell/s which produce them. More homogenous Hp is characterised by containing high levels of sulfation, ~2-3 sulfates per disaccharide. To obtain high levels of sulfation, regions of the chain are mainly made up of the trisulfated disaccharide, IdoA(2S)-GlcNS(6S), in high density around occasional unsulfated residues (Gallagher and Walker, 1985). HS broadly speaking is far more heterogeneous in its composition, having lower sulfated mono- and di-sulfated disaccharides, giving a lower level of average sulfates per disaccharides (~0.5-1.8) and a longer chain length 20-100 kDa (Hp 7-20 kDa - Zu and Esko, 2014).

However, Hp and HS are also produced by different cells in the body (Table 1.2). Hp is produced by mast cells, usually attached to a serglycin protein core, whereas HS is produced

by almost every cell type and has an abundance of protein core ligands. It should be noted that some very highly sulfated HS types that are Hp-like have been identified e.g. liver tissue (Lyon, Deakin and Gallagher, 1994).

Distinguishing Characteristics	Heparin	Heparan Sulfate
Site of Synthesis	Mast Cells	~All Cells
Size	7-20 kDa	20-100 kDa
Core Protein	Serglycin	Many
Sulfates per disaccharide	2.0-3.0+	0.5-2.0
Percentage of N-sulfation	>80%	<50%
Percentage of 2-O sulfation	>80%	<40%
Percentage of 6-O sulfation	>80%	<40%
Affinity to AT	30%	0.3%
Commercial Cost	$62.47 (10mg-FisherSci)	£529.00 (1mg-Sigma)

Table 1.2- A summary of the main differences between Hp and HS. Adapted from Zu and Esko, 2014.

1.4 Functions of HS

In the body HS plays a pivotal role in a very wide diversity of biochemical processes during homeostasis and disease. Reflecting this functional heterogeneity, the structure of HS varies significantly from tissue to tissue, in gender, age and in both normal and diseased states. These findings, along with the discovery of the pentasaccharide AT binding sugar, has led to extensive research into other HS/protein specific interactions.

1.4.1 HS-Protein Interactions

HS chains exert their functions through interacting with many different types of proteins. For example, HS can act as a sequestering molecule at the cell surface, increasing the concentration of growth factors, releasing them in active form for high affinity binding to their receptors, as well as protecting growth factors and cytokines from degradation (Herr *et al*., 1997).

There is considerable debate over whether proteins bind 'specific' HS motifs. Largely driving this theory was early work conducted into investigations of the binding of the

pentasaccharide binding site for ATIII, which prevents the conversion of AT to thrombin and the formation of a fibrin clot. This structure to date has been exploited widely as the gold standard for anticoagulation therapeutics (Thunberg *et al*., 1980). However, it is notable that other HS sequences have been found to bind with equal affinity to ATIII (Dawes, 1988; Hubbard *et al.*, 1984; Shimada & Ozawa, 1985). Work around protein specificity has largely been based on binding studies which use affinity chromatography, and based also on salt elution of unbound oligosaccharides. However, this method of deducing binding to growth factors inherently favours highly sulfated chains which require higher concentrations of salt to displace them and does not always select binders that will lead to activity (Ishihara *et al.*, 1993; Saksela *et al.*, 1988).

Research currently favours theories that HS binding to a protein is largely based on the charge density, size and conformation of the HS chain. The conformational flexibility of HS is largely due the presence of iduronate residues and the glycosidic linkage regions, which provide flexibility that allows the binding of certain sulfate groups to the protein, especially 2-O sulfates (Casu *et al*., 1988). Although some proteins have been found to bind with higher affinity to sequences containing certain sulfation groups, maintaining the order of these and their neighbouring structures are more than likely crucial for successful binding. Thus, a number of sequences with differing precise sulfation patterns may be able to fulfil binding requirements. However, the immediate surrounding (flanking) saccharides in binding regions can ultimately differ and may still lead to a successful interaction between the GAG and protein, thus the impact of these flanking sequences will vary depending on the protein involved.

Basic protein binding motifs are usually rich in lysine or arginine residues, which positive pockets along with hydrogen bonding glutamine and asparagine and non-polar aa e.g. valine, produce regions across the proteins surface to enhance Hp binding (Rudd *et al.*, 2017). Fibroblast growth factors (FGFs) are probably the most researched and best understood, in terms of their binding regions and ‘specificity’ for HS. FGF2 for example is known to have 3 conserved binding sites which bind 2-O and N-sulfated regions (Turnbull *et al.*, 1992). However, other groups have shown that specific sulfation patterns along the chain may be less important for activity, as other species still bind and may have varied levels of activity. All agree that a general decrease in sulfation led to weaker binding to FGFs (Jastrebova *et al*., 2010). Further details of interactions between FGFs, vascular endothelial growth factor (VEGF) and platelet derived frowth factor (PDGF) are given below (see 1.4.2).

Whereas cytokines such as the transforming growth factor β (TGF-β) family have members which show considerable binding with diverse HS motifs, potentially implying the different functional relevance of HS chains for these proteins, which are yet to be fully elucidated (reviewed by Rider and Mulloy, 2017). Data from previous experiments and pooled by Yates *et al*., 2017 have suggested that whilst there are small conserved areas of certain patterns of amino acids within the heparan binding sites (HBS) on proteins, these sites largely allow a degree of freedom for the size, sulfation pattern and conformation of HS structures that bind them.

1.4.1.1 Heparin as an Anticoagulant

Hp structure was elucidated in the early 1980's (Lindahl *et al.* 1984; Thunberg *et al.*, 1982). Since the discovery of the ATIII- binding pentasaccharide sequence, there has since been a long and extensive search into pairing other proteins with specific binding sequences of HS. The classic pentasaccharide porcine sequence, GlcNS(6S)-GlcA-GlcNS(3S,6S)-IdoA(2S)-GlcNS(6S) (Figure 1.3), was initially discovered due to the inability of nitrous acid to digest the GlcNS(3S,6S) residues (Cifonelli and King, 1972). The pentasaccharide was found to be the most avid binder to ATIII and to some extent, became labelled as the specific binder by default, when in fact there are multiple HS sequences that also bind to the protein, with the trisaccharide, GlcA-GlcNS(3S,6S)-Ido(2S), being the most important sequence for binding but ultimately the neighbouring structures can differ (Brito *et al*., 2014). Increasingly evidence has suggested the highly negative charge density of Hp plays a significant role in ATIII binding and this allows for some substitution of sulfation motifs in the residue (Seyrek *et al*., 2007).

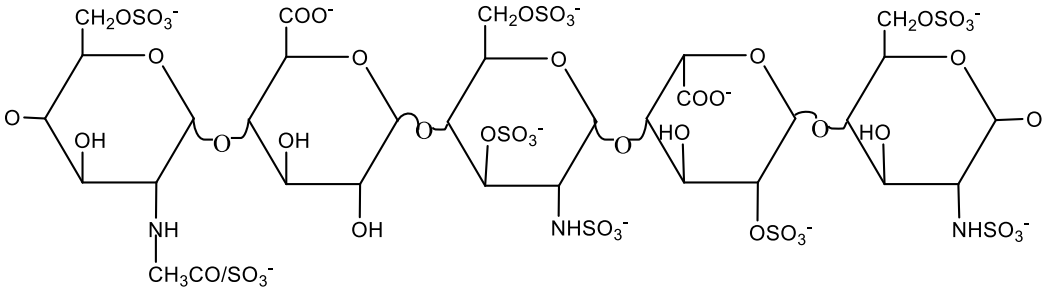

Figure 1.3 - ATIII pentasaccharide binding sequence. The sequence is made up of 5 sugar residues; GlcNAc(6S)-GlcA-GlcNS(3S,6S)-IdoA(2S)-GlcNS(6S) which bind ATIII and prevents coagulation (adapted from Walenga *et al.*, 1997).

This pentasaccharide sequence binds a linear, basic N-terminus binding site on ATIII with high affinity, enhancing the activity of the protein ~1000-fold (Pratt & Church, 1991). This leads to a conformational change in the protein which allows ATIII to bind to its ligand, thereby stabilising the protein and releasing a protease substrate, which cleaves a reactive loop

trapping proteins, such as thrombin, inhibiting their activity (Huntington *et al*., 2000 and Lima *et al*., 2013; Figure 1.4). However, on the other hand, it has also been shown that there is no linear between the conformational change induced in ATIII and activity, but rather a relationship between stabilisation and activity is observed (Brito *et al*., 2014; Lima *et al.*, 2013).

Other proteins in the blood clotting pathway are also able to bind heparin including; factors IXa, Xa and XIa. Thrombin engages with Hp to accelerate the inactivation of thrombin (FIIa). However, this action requires a longer sequence of monomers, ~18mer, which not only contain the pentasaccharide sequence which binds ATIII at the reducing end but at the non-reducing end of the oligosaccharide is also able to bind thrombin (Petitou *et al*., 1999). The identification of these Hp binding proteins and their importance in the coagulation cascade has led to pharmaceutical Hp products being commonly referenced by their anti FXa:FIIa activity. More recently, LMW species of Hp have been identified as more avid binders with better pharmacokinetics and have led to the production of many difference species of drugs, including the synthetic saccharide, Arixtra, for the treatment of thromboembolisms (Laforest *et al.*, 1991; reviewed by Bauer, 2001).

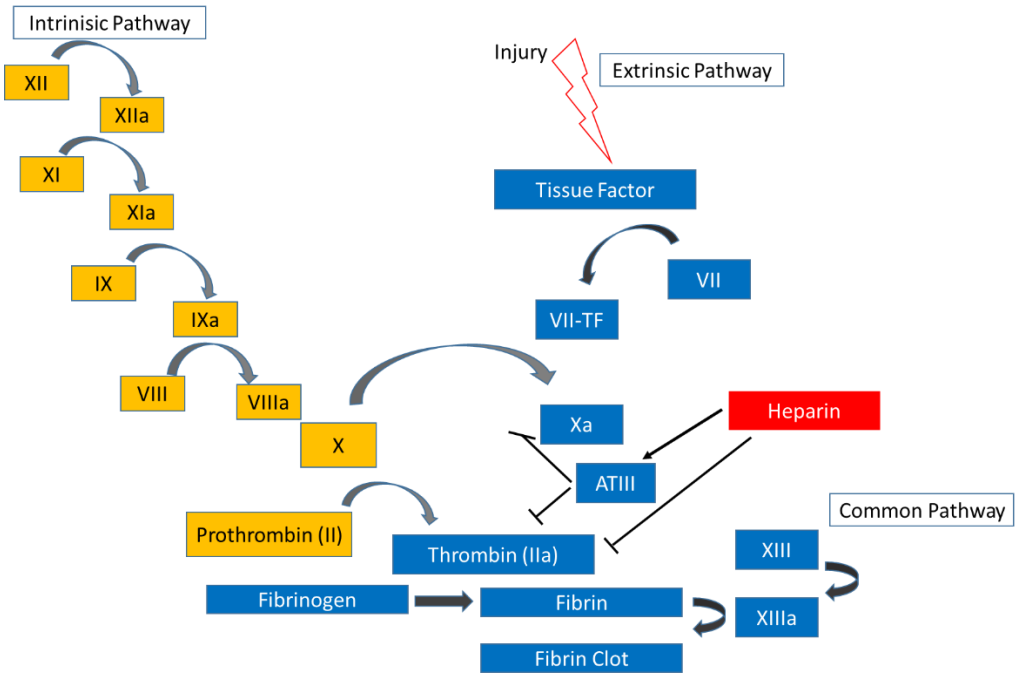

Figure 1.4- The major factors involved in the coagulation pathway. The coagulation pathway is particularly important when looking at the action of heparin and its related products. Heparin binds many factors in the cascade but it is its inhibition of the conversion of factor X to Xa by binding with ATIII and II to IIa an 18mer and ATIII, which is mainly responsible for to the failure of a fibrin clot to form (adapted from review by Wolber *et al.,* 2015).

1.4.2 Growth Factors and HS

It is hypothesised that GAGs play various roles on the cell surface, including sequestering of growth factors for signalling events and the activation, modulation of cell surface receptors by providing a ligand to which both the growth factor and the receptor can bind.

1.4.2.1 FGF2

There are 22 human FGFs, divided into seven subfamilies which largely share similar functions. FGF 1 and 2 belong to subfamily 1 and are by far the most extensively studied. FGF2 is produced in multiple splice variants from 17-24 kDa, which all bind to one out of five cell membrane receptors, FGFR1 (reviewed by Basilico and Mostcatelli, 1992). It is well recognised that FGF2 regulates epithelial-mesenchymal communication, organogenesis and pattern formation, which are essential for proper development, as well as many aspects of homeostasis and disease (Hu *et al*., 2009). The introduction of adenovirus antisense FGF2 RNA by Leconte *et al*. (1998) in 7 day mice embryos, resulted in abnormal vasculature, suggesting that FGF and its signalling events play a pivotal role in blood vessel formation. FGF2 interactions with HS have been extensively studied, and it has been shown that HS potentiates and is essential in its activation through binding with it and its receptor (Kan *et al*. 1999).

FGF2, like platelet derived growth factor (PDGF) and vascular endothelial growth factor (VEGF), is produced by various cells involved in wound healing including fibroblasts, macrophages, keratinocytes and vascular smooth muscle cells (Bennett *et al*. 2003). Lin *et al*. 1999 showed that HS and its biosynthetic enzymes can modulate FGF activity by knocking out the *Drosophila* equivalent of mammalian NDSTs. Sulfation events are the last biosynthetic steps in the formation of HS and the knockout of some upstream biosynthetic enzymes leads to the elimination of sulfation in the HS chain (Gallagher *et al.,* 1986). The resulting models were unsuccessful at binding and therefore activating FGF. Further understanding of FGF/HS binding has identified favoured sulfation groups required for FGF binding. Other work into FGF/HS binding has suggested that the FGF:HS complex acts as a regulator of FGF signalling by prolonging its activity, providing thermal stability and protecting the growth factor from degradation, it may also keep FGF in an inactive state until presented to its receptor complex (Folkman *et al*., 1988; reviewed by Zhang *et al*., 2012). This has been shown in the case of trauma, such as wound healing, once activated, with the potential HS protection, FGF2 signalling during the inflammation process allows rapid and prolonged signalling of FGF in the proliferation phase. This is followed by the promotion of the laying down of new extracellular

matrix in granulation tissue and re-epithelialization by the active migration of fibroblasts and keratinocytes respectively (Kato *et al*., 1992).

Three Hp binding sites (HBS) have been identified on FGF2, these binding sites are bordered by unfavourable, negatively charged, hydrophobic residues (Migliorini *et al.,* 2015). Several amino acids on FGF2, predominantly positively charged ionic binding arginine, lysine, non-polar aa (e.g glycine) and hydrogen bonding glutamine and asaparagine have been shown to make up the HBS that are capable of binding oligosaccharides (Lee *et al.,* 2007). The primary binding site at the canonical C-terminus of FGF2 has the highest binding affinity for N-sulfated residues (Sterner *et al*., 2014). Whilst this is still a modest interaction, at the cell surface an abundance of FGF2 at the site of interactions compensates for this and ensures successful activation and binding. HBS2 and 3 have lower binding affinities for HS; nevertheless, they still affect the activity of FGF2. HBS2 has been shown to bind with unsulfated regions of HS to ensure dimerization of the FGF monomers and is required for appropriate induction of FGFs into the ECM (Venkataraman *et al*., 1999). Removal of HBS3 at the N-terminus has been shown to cause a decrease in the mitogenic activity of the growth factor (Xu *et al*., 2012). It is suggested that HS causes the protein to undergo conformational changes from saturation of HBS1 through to 3, and Xu *et al*., 2012 discovered that the secondary structure of the FGF protein becomes more disordered as the concentration of HS is increased.

Stimulation of the FGFR requires the co-binding of HS, FGF2 and its receptor FGFR1 in a ternary complex. FGFRs consist of up to 3 immunoglobulin domains, a transmembrane region and a cytoplasmic domain which becomes phosphorylated and activates the tyrosine kinase pathways; PI3K-AKT, PLCϒ-ERK1/2, STAT and RAS-MAPK (Figure 1.5; Itoh and Ornitz 2004). FGF2 has been shown to bind the second Ig domain, with HS also being capable of binding the receptor here. HS-FGFR1 binding can occur independently of the growth factor, via a high affinity divalent cation interaction with the ectodomain to form a binary complex to which the FGF can attach (Kan *et al*. 1999; Burke *et al*., 1998). It is well established that 6-O sulfation is key in the binding of HS to FGFR1 (Guimond and Turnbull, 1999). Studies have shown that a decrease in 6-O sulfation by reducing HS6ST-1 expression led to an overall reduction in FGF2 dependant endothelial sprouting and inhibition of *in vivo* FGF2 induced angiogenesis (van Wijk and van Kuppevelt 2014).

Overall sulfation at the 2-O position of IdoA and N-sulfation of GlcNAc has been suggested to be a key modification for forming a bridge between FGF and its receptor, although it is not ultimately required for the growth factors activation, 6-O sulfation is required for

binding the receptor and supporting the formation of the FGF:FGFR complex (Faham *et al.,* 1998 - Figure 1.5). High affinity binding was first demonstrated to involve an N- and 2-O sulfated oligosaccharide (Turnbull *et al.*, 1992). Kreuger *et al*., 1999 have suggested, from testing a limited number of structures, that the shortest oligosaccharide sequence for FGF2 binding is GlcNS-IdoA(2S)-GlcNS-IdoA(2S). However, strong activators of the FGF2 pathway start from octasaccharides containing 2- and 6-O sulfation, with an increase in binding affinity up to ~14mer (Walker *et al*., 1994). Beyond the sulfation patterns it has been suggested by Nieto *et al*. (2011) that there is a preferential shift towards $^{2}S_{0}$ conformation of IdoA(2S) residues for FGF2 binding, with this selection being highly reinforced by FGFR binding, providing a selective difference over FGF1, which was shown to bind a high proportion of $^{1}C_{4}$ chair conformers (Nieto *et al*., 2013; Canales *et al*., 2005). The difference between FGF1 and -2 binding to HS has been further characterised by Rudd *et al.*, 2010, who showed that HS binding leads to the stabilisation of FGF1 which relates to its activity, which is not the case for FGF2.

It has been shown that dimerization of the growth factor occurs when FGF binds to HS and this in turn allows the binding of the receptor and its dimerization (independent of the contact between the 2 receptors; Lam *et al.*, 1998). However, there is still some controversy over the complete mechanism and the overall number of components involved in the activation of the FGF pathway. To date, two ternary binding structures have been proposed by several groups via crystallography and NMR studies (Figure 1.5). However, this topic is still under much discussion as it is yet to be determined whether either of these models are functionally active and therefore applicable to the *in vivo* situation. These models are;

- Asymmetrical model – one HS bridges 2 FGFs forming a dimer bringing together two receptors. The two receptors do not interact directly with one another but the receptors are bridged by connecting with both FGFs (Pellegrini *et al*., 2000; Harmer *et al*., 2004)

- Symmetrical model - this model proposes that one or two HS interact with two FGFs and two receptors. Both FGFs interact with two receptors and both receptors associate with each other. The FGFs and the FGFRs form a single binding cleft where two Hps bind both FGFs/Rs forming the ternary complex (Schlessinger *et al*. 2000; Nieto *et al*., 2013).

Both proposed systems lead to a basic protein cleft between the dimerized receptors and growth factors, which are distinct for each FGF. This positively charged residue, allows the interaction of either one or two negative HS chains to bind with nM affinity and activate downstream tyrosine kinase pathways (Figure 1.5).

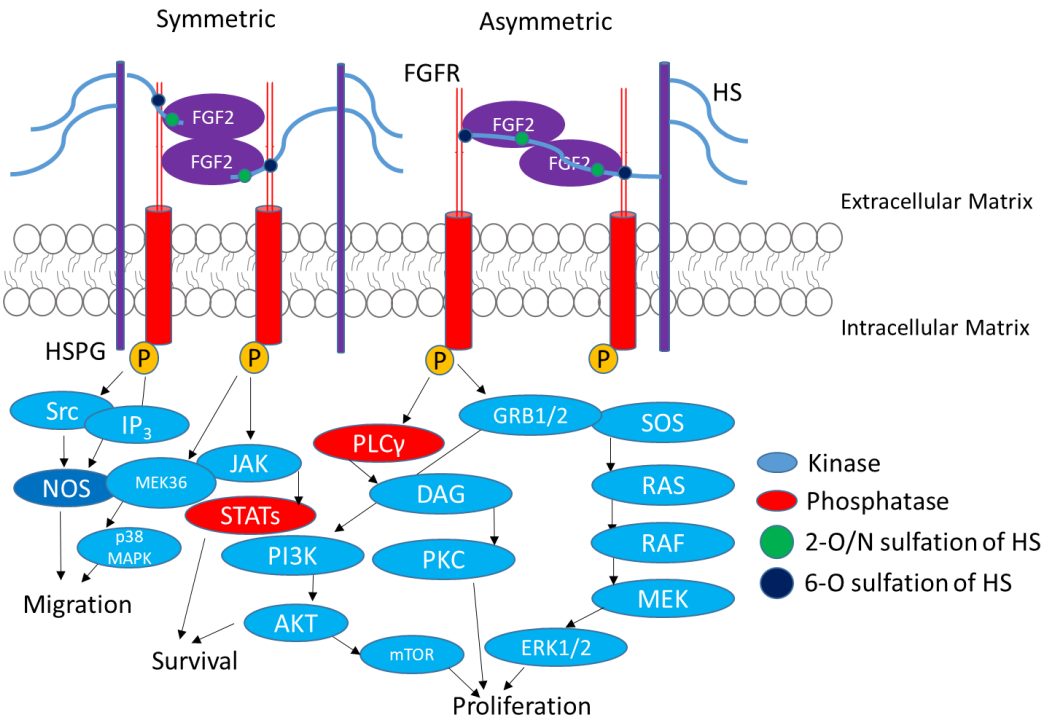

Figure 1.5- Diagrammatic representation of the two major proposed models of FGF-HS-FGFR ternary complex.

Symmetric model - a stable 1:1:1 complex forms between FGF/FGFR/HS this ternary structure then binds to another 1:1:1 complex, giving a biologically active 2:2:2 structure.

Asymmetric Model- Dimerization firstly occurs between two FGF molecules before attaching to one FGF receptor. This then induces dimerization of the receptors to form an active 2:2:1 FGF:FGFR:HS complex (adapted from review by Turner & Grose, 2010).

Src- sarcoma-family kinases, IP_3- inositol triphosphate, NOS- nitrous oxide synthase, MEK36-,mapk/ERK kinase 36 p38 MAPK-mitogen-activated protein kinase 38, JAK- janus family tyrosine kinase, STATs- signal transducer and activator of transcription, PI3K- phosphoinositide 3, AKT- AKT8 virus oncogene cellular homolog, PLCγ- phospholipase C gamma, DAG- diacylglycerol, PKC- protein kinase C, GRB1/2 – growth factor receptor-bound protein 1 and 2, SOS- son of sevenless guanine nucleotide exchange factor, RAS- Ras guanyl nucleotide-releasing protein, RAF- , MEK-MAPk/ERK kinase, ERK1/2- Extracellular signal-regulated kinase 1/2, mTOR- mammalian target of rapamycin.

1.4.2.2 VEGF-A_{165}

VEGF is encoded by a single gene, but alternate mRNA splicing gives rise to several isoforms that differ in their ability to bind HS through a binding site at the C-terminus. The family consists of VEGF-A of which there are multiple splice variants, B, C, D, E and F, as well as placental growth factor (PIGF).

The most abundant HS binding VEGF isoform is 165 (VEGF-A_{165}) (Robinson *et al.*, 2006; Bruns *et al.*, 2009). VEGF-A_{165} binds to its receptor VEGFR1 and promotes angiogenesis by increasing permeability of capillaries at the wound site and promoting the migration and

proliferation of endothelial cells. Hypoxic conditions in a wound bed are considered to be the main signalling cue for the upregulation of VEGF, building new blood vessels which reduces the oxygen deficient environment to allow other growth factors which favour less acidic conditions such as FGF2 to infiltrate (Eming and Hubbell, 2011). This influx of other growth factors increases vascular growth and therefore reduces apoptosis of newly migrated cells in the early stages (day 3) of healing (Stein *et al*., 1995; Watanabe *et al*., 1997). More recently VEGF has been shown to have multiple roles in wound healing, such as degradation of the current basement membrane by directly increasing the release of matrix metalloproteinases from endothelial cells, and chemotaxis through interaction with integrins (Unemori *et al*., 1992; Senger *et al*., 1996). This occurs through downstream signalling after phosphorylation of VEGFR, leading to the activation of AKT, ERK1/2 for survival and proliferation and NOS, p38 and other transcription factors inducing migration of cells and as described above, vascular permeability in endothelial cells (reviewed by Koch *et al.*, 2011 – Figure 1.6).

Mice with a reduction in VEGF-A survive to term but have significant postnatal vascular deformities, most commonly seen in major blood vessels supplying highly vascular structures like the kidney. Phenotypically the cell number is maintained in the capillaries of these mice, however the branching of the blood vessels is significantly reduced. To compensate somewhat for this, endothelial cells proliferate to increase the lumen diameter of the vessels, weakening the overall structure (Olsson, 2006; Carmeliet and Collen, 1999; Ruhrberg *et al*., 2002). A lack of Hp binding VEGF (VEGF-A_{165}) in mice, has been shown to cause cells to lose directionality, blood vessels were shown to extend into the spinal cord but appeared to terminate in a tuft of blood vessels where the ends coiled in on themselves. The presence of VEGF-A_{165} may act as an attractant for the growing vessel buds and the formation of a concentration gradient of VEGF may be required for correct assembly of the vascular network (Ruhrberg *et al*., 2002). Knockout of a single VEGF-A gene produces embryonic lethality, prior to E10, with mice presenting the same phenotypes as knockdown experiments in endothelial cell and blood vessel deformation (Carmeliet and Collen., 1999). Basal levels of VEGF-A continue in homeostasis but are upregulated in pathophysiological conditions, such as tissue damage and tumour growth, where a reduction in competent blood vessels causes tissue hypoxia and through the transcription factor HIF, an upregulation of VEGF-A (Reviewed by Ferrara, 2004; Germain *et al*., 2010).

Multiple VEGFRs bind VEGF-A through HS dependent interactions. VEGF-A binds both VEGFR2, which induces vigorous tyrosine kinase phosphorylation, and also to a lesser extent VEGFR1. Knockout experiments of VEGFR2 in mice show embryonic lethality prior to E10, much

like the KO of the growth factor, whereas VEGFR1 deficient mice show only minor vascular abnormalities (Quinn *et al*., 1993; Hiratsuka *et al*., 1998; 2001). The growth factor has been shown to dimerise at the cell surface once contact with HS has been established. However, like FGF, it is uncertain whether a single HS chain binds both growth factors (Venkataraman *et al*., 1999; Markovic-Mueller *et al*., 2017).

For binding optimum saccharides an ~8mer with several moieties within HS important for binding the growth factor including carboxylate groups, 2-O, 6-O and N-sulfation although not all are necessary to initiate signalling (Robinson *et al*., 2006; Figure 1.6). In NIH3T3 cells it was also established that N-desulfated HS was a much poorer competitor for VEGF binding than one with reduced 2 or 6-O sulfation, suggesting VEGF preferentially binds N-sulfated residues on HS. Mice completely deficient in 2-O sulfation with a compensatory increase in 6-O and N-sulfation maintained the same overall charge density and affinity to VEGF-A_{165}, whereas a loss of 6-O sulfation/carboxyl groups abolishes HS affinity to VEGF compared to the same size saccharide containing one or two 6-O groups (Ono *et al*., 1999; Robinson *et al*., 2006). Although 2-O sulfation might not be necessary for binding affinity, Zhao *et al*. (2011) and Robinson *et al*., 2006 have both suggested that the presence of all three sulfate groups are required for exhibiting the strongest level of competitive binding. This is primarily thought to be due to the flexibility of the backbone structure, associated with the presence of IdoA and possibly 2-O sulfation. Heparinase I and III treatment abolishes VEGF mediated activation, suggesting that the unsulfated residues as well as multiple sulfated residues are important for VEGF activation. This is supported by the findings of Robinson *et al.* (2006) showing that only one region of sulfated residues are required for VEGF binding.

1.4.2.1 PDGF-BB

Platelet Derived Growth Factor (PDGF) promotes a variety of cellular processes in fibroblasts, smooth muscle and endothelial cells, including mitogenesis, migration, activation of inflammatory cells and stabilization and integrity of newly formed blood vessels (Hellstrom *et al*., 1999; Abramsson *et al*., 2007; Feyzi *et al*., 1997). The protein exists as two main peptide chains, A (~200 amino acids) and B (~241 amino acids), as well as the more recently discovered PDGF- C and D for which 4 different genes are responsible for their production. In the ECM, the protein exists as a disulphide linked dimer, with primarily AA, AB and BB existing in higher quantities than others at the cell surface (such as PDGF-CC/DD). Knockout models of either the growth factor or receptor show embryonic lethality due to weakness of the majority of blood vessels, leading to aneurysms and haemorrhaging (Tallquist and Kazlauskas, 2004; Stenzel *et*

al., 2009). Current knowledge about PDGF is lacking somewhat compared to other growth factors, especially for isoforms C and D, so from here on this thesis will only discuss isoforms A and B.

The C and N terminus of the protein are both required for the regulation of cellular processes and exist in two splice forms, long (L) and short (S). To be released into the ECM the N terminal amino acids undergo proteolytic cleavage during the activation of the growth factor signalling pathway (Lokeshwar *et al.*, 1990). The C terminus is understood to bind to HS and elicit this activation. Crystal structure analysis of the growth factor has suggested that anti-parallel β-sheets of PDGF give rise to a very similar structure to VEGF when bound to HS, they mediate the same downstream signalling pathways, and ultimately serving similar roles, primarily in angiogenesis but act through distinct receptors. However, to further support the similarity between the two growth factors, both can bind and activate PDGFR's (albeit VEGF far less efficiently), suggesting some synergy between the two (Muller *et al*., 1997; Wu *et al*., 2008). Compensatory effects have also been suggested in smooth muscle/fibroblasts cells with a reduction in VEGF, where in areas of hypoxia and damage, VEGF is able to indirectly activate PDGFRα, reducing the levels of p53 and promoting cell survival whilst new blood vessels are made to reduce tissue hypoxia and stress (Pennock and Kazlauskas, 2012).

PDGF-BB signals via its receptor PDGFR-β (which has also been shown to bind and activate the heterodimeric PDGFR-αβ), resulting in dimerization by contact with PDGF dimers. Prior to this they are found as monomers on the membrane. PDGF-BB is produced by endothelial cells and its receptor by pericytes and vascular smooth muscle cells (Hellström *et al*., 1999). The BB isoform is highly expressed in heart and placental tissue and through the recruitment of mural cells it plays a significant role in the stabilization of newly formed blood vessels as they mature (Hellberg *et al*., 2010).

PDGFR activation by autophosphorylation causes downstream tyrosine kinase activation through many SH2 domain proteins such as PI3K, as well as the independent PLCγ path. The activation of the receptor also signals its internalisation and degradation, thus ending its signalling (Engelman *et al*., 2006). Unlike PDGFR-α, PDGFR-β also directly engages RasGAP, inactivating Ras (Figure 1.6).

PDGF is thought to exert its effects on cells in a concentration dependent manner, providing newly migrated cells with directional cues. De Dontis *et al*, 2008 showed that fibroblasts exposed to lower concentrations of PDGF (~1 ng/ml) migrate towards the site where they are needed e.g. wound bed, at this point the cells meet a threshold concentration (~5+

ng/ml), where cells cease movement and start proliferating. Embryonic knockout models of either PDGF/R-β reduce the number of pericytes and vascular smooth muscle cells, thereby increasing the probability of vascular failure in blood vessel rich organs such as the brain, heart, kidney and eye (Lindahl and Betsholtz, 1998).

Garcia-Olivas *et al*. (2007) showed that PDGF-AA long isoforms have a greater binding affinity to HS on the cell surface than other species, as well as the long isoforms, AA/BB, show greater colocalization with GAGs on the cell surface. PDGF-BB has a 10-fold reduction in its affinity to bind HS than the AA (Lustig *et al*., 1999). This could potentially be cell specific, as the PDGF-BB short isoform shows greater ability for increasing cell responses, such as proliferation in hASMCs (up to 10 ng/ml). This characteristic may be more dependent on which cell surface proteins are present and to a lesser extent the HS chains, as short splice variants are unable to bind CS, like other PDGFs, and still exert some activity after chlorate and heparinase treatment in CHO cells (Garcia-Olivas *et al*., 2003).

As PDGF-B chains can bind both PDGFR-A/B it is suggested that lower concentrations of growth factor needs to be employed to exert greater effects than PDGF-A which can only bind receptor A. Although it has been established that PDGF-AA requires ECM-based HS chains in order to activate signalling. Unlike FGF, it is not the O-sulfated regions of HS which are immediately important for binding PDGF, but N-sulfation (Abramsson *et al.*, 2007).

Both isoforms contain basic regions where the HS binding sites are located. The growth factor contains three basic loop receptor binding residues which have been shown to bind evenly spaced N-sulfated residues with a further need for 6-O and to some extent 2-O sulfation (Abramsson *et al*. 2007; Feyzi *et al*., 1997; Schilling *et al*., 1998). Removal of HS by heparinase treatment, significantly diminishes PDGF-BB binding and therefore its receptor activity (Garcia-Olivas, 2003).

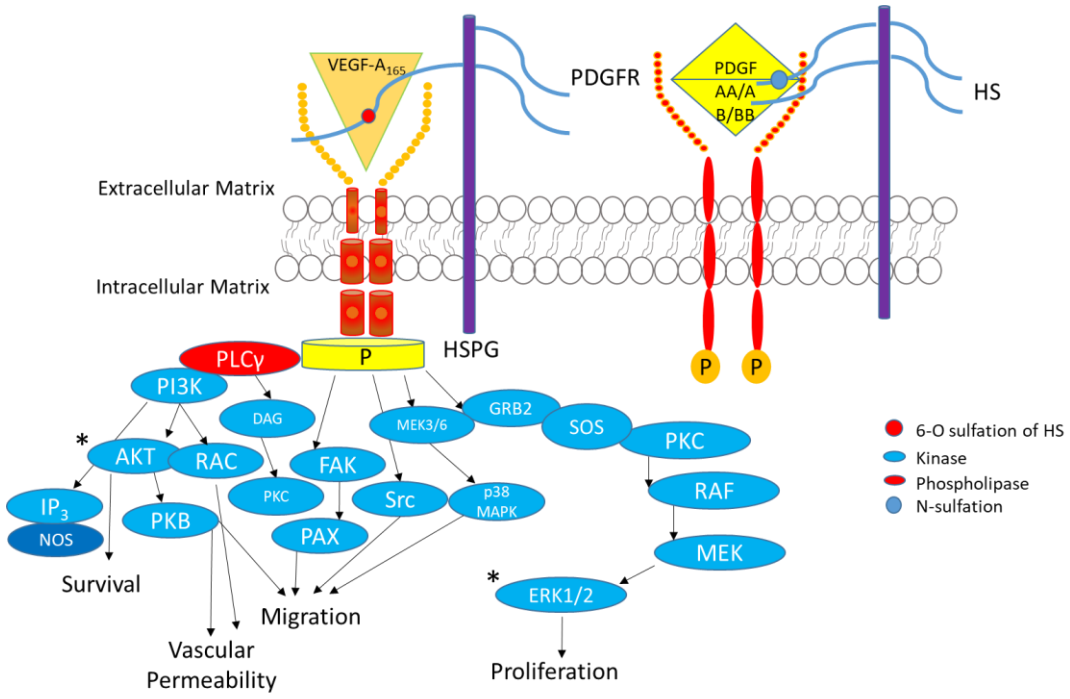

Figure 1.6- A diagrammatic representation of the main signalling events of VEGF-A_{165} and PDGF. Activation of the receptors by interaction with the growth factor and HS. *Represents parts of the signalling pathway investigated in Chapter 5 of this thesis (adapted from review by Takahashi & Shibuya, 2005).

RAC- Ras-related C3 botulinum toxin substrate 1, PAX- paxcillin, PKB-protein kinase B

1.5 HS/Hp in Viral Infections

The role of HS in maintaining normal homeostasis has been intensely researched over many decades. However, more recently HS has been shown to be responsible for the many other activities, for example the transmission and survival of many Flaviviruses, both in the primary insect host and the final host, humans. Recent research has suggested that positively charged conserved pockets on the protein envelope of the virus provide the ideal environment for a strong interaction with HSPGs. As the most negatively charged macromolecule in the body, this is perhaps unsurprising, although the regions and strengths of binding differ between the family of Flavivirus. For example, NS1, viral glycoprotein on the viral envelope of Dengue fever has been implicated in the initial attachment of the virus to the cell membrane by CS and HS (Avirutnan *et al.*, 1998). Furthermore, there is some evidence for similar mechanisms in the other family members; Zika, yellow fever and West Nile Virus, suggesting that from the outset HS plays a pivotal role in the viral propagation and subsequent infection of the Flavivirus family (Chen *et al.*, 1997; Germi *et al.*, 2002; Hilgard *et al.*, 2000; Dalrymple *et al.*, 2011; Lee and Lobigs, 2008).

1.5.1 The Role of GAGs in Zika Virus Biology

From 2015/16 the study of Zika virus has become of great importance, this is primarily due to the newer INMI-1 strain of Zika found in Brazil, having serious health implications. The INMI-1 strain is relatively harmless to adults in good health, usually presenting in flu like symptoms and in some serious cases Guillain-Barré syndrome (an autoimmune disease). However, infants born to mothers infected with Zika virus present with neurological deficits, possibly due to aberrant autophagy activation and subsequent alterations in normal neurogenesis (Liang *et al*., 2016). HS has been suggested to play an important role in the control of this process. Kim *et al*., 2017 have investigated structural specificity of HS and its binding to the positive region of the virus protein envelope. Zika virus has been shown to favour Hp over other GAGs and has higher affinity for longer chains, octasaccharide or above, which contain extensive tri-sulfated structures or those with 6-O sulfation in particular. However, Hp was not found in abundance in either brain (contained in many cell types in foetal brain, particularly neural stem cells) or placental tissues (through which it is passed from mother to foetus), where the virus primarily exerts its effects.

More recently, exogenous Hp has been shown to decrease cytopathic effects of Zika infected cells, shown by monitoring levels of adenylate kinase released into the culture. Adenylate kinase is released when the cell membrane is damaged and is used as an early marker of apoptosis. Further evidence for the role of exogenous Hp reducing apoptosis is the reduction of Caspase 3 (CASP-3) activity in infected cells and ultimately cell death. Although not reducing the viral burden in these cells, this evidence has led to the suggestion that Hp can exert a neuroprotective role in Zika infected cells that may lead to a reduction in cell death seen in brain embryology of infected patients and therefore reduce the severity of the disease. However, it should be noted that Hp could potentially ensure the propagation of the disease as these cells do not die and therefore the virus can continue to replicate (Ghezzi *et al*., 2017).

1.6 Production of HS

As described above, HS provides a potential therapeutic target for many diseases. For this reason, the ability to make copious amounts of high quality HS, which can be tailored to have specific activities for extensive research and the eradication and treatment of many diseases, is highly desirable.

1.6.1 Methods of HS Production

Alternative methods for the production of Hp have been sought since the 2008 contamination crisis due to over sulfated CS (FDA, 2009). The ability to characterise all Hp products will enable quicker, more rigorous checking of batches and permit future FDA approval for new HS related drugs. To date there are still far more naturally sourced Hp and LMWH products on the market, despite some synthetically derived materials showing greater selectivity and pharmacokinetics (Laforest *et al.*, 1991). However, the latter can also create problems with reversibility of the drug due to high affinity binding (reviewed by Nunnelee, 1997). The failure of many synthetic products to reach the market apart from Arixtra, is partly due to synthetic production failing to produce the yields of material required at a reasonable cost for the pharmaceutical industry (Driguez, 2004). This may change with recent advances in chemoenzymatic methods for Hp production (Liu & Linhardt, 2014)

To date there are three main strategies for synthesising HS structures; multi-step solution-phase synthesis, automated synthesis and the chemoenzymatic approach.

Multi-step solution-phase synthesis still remains the most popular way of producing oligosaccharides and has allowed other approaches to be established. Chemical glycosylation requires a donor, and nucleophilic attack on the acceptor to form new glycosidic bonds. Removing the protecting group on the non-reducing end of the newly formed disaccharide allows further glycosylation. This requires a large number of steps to create intermediates, removing the protective group on the non-reducing end and the final addition of disaccharides to the chain, therefore this process is most often used to produce short HS chains for bioassays and structure-activity studies (Haller and Boons, 2001; Prabhu *et al.*, 2003; Schworer *et al*., 2013; reviewed by Dulaney and Huang, 2012).

The second process, the automated synthetic approach, requires far fewer steps, allowing the synthesis to take place more rapidly, although it still requires the manipulation and addition of sensible building blocks for this to take place. These are subject to finding the appropriate conditions for each step, as well as addressing a substantial need for glycosyl donors and other synthetic modifications (Plante *et al.*, 2001; Weishaupt *et al.*, 2010).

Finally, chemoenzymatic synthesis manipulates saccharides of varying sizes which are modified by the introduction, modification or removal functional groups. This is perhaps the easiest method and most utilised for GAG production (Blixt and Razi, 2006). Initially a sugar backbone is produced which can then be elongated, epimerised and sulfated at the 2-, 6-O and

N-positions and if required the 3-O position to produce the Hp pentasaccharide. One approach is the production of a sugar backbone, which is achieved from disaccharide building blocks produced from an initial nitrous acid digestion of longer oligosaccharides (Liu *et al.,* 2014). However, more recently, related methods have been further developed systematically producing larger libraries of HS/Hp saccharides (Zhang *et al.*, 2017). Xu *et al.* (2017) have reported a 10% yield of a purely synthetic ~22 step anticoagulant Hp ~12mer production method with the use of an initial GlcA-NP (nitrophenol), rather than animal saccharide building blocks. This monomer, like the disaccharide building blocks, was elongated by incubations with UDP-GlcNAc, UDP-Glc-PNP (paranitrophenol) in the presence of KfiA (N-acetyl-D-glucosaminyl transferase of K5 strain of *E. coli)* and the addition of GlcA residues by PmHS2 (a dual action glycosyltransferase), this produces a mixture of different length saccharides with a GlcUA-GlcNAc- repeats, this method can be repeated until the desired chain length is achieved (up to ~dodecasaccharide - Liu and Linhardt, 2014; Xu *et al.,* 2017). Once made these saccharide chains are then purified by HPLC (high performance liquid chromatography), followed by desalting and purification to pick the same size species for further modifications (Guixin *et al.,* 2017). 2-O sulfation can be added to the backbone chain by incubation with NDST and PAPS, at the same time as C5 epimerisation. A further incubation with HS6ST-1 and 3 in the presence of PAPs introduced 6-O sulfation to the chain, and finally the important 3-O sulfate can also be added by HS3STs before the final pentasaccharide product was purified (Liu *et al.*, 2010). Earlier reported yields from this method for the production of the Hp pentasaccharide achieved around ~1.1%, the loss of product was attributed to purification strategies (Kuberan *et al*., 2003). Further to this other groups such as those of Liu and Lindhardt have utilised the method described above in place of the hexasaccharide starting saccharide of Kuberan *et al*. The group have shown a significant increase in yields, 38%, compared to Kuberan (1.1%), suggesting that there is the possibility of producing gram quantities of not only the bioactive pentasaccharide, but also other HS structures using this method (Liu *et al*, 2010).

Arixtra is used in the treatment of thromboembolisms and is one of the few synthetically produced carbohydrate drugs on the market. To produce the classic pentasaccharide ATIII binding sequence, about 50 steps are required in the chemical synthesis, which not only is an arduous task but also increases the cost of the drug due to a reduction in product yields at each stage (Sinaÿ *et al*., 1984). Due the cost, scientists have strived to refine and slimline this production and currently the process has been reduced to around 15 steps, reducing the loss of yield and cost of the final drug (reviewed by Driguez *et al.*, 2014).

1.6.1.1 Production of Hp and LMWH from Natural Sources

The production of Hp and LMWH has been refined over the last few decades, sourced predominately from porcine intestine and to a lesser extent bovine intestine and lung. LMWH has been more favoured for use in hospitals since the 1980s over its Hp counterpart, as they show more specificity to binding ATIII and a reduction in off-target effects. They are derived from the initial production of pharmaceutical grade Hp, but samples undergo more processing than standard pharmaceutical Hp. The initial production of LMWH has been patented and published, whilst company specific protocols are highly guarded industry secrets.

There are 5 steps from the crude animal product to purified Hp; 1) preparation of tissue, 2) extraction of Hp from the raw tissue 3) recovery of raw Hp 4) purification of pure Hp and 5) recovery of pure Hp (Lindhardt and Gunay, 1999). This process is discussed further in detail in Chapter 3, as this is the process from which the by-products were obtained.

1.7 Aims

This aims of this thesis were to investigate the HS/Hp content in a range of by-product material from the Hp stage in the production of LMWH. For this the by-products were refined by enzymatic digestion to produce an economical source of HS, for activation of growth factors and other biological applications, whilst also maintaining a low level of off target, undesirable effects. The principal aims were: -

1. To purify and characterise by-products from the production of Hp and compare their structure and content to Hp from a commercial manufacturer.

2. Digest by-products D1 and F1 with heparinase enzymes and separation into more refined fractions of HS oligosaccharides by size and charge.

3. Explore the bioactivity of the intact, parental by-product material versus Hp and oligosaccharide fractions of D1 and F1 in bioassays with FGF2, PDGF-BB and VEGF-A_{165}.

5. Compare the side-effects of the by-products and Hp through anticoagulant activity and cytotoxicity in cell assays.

6. Explore the potential of the by-products to reduce cell death associated with Zika Virus infection, as an example of a biological application for the by-products.

Chapter 2 – General Materials

Buffer List

Chondroitinase Buffer – 100 mM Tris acetate (Sigma, UK), pH 8.0

DNase Buffer- 10 mM Tris acetate, 25 mM magnesium chloride (Sigma, UK), 0.5 mM calcium chloride (Sigma, UK)

RNase Buffer – 10 mM Tris acetate (pH8.0), 5 mM EDTA (Sigma, UK), 8 mM sodium acetate (Sigma, UK)

Pronase Buffer – 10 mM Tris acetate, 10 mM calcium acetate (Sigma, UK)

Heparanse Buffer – 100 mM sodium acetate, 0.1 mM calcium acetate, pH 7.0

Acrylamide Buffer for sugar gels-

- Resolving gel - 4.5 ml GlycoMap buffer (20 ml 895 mM tris acetate (pH 7), 35 ml ethylene glycol, 35 ml ddH_2O.), 5.5 ml acrylamide (50%, 19:1 bis-acrylamide: acrylamide, Sigma, UK), polymerised with 28 µl 10% APS, 6.6 µl TEMED

-Loading gel – 2.25 ml GlycoMap buffer, 0.75 ml Acrylamide, 2 ml ddH_2O

RIPA Buffer (x1.1) – 50 mM tris acetate pH 6.8, 150 mM NaCl, 2 mM EDTA, 1% IGEPAL, 0.5% deoxycholate, 0.1% SDS, make up to 10 ml ddH_2O

Media List

BaF3-1c – 500 ml RPMI, 10% foetal bovine serum (FBS) 50 µM L-glutamine, 100 U/ml penicillin G, 50 µg/ml streptomycin (ThermoFisher Scientific, UK) and supplemented with 2 ng/ml IL-3 (R&D Systems, UK)

NIH3T3- 500 ml DMEM (Dulbecco's modified eagle's medium - Gibco Lifesciences, UK), 10% FBS and 50 µg/ml streptomycin

HUVEC - Endothelial media kit 2 (Promocell, UK), 10% FBS, 50 µg/ml streptomycin

Starvation Media – 500 ml DMEM, 50 µg/ml streptomycin, 0.1% BSA (Sigma, UK)

Chapter 3 – Purification and Characterisation of Heparin By-Products

3.1 Aims

The aim of the work described in this Chapter was to purify and characterise by-products from the production of porcine Hp. Four samples were obtained as by-products from different stages in the production of Hp (Shandong ChenZhong Biopharma, China). These by-products are usually discarded at the point they are produced, as the progressive removal of other contaminating species allows the retrieval of pharmaceutical grade Hp before LMW species are generated. Following the characterisation of the HS/Hp content via several methods, samples were compared to porcine mucosal Hp (PMH, Celsus, USA) as a representation of commercially available Hp, from a reputable company with batch identification. It was hypothesised that HS/Hp fractions removed from later stages in the process would have characteristics more similar to Hp, for example being highly sulfated.

3.2 Introduction

3.2.1 Background of Hp and LMWH Production

As mentioned previously, the full details of the production of pharmaceutical Hp is highly guarded proprietary information. The practice has undergone some changes over the years, primarily due to the sourcing of the material changing predominantly to porcine intestine and away from bovine intestine or lung. Bovine sources largely fell out of favour in the 90's, except in South America and has since been limited in its use, due to bovine encephalopathies which could potentially be in batches of Hp (Linhardt and Gunay, 1999). However, as a source, bovine Hp may potentially be making a comeback owing to a perceived need to diversify sources, primarily due to a reduction in the availability of porcine material after the Hp crisis of 2008. With the increasing demand placed on a limited number of species, contamination from animal sources will always be potentially problematic, until more rigorous analysis of pharmaceutical batches for contaminants can be established. Using current purification methods there is a need to successfully remove and check for other GAGs such as CS/DS which can co-purify with Hp, or for intentionally altered products, until the synthetic production of Hp is able to meet demand (Laveran *et al*., 2009).

The preparation of the material is summarised in Figure 3.1. There are 4 main steps in the production from tissue to final product.

1) The preparation of tissue.
2) Extraction and recovery of raw Hp.
3) Purification of the raw Hp.

4) Recovery of the clean Hp product.

The following method outline (Fig 3.1) has been provided by Shandong ChenZhong Biopharma (China) who have also provided the by-product samples used throughout this project.

The preparation of raw material usually takes place at the slaughterhouse; this includes removing the endothelial lining from the intestinal lumen.

Using high temperature and pressures, GAGs are solubilized in purified water in batches of ~100 kg. After dissolving, the material is filtered to remove any large debris.

Proteolytic digestion occurs over a 5 hour time period. The solution is then heated to 90°C with an increase in pH to kill the enzyme and also remaining bacteria. The first oxidation and ethanol precipitation step produces the first by-product sample, M1 (Fig 3.1).

GAGs bind to positively charged anion exchange beads which are added at this stage and the loaded beads are transferred into a good manufacturing practice (GMP)-compliant laboratory. Dissociation of GAGs from the beads occurs by applying an increasing concentration of salt. At this point, the volume of the sample is around 700 L, which is doubled to reduce the concentration of the salt for further steps. A second precipitation is where the second by-product sample, -D1, is removed. In quick succession, nanofiltration and a second precipitation occurs and this is where by-product F1 is removed.

Heavy metals are removed with the addition of silica and this is followed by oxidation of the solution using 30% hydrogen peroxide. Oxidation bleaches the sample to leave a whiter product, whilst also working as a sanitation step.

Following wash steps, adding acid and neutralising with a base are repeated to remove any remaining protein. Ethanol precipitation and a further oxidation step give rise to the final by-product sample, H. Continual repeats of the above step lead to the production of Hp sodium, which is pharmaceutical grade unfractionated Hp (UFH).

For the subsequent production of LMWH, partial depolymerisation is required. For example, for enoxaparin production a secondary intermediate is produced before being dissolved and an esterification step precedes another precipitation step with anhydrous sodium acetate and ethanol. Alkaline depolymerisation by the addition of sodium hydroxide occurs before several rounds of precipitation, oxidation, ultrafiltration and lyophilisation finally gives rise the LMWH final product.

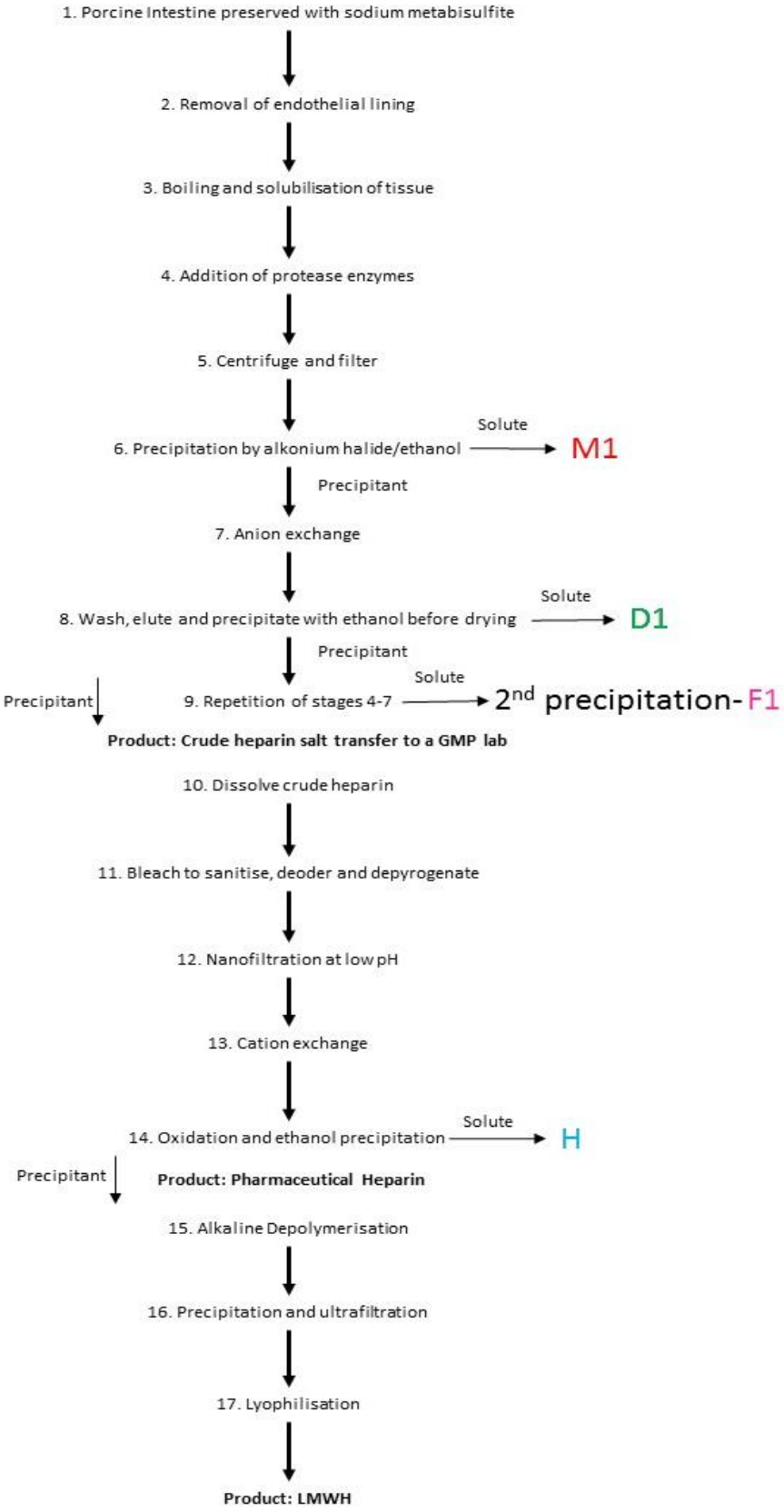

Figure 3.1- A flowchart depicting the major steps of the production of pharmaceutical Hp and LMWH. The production from porcine intestine at a slaughterhouse to final pharmaceutical Hp and LMWH, involves a clean-up process with multiple steps to ensure that all contaminants are removed, providing final products pharmaceutical grade for human use.

3.2.2 Background to Characterisation of the By-Products

Currently, commercial research grade Hp/HS does not undergo vigorous characterisation and products have recently been shown to vary greatly in their composition (Mulloy, 2016). However, there has been an increase in testing and maintenance of higher standards for pharmaceutical Hp since the contamination with exogenous oversulfated CS, which in 2008 led to adverse effects and the death of several hundred patients worldwide (WHO, 2008). Along with this obvious issue for clinical usage, there is also a need for consistency in products used for scientific research. Following this, well documented techniques published from our laboratory and others, have been used to identify HS related structures and to also ensure the removal of contaminating species.

Digestion with the full complement of heparinase enzymes gives rise to disaccharides which can be compared to known, authentic structures. Heparinase I and III, in particular, have preferred substrates and therefore give rise to specific disaccharides (Table 3.2). The products of digestion are typically separated over a strong anion exchange column using a sodium chloride (NaCl) gradient, displacing the negatively charged disaccharides from the beads. HS composition has been used by several laboratories to compare samples with reference to the 8 known major disaccharides (Table 3.3). A method employing UV detection at 232 nm identifies the unsaturated bond at the non-reducing end of the original glucuronic/iduronic acid (termed ΔUA products), with the ability to detect quantities as low as ~1 μg in mixtures of starting material (Turnbull *et al.*, 1999). The production of this unsaturated double bond during digestion causes the loss of identity between glucuronic and iduronic acid, therefore this monomer is referred to simply as ΔUA in compositional analysis (Linhardt *et al.*, 1988). More recently other methods have been developed which have increased sensitivity to small amounts of material. Labelling the disaccharides with fluorophores such as BODIPY FL hydrazide, makes HS extraction and analysis from tissue possible based on low fmol range of detection permitting use of ng quantities of starting material (Skidmore *et al*., 2006 & 2010). Fluorophores are generally tagged onto the reducing end of the disaccharide by a reaction with a nitrogen containing functional group and the carbonyl group of the disaccharide (Deakin and Lyon, 2008), also known as a Schiff's base reaction (see Figure 3.2). These are detected by fluorescence rather than UV (for example BODIPY, Ex 488 nm and Em 520 nm) (Skidmore *et al*., 2010).

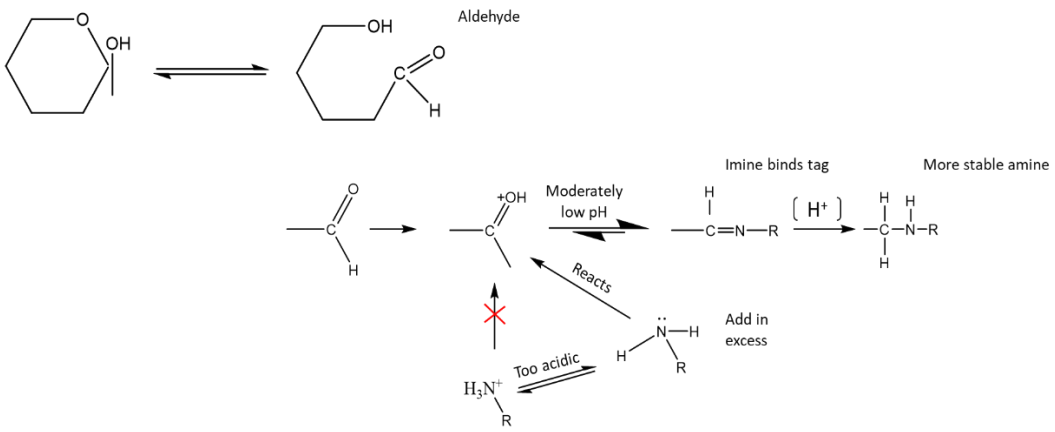

Figure 3.2- A diagrammatic representation of a Schiff's base reaction. A Schiff's base reaction forms an imine group at the reducing end of the sugar with the amine group of the fluorophore tag. In conditions which are too acidic, excess protons are available, lone pairs become no longer available on the nitrogen and more stable but unreactive ammonium ions are formed.

Nuclear magnetic resonance (NMR) is frequently used to identify HS related structures in complex mixtures. Selective observation of the material via ^{13}C and ^{1}H NMR are very informative techniques to quantify and identify structures contained within the samples. Insights into altered sulfation/N-acetylation patterns, uronic acid content and even ring conformations allow different compounds to be compared (Mulloy *et al.*, 1993). More information can be gleaned when these NMR techniques are used in combination, for example, heteronuclear single quantum coherence spectroscopy (HSQC), where 2D peaks are produced that have both volume and height. These provide improved resolution and are more informative when exploring quantities of a specified structure, they can be used to compare directly with compositional analysis providing more power to the analysis (Yates *et al.*, 1996). Other methods in general, like mass spectroscopy of samples alone, are impracticable in these circumstances due to it not being a fully quantitative method.

3.3 Methods

3.3.1 Clean-up of Crude By-Products and Recovery of HS

20 g of each crude by-product sample was dissolved in 100 ml of chondroitinase buffer. Samples were incubated until dissolved and fluid, losing their gelatinous form. For chondroitinase digestion samples were incubated with 500 mU of chondroitin ABC-ase (Sigma-Aldrich, UK) overnight at 37˚C (all subsequent incubations are at 37˚C). After 24 hours, 20 ml of 5x DNase buffer was added to the sample and in the presence of 500mU DNase and incubated for a further 4 hours. Further overnight digestions with 250 mU RNase in 20 ml of standard 5x RNase buffer and subsequently 280 U of Pronase in 20 ml of 5x buffer followed (Table 3.1).

Step	Enzyme	Final Buffer Concentrations	Incubation time
1	Chondroitin ABC-ase	100 ml – 100 mM TAE, pH 8	Overnight
2	DNase	20 ml – 10 mM TAE (pH 7.5), 25 mM $MgCl_2$, 0.5 mM $CaCl_2$	4 hours
3	RNase	20ml – 10 mM TAE (pH 8), 5 mM EDTA, 8 mM NaOAc	Overnight
4	Pronase	20 ml – 10 mM TAE (pH 8), 10 mM $Ca(OAc)_2$	Overnight

Table 3.1 – A table showing the sequential conditions for enzymatic clean-up of by-product samples.

HS was separated from the subsequent products of enzymatic digestion by weak anion exchange chromatography on diethylaminoethanol (DEAE) beads (either in a 5 ml prepacked DEAE column, or beads self-packed into a 20 ml column or batch preparation in 50 ml Falcon tubes) (beads and columns - GE Healthcare, UK). 10 column volumes of 0.01 M phosphate buffered saline (PBS- Sigma, UK) and 100 ml of 0.3 M NaCl (ThermoFisher Scientific, UK) were used to clean the column of all unbound non-HS products, HS was eluted with 100 ml of 2.0 M NaCl.

To remove the salt, the sample was dialyzed in tubing (ThermoFisher Scientific, UK) with a 3.5 kDa cut off over a 24-hour period with two 5 L changes of ddH_2O.

A rotary evaporator (Heidolph Labarota 4000 Efficient, Sigma, UK) was used to reduce the volume of the sample to ~5 ml before it was freeze dried completely. Samples were weighed to calculate the mass of HS obtained from the initial crude samples

3.3.2 Sizing of Initial By-Product Samples

16 mg of a clean, intact sample were separated on a Superdex 30, 16/60 column at 0.5 ml/min in ddH_2O. Products were identified by UV at 232 nm. The column was calibrated with dextrans of known size (16230, 11600, 9980 and 7200 Da – American Polymer Standards Corporation, USA) under the same conditions.

50 mg of 4 dextrans were separated on the same column as the by-products and 1 ml fractions were collected. These, unlike HS/Hp, do not have an unsaturated double bond chromophore and therefore cannot be detected by UV. However, due to the quantity used and the water running buffer, dextrans can be identified by freeze drying the samples completely, where they are then visible and the peak maxima was identified by weighing.

From previous work it has been established that a 1.6 cm diameter column of length 60 cm, will separate Hp and samples partially enzymatically digested from size 2-20mer, using Superdex 30 beads (GE Healthcare), which are robust and consistent in their separation (Powell *et al.*, 2010).

3.3.3 Analysis of Sulfation Levels of Purified Intact By-Products by Weak Anion Exchange Chromatography

For analytical purposes 200 µg of intact, clean sample was separated on a 1 ml Hitrap Q HP column (GE Healthcare, UK) over a 45 min programme set with two column volume washes of 0.5 M NaCl followed by a step gradient of 0.5, 1.0, 1.2, 1.4, 1.6, 2M NaCl (10 ml of each) following a protocol similar to Griffin *et al*. (1995). Peaks were detected by following the increase in UV absorbance at 232 nm with the expectation that peaks would be visible across the range of NaCl concentrations, with more highly sulfated structures eluting at higher concentrations.

3.3.4 Compositional Analysis of By-Products by Digestion with Heparinase I, II and III

Following clean-up of the by-products they were solubilised in heparinase buffer to make a solution of 10 mg/ml. 200 µg of by-products were digested with 2.5 mU of heparinase III, I and II (IBEX, Canada) added sequentially at 2 hour intervals, with heparinase II left incubating at 37˚C overnight. Addition of the same amount of all three heparinases were then

left to incubate for 2 hours the following day, to ensure samples were digested to the fullest extent of the enzyme (Appendix 1.A); the addition of more enzyme did not elicit any different products (data not shown).

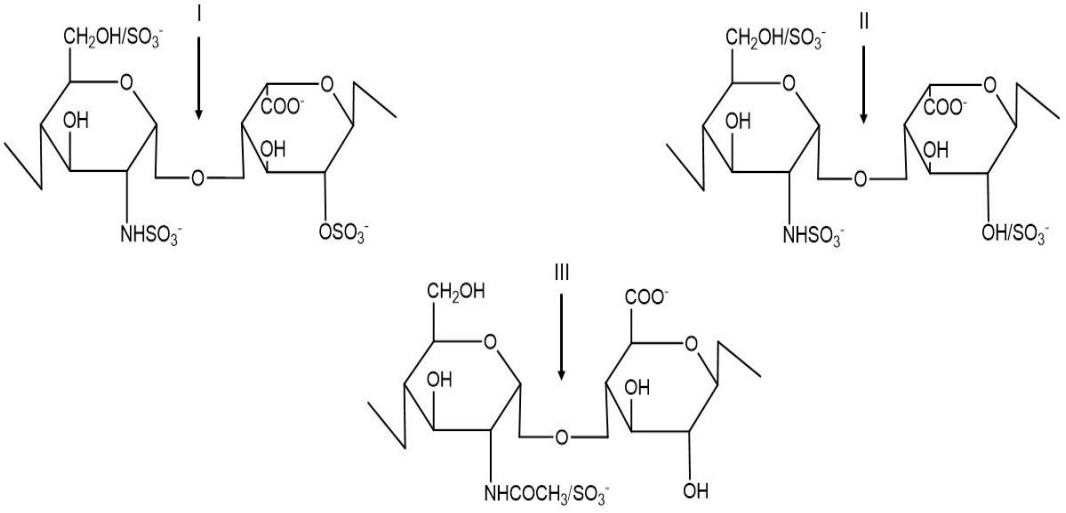

Heparinase	Size	Principal glycosidic cleavage site	Preferred substrate?
I	43 kDa	GlcNS(±6S)α(1-4)IdoA2S	Heparin
II	86 kDa	GlcNAc/NS(±6S)α(1-4)GlcA/IdoA	Both
III	74 kDa	GlcNAc/NS(±6S)α(1-4)GlcA	HS

Table 3.2 - Heparinase enzymes have substrate preference along the saccharide chain. Digestion of 200 µg of by-products with addition of 2.5 mU of individual enzymes at 2 hour intervals, depolymerises the HS chain producing constituent disaccharides. The digestion of the chain leaves unsaturated double bonds, which can be detected by UV at 232 nm, allowing for the disaccharides identification (Linhardt *et al.,*1986; Linhardt *et al.,* 1990).

The products of digestion were then separated according to charge on a Propac PA1 column (4 mm diameter x 250 mm length- Dionex, UK), eluted with a linear gradient of 0-2 M NaCl, over 60 mins at 1 ml/min. Product peaks were detected by UV at 232 nm and samples were compared to 8 disaccharide standards of known structure (Table 3.3 - Dextra Labs, UK) also separated on the same column, under the same conditions.

Peak (in elution order)	Structure
1	Δ-UA-GlcNAc
3	Δ-UA-GlcNS
2	Δ-UA-GlcNAc(6S)
7	Δ-UA(2S)-GlcNAc
4	Δ-UA-GlcNS(6S)
5	Δ-UA(2S)-GlcNS
8	Δ-UA(2S)-GlcNAc(6S)
6	Δ-UA(2S)-GlcNS(6S)

Table 3.3- The structure of 8 standard disaccharides used for HS/Hp comparison. These 8 standards have defined structures and elute in a reproducible order.

3.3.5 HSQC NMR

HSQC NMR of the by-products were run by Dr Timothy Rudd (NIBSC, UK) and subsequent analysis was conducted by the thesis author. The Hp and by-product samples were prepared by dissolving 20 mg of each in 0.6 mL of 0.15 mM TSP (trimethyl-silyl-3-propionic acid) solution in deuterium oxide. Spectra were recorded on a Bruker AVIII-600 instrument operating at 600.13 MHz (Bruker, Germany). $^{1}H–^{13}C$ HSQC experiments were acquired with 16 scans for 320 increments in the F1 dimension. The matrix size 1 k × 512 was zero filled 2 k × 1 k by application of a squared cosine function prior to Fourier transformation. The samples were held at a temperature of 298 K during data acquisition. Line broadening of 1.0 and 0.3 Hz, respectively, for F2 and F1, were applied before Fourier transformation and data sets were processed using TOPSPIN 3.1 (Bruker, Germany).

3.3.6 Carbon-13 NMR

Carbon-13 NMR was run by Dr Igor Barsukov (Liverpool University, UK). All spectra and analysis of scans were conducted by the thesis author. 20 mg of clean samples were dissolved in 0.7 ml of deuterium water (Sigma-Aldrich, >90% D, UK), particulate matter was removed by centrifugation (13,000 RPM, 5 mins) and the sample then placed in a 5 mm NMR tube. One dimensional ^{13}C spectra were recorded at 313K on a Bruker 600 MHz spectrometer (Bruker, Germany) with TSP as the external reference (0 ppm). Data sets for all spectra were processed in Mestrenova (Mestrelab, Spain). Signals were assigned according to the literature (Casu *et al*., 1994; Yates *et al*., 1996).

3.4 Results

3.4.1 DEAE Recovery of HS

Following the initial crude clean-up of the digested products, HS was separated from the products of digestion by using weak anion exchange DEAE beads. Several methods were tested to develop a method providing the maximum yield of HS from the sample. Figure 3.3 showed the recovery in milligrams of HS from an initial starting 20 g. Methods were developed which included using the purchased DEAE Hitrap columns, packing DEAE Sephacel beads into a column and finally batch adding samples to 50 ml falcon tubes containing 20 ml of initial DEAE bead material in 20% ethanol (which was removed before the sample was added). From Figure 3.3 it is clear that batch purification provided the best yield. The DEAE 5 ml Hitrap column recovered around ~300mg (1.5%) of material, this yield was increased to ~1.5 g (~7.5%) in 20 cm self-packed DEAE-Sephacel columns. Finally, large quantities of samples D1 and F1 were purified using batch DEAE and this method recovered 3.5 g per 20 g of crude material (~15%).

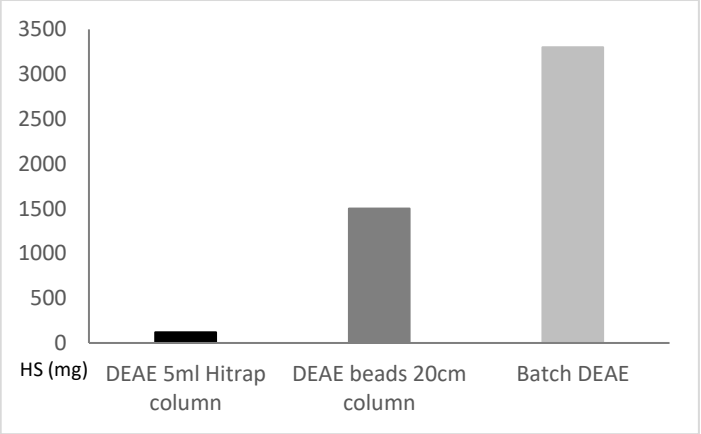

Figure 3.3- Comparative yields of HS by-products from alternative DEAE purification methods. HS bound to DEAE beads was eluted by washing with 2 M NaCl using three methods to assess the recovery yields of HS for subsequent work (n=1)

3.4.2 Sizing of Intact By-Products

Following the initial enzymatic clean up, 16 mg of each sample was separated on Superdex 30 beads packed into a 16 mm/60 cm column. Samples were run according to the method above in ddH_2O and identified by UV at 232 nm. The column was also calibrated

using dextrans of known molecular weight, allowing a tentative size to be assigned to each of the samples.

Dextran samples with known molecular weights; 16230, 11600, 9980 and 7200 were found to primarily elute at 1ml, 40, 52 and 90 ml, respectively. From this a calibration curve was used to assign molecular weights to each of the samples (Figure 3.4). It must be noted the Hp was not homogenous in its elution and was identified in a broad peak from 35-90 ml, with ~50% of the material having eluted by 70 ml (~12000-9000 Da- Appendix 2). This is consistent with the known typical molecular weight of UFH, confirming the validity of the molecular weight determination (Mulloy *et al.,* 2010). The peak maxima for samples M1, D1 and F1 were all around 40 ml (40-45 ml). From the calibration, it can be seen that the dextran of molecular weight ~11,600 elutes at approximately the same volume, suggesting that these samples are around 11,500-12,000 Da (Figure 3.4). Sample H was by far the smallest of the by-products with peak maxima elution at ~70 ml and a tentative value of ~8800 Da was assigned (Table 3.4 & Appendix 2.B).

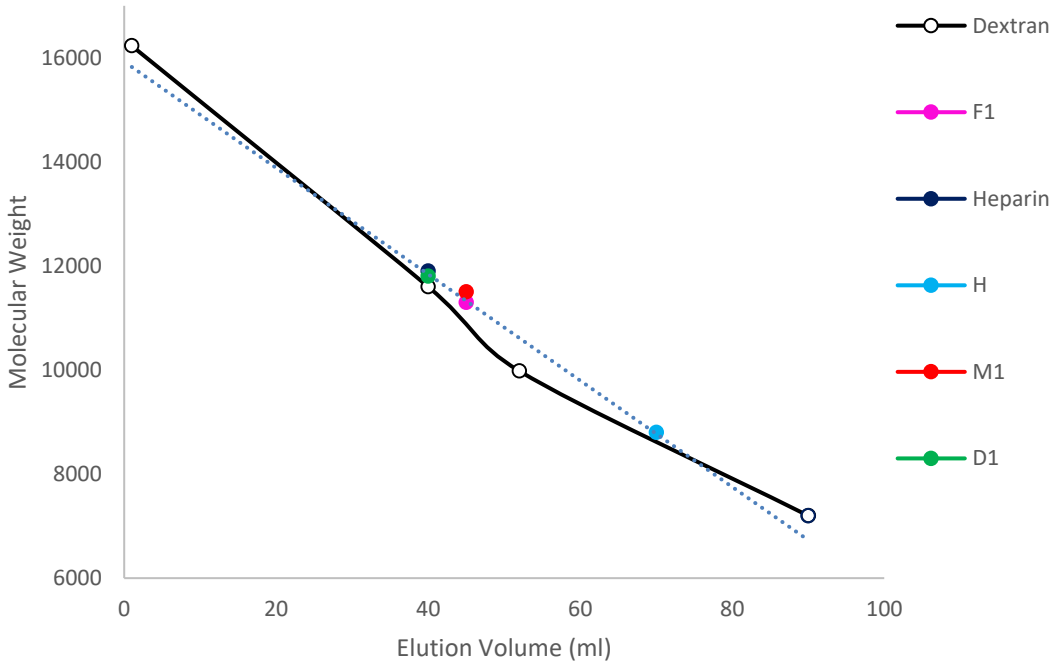

Figure 3.4 – Superdex 30 gel filtration chromatography of purified intact HS by-products. 16mg of four dextrans of known size; 16230, 11600, 9980 and 7200 Da were separated in ddH_2O on a Superdex 30, 16/60 column. All by-products and Hp were separated using the same method and tentatively assigned a molecular weight based on the calibration curve line of best fit produced by the elution of the dextrans.

Sample	Size (kDa)
Hp	**9-12**
H	**8.8**
M1	**11.5-12**
D1	**11.5-12**
F1	**11.5-12**

Table 3.4 – Hp and by-products were assigned a molecular weight after separation on a 16/60 Superdex 30 column. 16 mg of purified, intact by-product and Hp were separated in ddH_2O over a 45 min programme at 0.5ml/min, samples were detected by UV at 232 nm. By-products and Hp were assigned a size after comparison to elution times of dextrans of weight 16230, 11600, 9980 and 7200 Da (see appendix 2 for further details).

3.4.3 Determining Approximate Sulfation Levels by Weak Anion Exchange Chromatography

After the crude clean up phase, 200 µg of intact by-products were separated on a Hitrap Q column (weak anion exchange). Samples were separated using a 0-2 M NaCl gradient in steps of 0.5 M, followed by 0.2 M at a flow rate of 0.5 ml/min; peaks were detected with UV at 232 nm. The initial analyses of the crude by-product material were used to compare the relative levels of sulfation in the intact samples to that of Hp. Hp, is known to be highly sulfated (~2.5 sulfates per disaccharide). Therefore, it is unsurprising that it elutes almost entirely at the higher salt concentrations, 1.8-2 M, as has been observed previously in many studies, with some initial material eluting at 0.5 M (Figure 3.5).

From an overview of the by-products, it is evident that H is the most homogenous, when separated via weak anion exchange, but has a very different elution pattern to Hp, with a large proportion of product being eluted between 1-1.2 M and the rest at 2 M NaCl, this data suggests that it contains primarily chains with large proportions of low-moderate levels of sulfation and moderate proportions of higher levels, with negligible material eluting between ~1.5-1.9 M.

In comparison D1 and F1 have an even distribution of products across multiple concentrations, but peaking primarily between 1.4-1.6 M, suggesting an even proportion of low and high levels of sulfation, and a large proportion of moderately sulfated chains, within the intact material.

M1 appeared to have a large proportion of material that elutes early, between 1-1.4 M, suggesting that it is less sulfated than Hp and H, but moderately sulfated like D1 and F1.

Thus far, as expected, none of the samples appear to show a close resemblance to Hp or to be as highly sulfated. This will be explored further by digesting the intact chains into their constituent disaccharides and then separating them by SAX-HPLC for compositional analysis, and also by NMR analysis later in this Chapter.

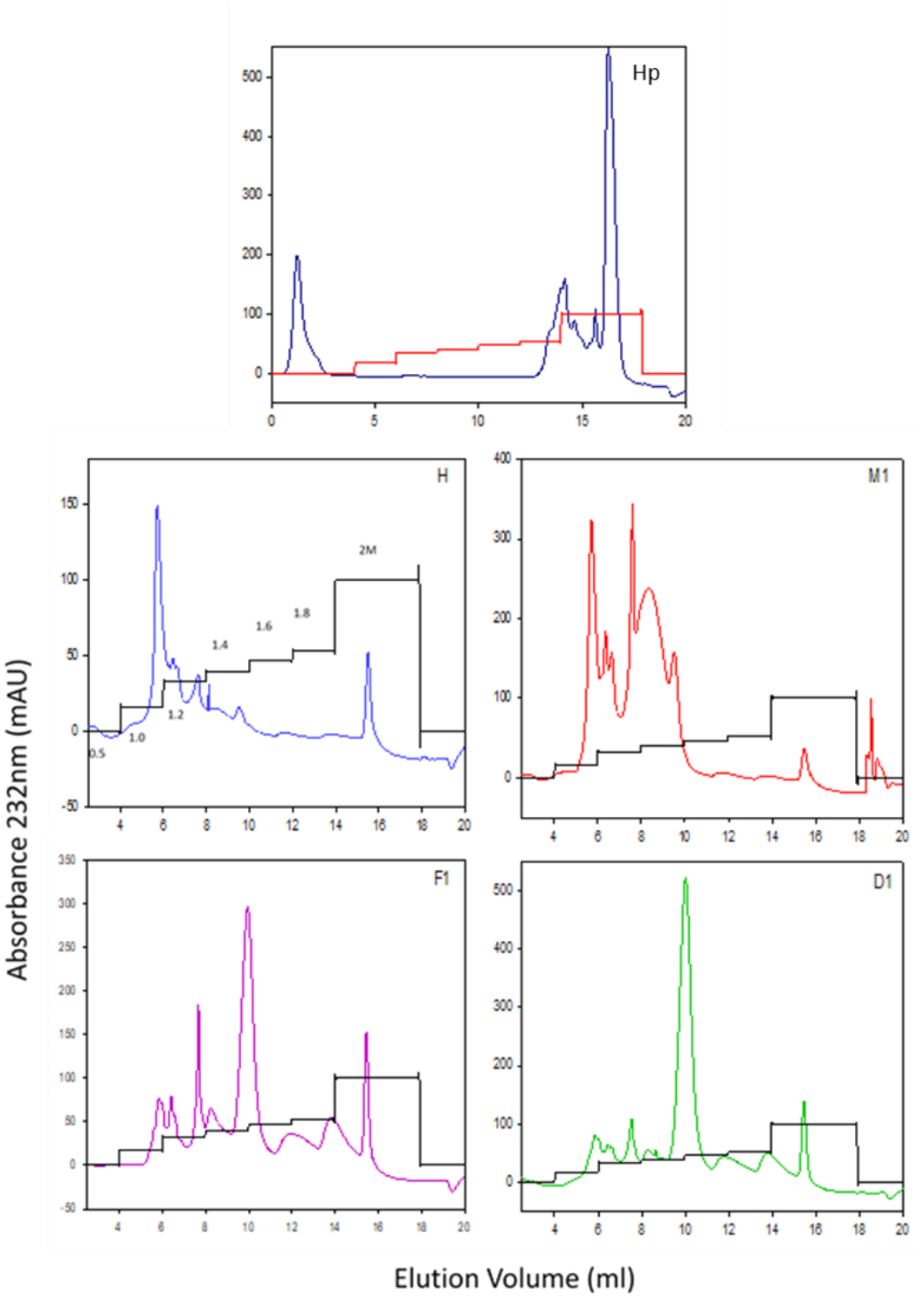

Figure 3.5- Weak anion-exchange chromatography of Hp and by-products. 200 µg of Intact samples were separated by a step increase in concentration of NaCl, 1.0, 1.2, 1.4, 1.6, 1.8 and 2 M (black/red line is conductance) at a flow rate of 0.5 ml/min, samples were detected by UV at 232 nm.

3.4.4 Compositional Analysis

Following clean-up, the samples were fully digested using heparinase I, II and III enzymes, derived from *Flavobacterium heparinum* (IBEX, Canada). Enzymatically digested samples were separated on a Dionex Propac PA-1 column (GE Healthcare, UK), using a 0-2 M NaCl gradient over 60 minutes, and products were detected by the unsaturated C=C double bond by UV at 232 nm. A set of authentic disaccharide standards of known structure were also separated under the same conditions and used to identify structures in test samples by overlaying chromatographs (Figure 3.6). However, L-iduronic and D-glucuronic acid yield the same unsaturated residue after lyase digestion, so although this is a sensitive method for analysis, the identity of the original non-reducing terminal uronic acid is lost (Linhardt *et al*., 1990). Initially for compositional analysis, the percentage peak area for each disaccharide structure was calculated and the means ± SEM are shown in Figure 3.7. A table of the data is given in Appendix C.1.

Multiple grouped t-tests were carried out on data from all samples compared to Hp as a control (Table 3.5). Sample H has significantly more mono-sulfated Δ-UA-GlcNS (P=0.0001), as well as the di-sulfated disaccharides Δ-UA(2S)-GlcNAc(6S) (P=0.004) and Δ-UA(2S)-GlcNS (p=0.004) than Hp. The other disaccharide structures do not vary significantly to Hp and comparatively the compositional analysis suggests that H, overall, is the most similar in its sulfation patterns to Hp.

M1 from its composition is the next most similar to Hp, with significant changes seen in an increase of the mono-sulfated Δ-UA-GlcNS and Δ-UA-GlcNAc(6S) structures ($p<0.0001$ and p=0.003, respectively). An increase in the di-sulfated disaccharide Δ-UA(2S)-GlcNAc(6S) (p=0.003) is also evident. These results indicate that M1 is less sulfated than Hp, as not only does M1 display an increase in mono- and di-sulfated structures, M1 showed a near statistically significant decrease in the most sulfated disaccharide, Δ-UA(2S)-GlcNS(6S) compared to Hp (p=0.069).

F1 differs greatly in its structure compared to Hp, with the levels of 6 of the 8 disaccharides being significantly different. A large decrease is seen in the level of tri-sulfated disaccharide when compared to Hp (p=0.0001). However, F1 does show statistically significant increases in all of the other disaccharides except Δ-UA-GlcNAc and Δ-UA-GlcNS(6S), indicating that it is markedly lower in its overall sulfation than Hp. In the order in which they elute, F1 has an increase in the following structures; mono- Δ-UA-GlcNS p=0.003,

Δ-UA-GlcNAc(6S) p=0.01, Δ-UA(2S)-GlcNAc p=0.001, for both di-sulfated Δ-UA(2S)-GlcNS and Δ-UA(2S)-Glc(6S) p<0.0001.

D1 is also structurally different to Hp, with significant differences seen in the full range of disaccharides. Although it has the largest overall differences compared to Hp, compositional analysis does not suggest D1 is less sulfated than Hp. D1 showed a significant decrease in the tri-sulfated disaccharide compared to Hp (p=0.003), it also showed a sizeable decrease in the level of the un-sulfated Δ-UA-GlcNAc disaccharide (p=0.01) and a decrease in Δ-UA-Glc-NS(6S) (p=0.002). D1 showed a significant increase in all other structures including; all three mono-sulfated disaccharides (in the order in which they elute p=0.002, 0.05, 0.0004), di-sulfated Δ-UA(2S)-GlcNS (p=0.0004) and Δ-UA(2S)-GlcNAc(6S) (p=0.01).

D1 and F1 were also compared since they were the samples taken forward for further investigation in Chapters 4, 5 and 6. There are a few significant structural differences to be noted between these samples. D1 has a higher level of tri-sulfated residues (p=0.0004) but a reduction in both di-sulfated Δ-UA-GlcNS(6S) and Δ-UA(2S)-GlcNAc(6S) structures (p=0.0005 and p<0.0001, respectively). This could potentially suggest that D1 is overall more sulfated than F1, but F1 contains a general higher level of di-sulfated disaccharides compared to D1, making them structurally distinct.

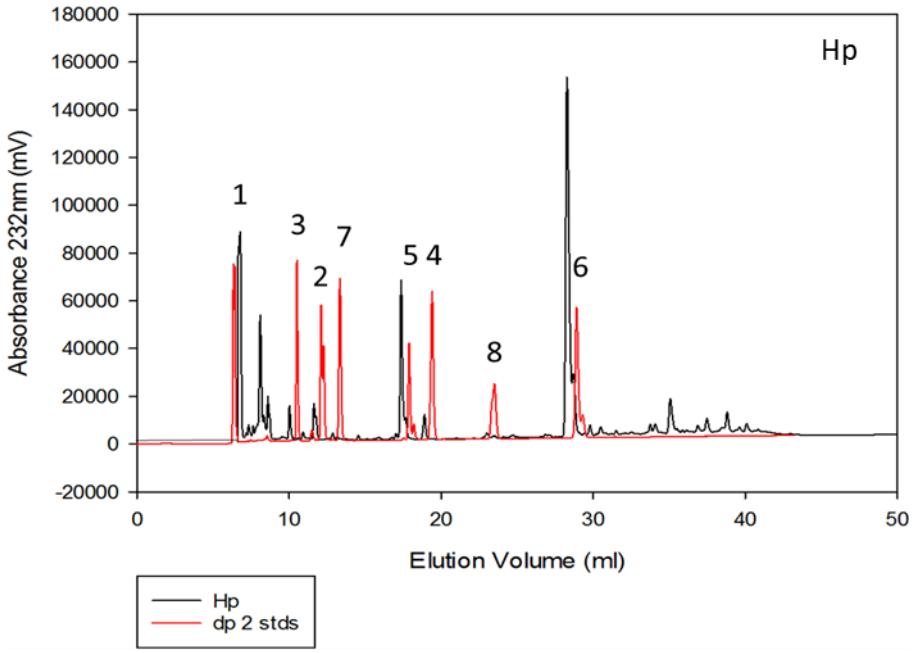

Figure 3.6 –SAX-HPLC analysis of Hp and standards. 200 µg of the by-products of digestion were separated over an hour long linear gradient of 0-2 M NaCl, at 1 ml/min and products were identified by UV at 232 nm. A set of 8 known authentic disaccharide structures were also run under the same conditions and these were used to identify peaks from the samples. In the order in which they elute 1- Δ-UA-GlcNAc, 3- Δ-UA-GlcNS, 2- Δ-UA-GlcNAc(6S), 7- Δ-UA(2S)-GlcNAc, 4- Δ-UA-GlcNS(6S), 5- Δ-UA(2S)-GlcNS, 8- Δ-UA(2S)-GlcNAc(6S) and 6-Δ-UA(2S)-GlcNS(6S).

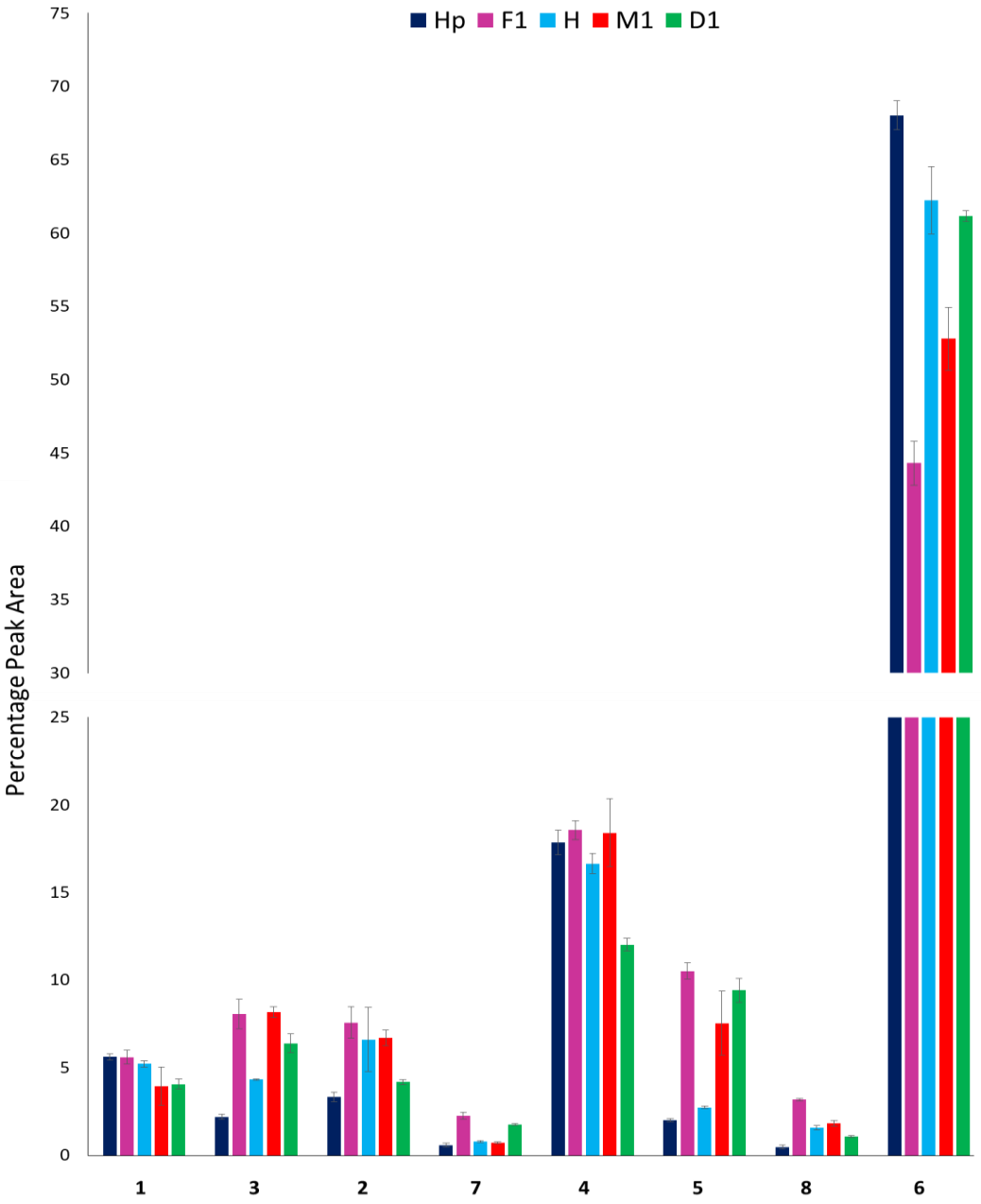

Figure 3.7- Disaccharide analysis of Hp and by-products. Following enzymatic digestion with heparinase I, II and III samples were separated on a Dionex PA-1 column (GE Healthcare, UK) over a 0-2 M NaCl gradient, at a flow rate of 1 ml/min and products were identified by UV at 232 nm. A set of 8 known structures were also run under the same conditions and these were used to identify peaks from the samples (Table 3.3). Percentage peak areas were calculated for each sample, along with the SEM and multiple t-tests comparing heparin to the other samples (P=0.05, n=3).

Peaks	1	3	2	7	4	5	8	6
F1		0.003	0.01	0.001		< 0.0001	< 0.0001	0.0002
H		0.0001				0.004	0.004	
M1		< 0.0001	0.003				0.003	
D1	0.01	0.002	0.05	0.0004	0.002	0.0004	0.01	0.003
F1vD1	0.03		0.02		0.0005		< 0.0001	0.0004

Table 3.5- P values from t-tests for the disaccharide composition of by-product samples vs Hp or F1 vs D1. Red indicates a statistically significant decrease and green and increase.

The compositional analysis data was used to compare the percentage of sulfate groups in each sample, highlighting a further level of analysis compared to that at the individual disaccharide level (Figure 3.8a). Analysing the data by the number of sulfate groups, e.g. percentage of un-, mono-, di- and tri-sulfated disaccharides, showed that all of the samples are significantly different to Hp (Table 3.6). This analysis suggests that D1 still maintains the greatest difference when compared to Hp, with an overall increase in the mono- and di-sulfated structures (p=0.001) but a decrease in both the un-sulfated and tri-sulfated residues (p=0.01 and 0.003, respectively). F1 showed a difference in a range of structures, with increases in un- (p=0.01) and mono-sulfated (p=0.001) structures and a decrease in tri-sulfated (p=0.002). M1 showed only one statistically significant difference with an increase in overall mono-sulfated disaccharides (p=0.0005). However, a decrease in the tri-sulfated disaccharide approaching statistical significance signifies that it may be less sulfated than Hp, (p=0.069). Overall, these results suggest that H is still the most structurally related sample to Hp, with only a significant increase in the mono-sulfated structures (p=0.04) and no other notable results approaching statistical significance.

As the disaccharide composition indicated, F1 has significantly increased levels of all structures except for the tri-sulfated disaccharide when compared to D1. This is in line with previous comparisons to Hp suggesting D1 to be moderate to highly sulfated (tri- p=0.0004 - F1 increase in NA p=0.03, mono- 0.01 and di- 0.0003).

When looking at the overall levels of specific types of sulfation - 2-O, 6-O, N-sulfation and unsulfated residues (Figure 3.8b), F1 has the most appreciable differences, having a decrease at all levels of sulfation compared to Hp (NS p<0.0001, 2S p=0.004 and 6S p<0.0001), and also showing an increase in unsulfated residues (p=0.003 – Table 3.7). This data further supports the evidence that it contains lower overall sulfation compared to Hp. Surprisingly it is M1 rather than H that more closely represents Hp in this analysis, with no significant results and only one approaching significance, a decrease in 2S (p=0.068). Both H and D1 show

similar differences when compared to Hp, as both contain significantly less N- (p=0.05 and p=0.0003) and 6-O sulfation (p=0.0005 and p<0.0001).

Perhaps unsurprisingly when comparing D1 and F1, D1 was found to contain significantly more sulfated residues in all 3 sulfation positions; NS (p=0.002), 2S (p=0.002) and 6S (p=0.01) and therefore still appeared to be overall more sulfated; this was further supported during this analysis as F1 contains significantly increased levels of un-sulfated NA residues (p=0.006).

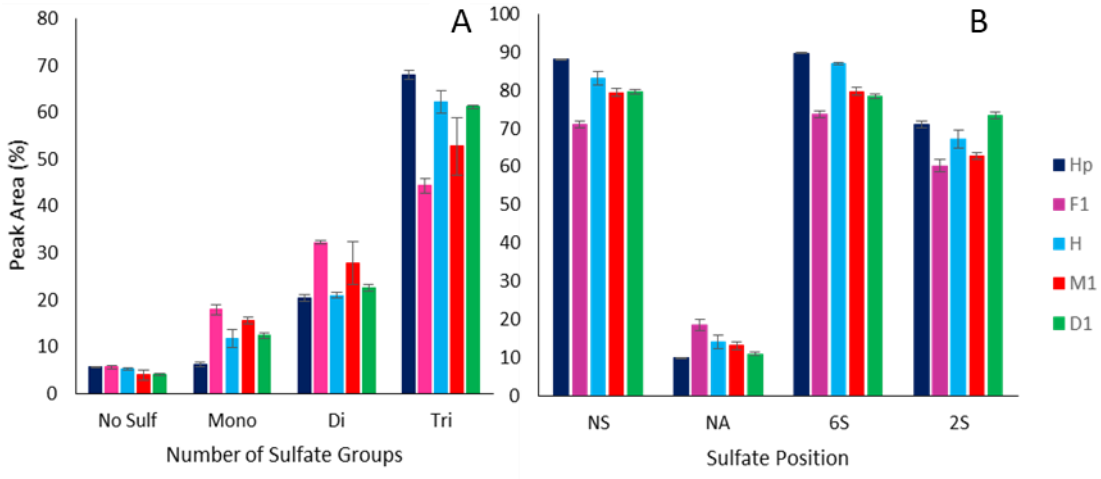

Figure 3.8- Analysis of sulfation levels and types from disaccharide composition data. From the same data used in Figure 3.6 percentage peak areas for each sample were grouped into categories to determine other structural compositions. Figure 3.8a percentage peak areas for no sulfates (1), mono- (3,2,4), di- (5,7,8) and tri- (6) were calculated, with mean and SEM. Multiple comparison t-tests (P=0.05, n=3) between all sample vs Hp and F1 vs D1 were carried out. Figure 3.8b percentage peak areas were grouped to look at the placement of sulfate groups; NS (3,4,5,6), NA (1, 2, 7,8), 2S (7, 5, 8. 6) and 6S (2, 4, 8, 6) were calculated, with mean and SEM. Multiple comparison t-test (P=0.05, n=3) comparing all samples vs Hp and F1 vs D1.

Sulfs per disaccharide	0	1	2	3
F1		0.0005	0.0001	0.0002
H		0.04		
M1		0.0005		
D1	0.01	0.001		0.003
F1vD1	0.03	0.01	0.0003	0.0004

Table 3.6- P values from t-tests for numbers of sulfates per disaccharide of by-products compred to Hp or F1 vs D1. Red indicates a statistically significant decrease and green and increase.

Structure	NS	NA	6S	2S
F1	< 0.0001	0.003	< 0.0001	0.004
H	0.05		0.0005	
M1				
D1	0.0003		< 0.0001	
F1vD1	0.002	0.006	0.01	0.002

Table 3.7 – P values from t-tests for types of sulfation of by-products compared to Hp or F1 vs D1. Red indicates a statistically significant decrease and green and increase.

Finally, when the average number of sulfates per disaccharide were compared, although both D1 and H on average show similar levels of overall sulfation to Hp (~2.2 vs ~2.0), statistical testing showed that D1 contains significantly lower levels of sulfation per disaccharide than Hp (p=0.003) and although approaching significance H still maintains the same level of sulfation on average (p=0.08). F1 appeared to be the least sulfated of the group (1.6 – p=0.0002 (vs Hp), p=0.0005 (vs D1)), closely followed by M1 (~1.8).

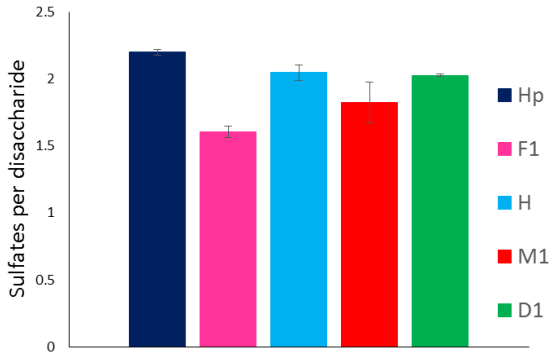

	Hp	F1	H	M1	D1
Sulfates per disaccharide	2.2	1.6 p=0.0002	2.0	1.8	2.0 p=0.003

Figure 3.9- Average number of sulfates per disaccharide in Hp and by-products. Values were calculated from each sample triplicate values from Figure 3.7. The SEM was calculated and all samples were compared via multiple t-tests (P=0.05, n=3) to Hp or F1vsD1. Red indicates a statistically significant decrease compared to Hp.

3.4.5 HSQC NMR

HSQC NMR has frequently been used to elucidate HS/Hp structure as sulfates provide characteristic shifts in both ^{13}C and ^{1}H spectra (Mulloy *et al.*, 1994; Yamanda *et al.*, 1992; Yates *et al.*, 1996).

Using papers from Yates *et al*., 1996 and Casu *et al*., 1994 as references for structural shifts, the 2D spectra were assigned (Figure 3.10). All of the spectra were produced from the same plane on the z axis. It has been established from the spectra that all samples contain sulfation at carbon 2 of uronic and carbon 2 and 6 of glucosamine. From this brief overview, it is apparent that the by-product samples contain 2-O sulfation of glucuronic acid (G2(2S)).

Further analysis by NMR was undertaken by ^{13}C on the next page, where ratios of 2S/2OH, 6S/6OH and NS/NA were calculated by identifying non-overlapping signals from the carbon-13 spectra (Figure 3.11 and Table 3.4).

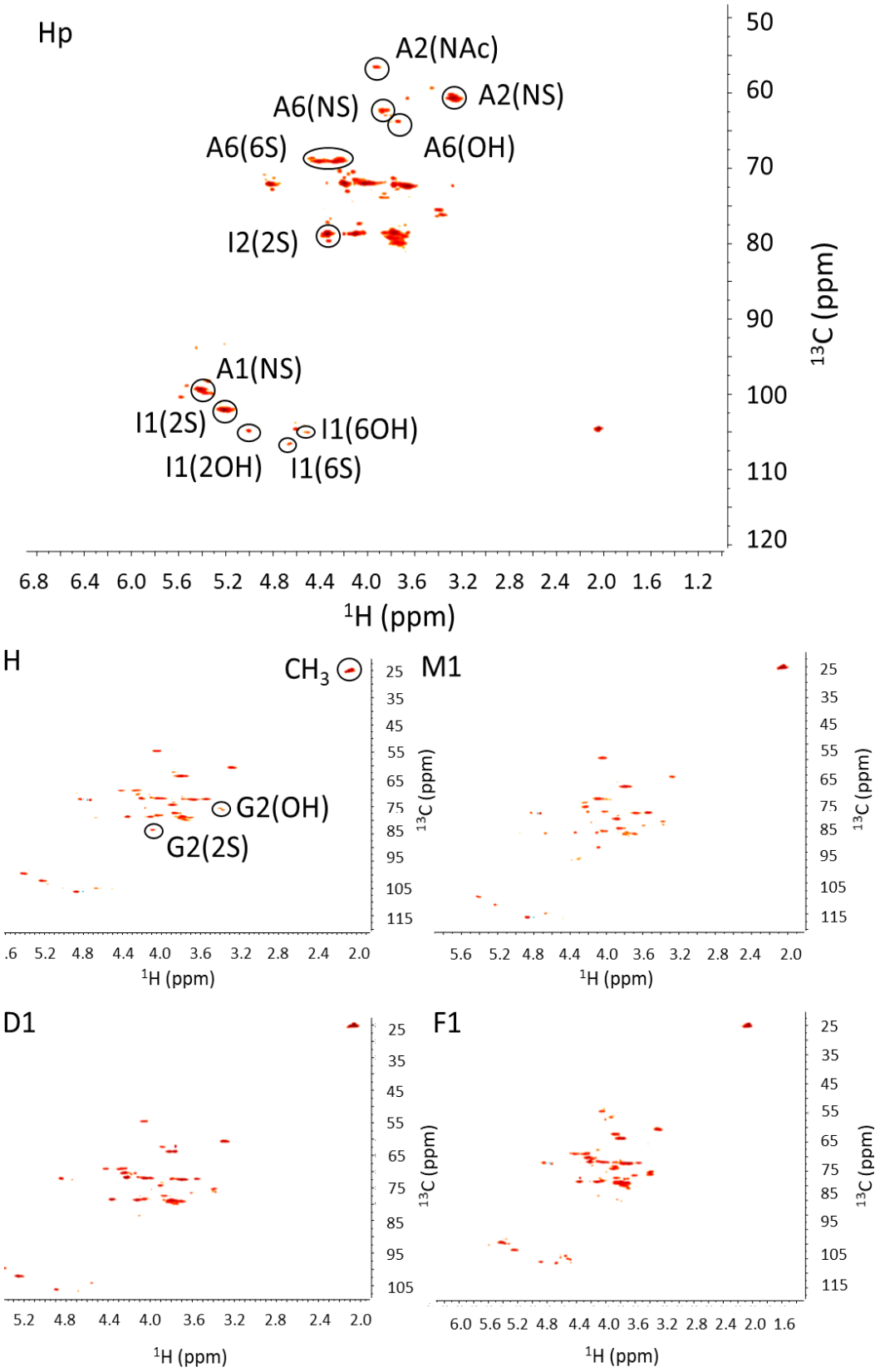

Figure 3.10- HSQC NMR analysis of Hp and by-products. 2D HSQC NMR spectra were recorded for 20 mg of each sample. Spectra of scans were made on Mestrenova and assigned according to reference peaks for HS/Hp from Casu *et al.*, 1994; Yates *et al.*, 1996.

3.4.6 Carbon-13 NMR Compares the Ratios of Relative Levels of Sulfation in All Samples

^{13}C NMR has been used in conjunction with HSQC to enable additional characterisation of the complex mixture. For further work, commenting on sulfation levels in the samples is the most appropriate way of analysing these spectra.

The relative peaks for 2-O, 6-O and N-sulfation were identified (Figure 3.11) and referenced from Yates *et al*., 1996. The shifts of carbon 2 (56 ppm) and 6 (69 ppm) of glucosamine, were used for identification of amounts of N- and 6-O sulfation, respectively (Table 3.8), as these are the carbons to which the sulfate groups are bound. For the identification of 2-O sulfation the carbon adjoining the sulfate group I-2 (iduronic acid residue) was not used, this is due to this peak being in a highly dense area of the spectrum, which could have been influenced by other structures. The signal for I-1 was used for the identification of 2-O sulfation instead, as the neighbouring carbon, it is highly influenced by the presence of a large, electronegative sulfate group. In the presence of sulfates at 102.3 ppm it is relatively unobscured by other peaks and the chemical shift is easily identified, moving to 104 ppm if unsulfated. After identification, the peak areas were taken and a ratio of sulfated to unsulfated shifts were calculated for the relevant carbons described above.

F1 appeared to be the least sulfated with all ratios of sulfation under 1, when compared to unsulfated residues. However, the levels of sulfation appear to be evenly distributed for 2-O (0.8), 6-O (0.7) and N- (0.7) sulfation (Table 3.8).

H and D1 are shown to contain more N sulfation, 1.25 and 1.29 respectively, than either 2-O or 6-O. D1 has slightly more 6-O sulfation (0.89) than H (0.73), whilst 2-O sulfation is broadly speaking the same in both (0.67 D1, 0.69 H). M1 appeared to be more highly sulfated than F1 but less than H and D1, due the decrease in 6-O sulfation, the ratios of N- and 2-O sulfation in M1 are broadly similar. Although having not analysed the data in depth, the NMR data for the by-products is consistent with the compositional analysis. However, it should be noted that the NMR data for Hp show greater increase in sulfation than the by-products compared to the disaccharide analysis, although both are in agreement that Hp is the most highly sulfated sample (Table 3.8).

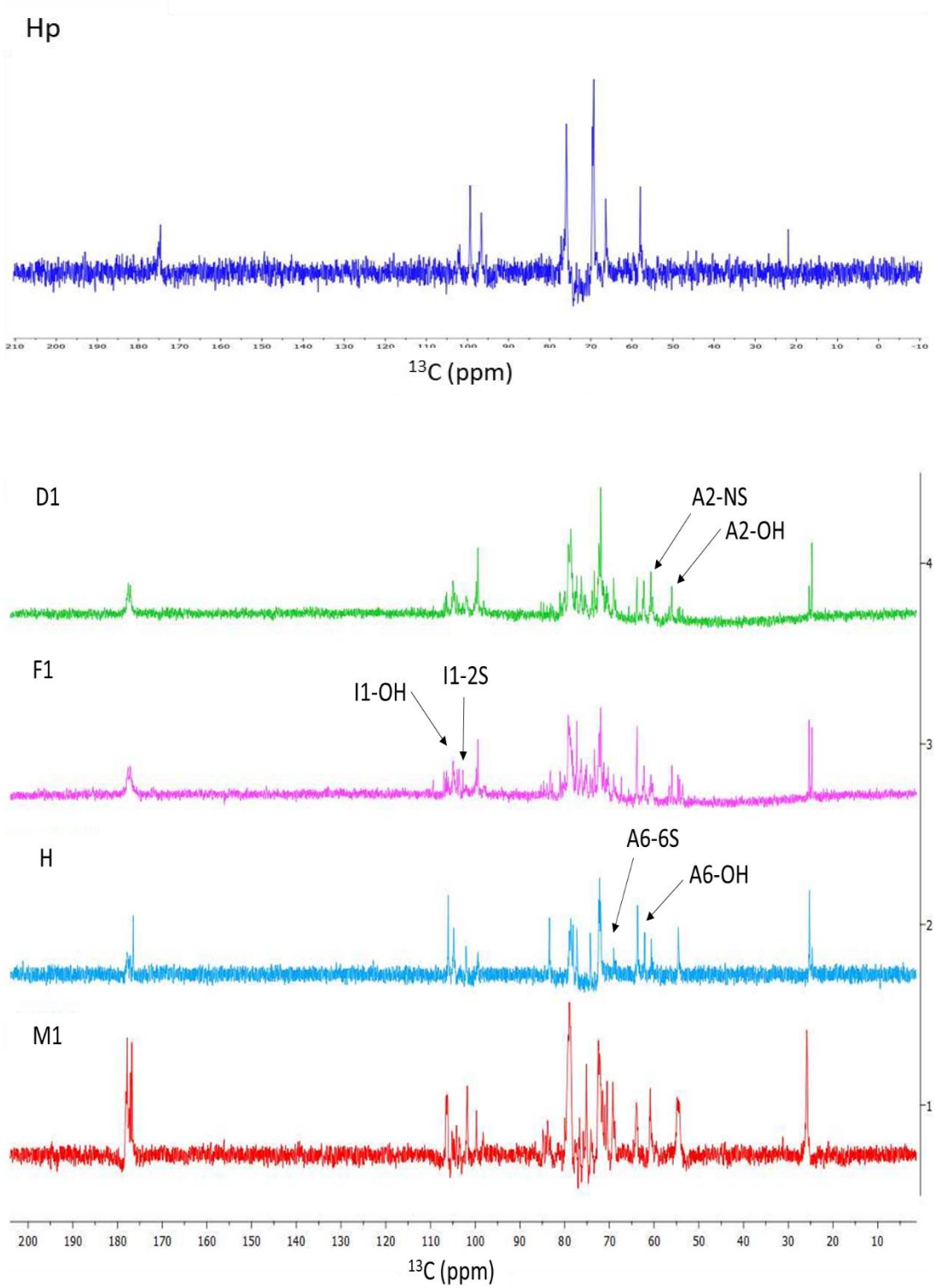

Figure 3.11- One dimensional ^{13}C NMR of Hp and by-products. 20 mg of samples were recorded at 313K on a Bruker 600 MHz spectrometer with TSP as the external reference (0 ppm). Signals were identified for all relevant Hp/HS structures in this thesis and were assigned according to Yates *et al*., 1996.

	S/OH		
Sample \ Carbon	A6 (69ppm)	A2 (57.6ppm)	I1 (102.32ppm)
Hp	3	2.7	2.6
D1	0.9	1.3	0.7
F1	0.7	0.7	0.8
H	0.7	1.3	0.7
M1	0.7	0.8	0.9

Table 3.8- Ratios of peak height of sulfated/unsulfated residues at A-6, A-2, and I-2 for Hp and by-products. 2-O sulfation of iduronic acid is most clearly identifiable by the chemical shift of carbon 1 at 102.32 ppm. N and 6-O sulfation are best identified by changes in signal of carbon 2 and 6 of N-acetylglucosamine at 57.6 and 69 ppm, respectively. Measurements from baseline to the tip of the peak were measured at the points described above, the sulfated measurement was divided by the peak size of the unsulfated domain to calculate a ratio.

3.5 Discussion

This Chapter has described the purification of the by-product samples, and their subsequent characterisation using several different methods including, weak anion exchange, NMR and SAX-HPLC. As these by-products were removed during the production of unfractionated Hp, the results have been interpreted by comparison to an existing commercial UFH, Celsus Hp. Two samples, D1 and F1, owing to their composition and availability, have also been compared to each other, as they were selected as the main focus of continuing work in further Chapters for the production of refined fractions in reasonable quantities.

From the compositional analysis, by-product H appeared to be the cleanest sample, consistent with the fact that it was removed from one of the last steps before the clean Hp product was obtained (Figure 3.1). Perhaps unsurprisingly it showed the closest resemblance to the Hp control. The largest difference relates to its size, since H is smaller than typical Hp, at around ~8800 Da. It could thus be suggested that H was obtained from the last ethanol precipitation mainly because of its size, rather than other characteristics, such as sulfation. Initial screening of the by-product samples by weak anion exchange also indicated that H is distinct from Hp in its overall sulfation prior to digestion. Most of the product elutes at low salt concentrations, 1.1-1.3 M NaCl. However, it must be noted that this is not a sufficiently rigorous method of analysis to allow comment on the overall characteristics of the sample. More thorough and descriptive analysis of sample H, where the sample was digested into its constituent disaccharides by heparinase enzymes and then separated by strong anion exchange suggested that this sample is highly sulfated and a close structural relative of Hp. From closer inspection, the combination of NMR and compositional analysis of H can also be used to examine the varying levels of NS, 2S and 6S. HSQC was not able to establish disaccharide or chain structure due to the diverse mixture of sugars, but carbon-13 NMR allowed comparison of the ratios of sulfated to unsulfated sugars, where the largest difference appeared to be in an overall increase in N-sulfation of H compared to the other by-products, as supported by compositional analysis.

To better reveal structural diversity and characterise the sample, it is important to look at the individual disaccharides in combination with NMR. Initially compositional analysis agrees with H having high levels of sulfation, with significantly more mono-sulfated Δ-UA-GlcNS and Δ-UA-GlcNAc(6S), di-sulfated Δ-UA(2S)-GlcNAc(6S) and Δ-UA(2S)-GlcNS and minimal variation in other structures compared to Hp. These results suggest that the long

chains of the undigested H material (separation shown in Figure 3.6) must contain extended regions of tri- and di-sulfated disaccharides, particularly di-sulfated, with additional regions of mono-sulfated disaccharides compared to Hp.

Size elution of by-product sample M1 suggests that it is similar in size to Hp (~11,300 Da). However, anion exchange separation of the intact chains indicates that it is less sulfated overall. M1 has a slightly wider spread by weak anion exchange, primarily eluting between 1-1.4 M NaCl. Although only just approaching statistical significance, this evidence was also supported by M1 having an overall reduction in the number of sulfates per disaccharide, ~1.8 compared to ~2.2 in Hp ($p=0.07$). A more in-depth look at M1 by grouping the disaccharides by individual numbers of sulfates (mono, di, tri) also suggests this to be the case, but more specifically suggests a reduction in the trisulfated disaccharides of M1 compared to Hp. M1, however, only showed a decrease in the prevalence of 2-O sulfates and all others remain similar to that of Hp. The most common disaccharide structures are Δ-UA-GlcNS and Δ-UA-GlcNAc(6S). This hypothesis can be further supported with the individual disaccharide structure of M1 showing a higher level of the mono-sulfated saccharide Δ-UA-GlcNS (8.2%, versus Hp 2.2%) and 6S structures, Δ-UA-GlcNAc(6S) and Δ-UA(2S)-GlcNS, with both being significantly increased when compared to Hp. ^{13}C data also agrees with the suggested increase in prevalence of 6-O sulfation, over either 2-O or N-sulfation. It is also important to note that compositional analysis is unable to distinguish iduronic acid and glucuronic acid; however, by HSQC NMR M1 is shown to contain a mixture of IdoA and GlcA.

By-product F1 showed the lowest level of average sulfates per disaccharide (~1.6) but still appeared to be of similar size to the other by-product samples (~11,300 Da). Initial anion exchange separation suggests this sample is the most heterogeneous, with products seen at all salt concentrations but primarily at 1.5 M (similar to D1, see below). It is perhaps surprising that F1s initial elution is similar to D1 and yet there is a large appreciable difference in average number of sulfates per disaccharide; this suggests a very different pattern of sugars in the intact chain. F1 has the lowest level of tri-sulfated disaccharides of all the samples and is significantly below that of Hp (68% vs 44%). From Figure 3.8b, it can be seen that there is a decrease in N-sulfation compared to all other samples compensated by a large increase in N-acetylated disaccharides (19%) that could make up NA domains. A large decrease in 2S and 6S structures can also be seen. However, overall compositional analysis suggests that F1 primarily contains an increase in Δ-UA(2S)-GlcNAc(6S) (3.1%) and Δ-UA(2S)-GlcNS (10.5%) compared to Hp, and it is these which provide the by-products with a moderate average level of sulfation and subsequent anion elution properties. This is largely

confirmed when looking at the disaccharide composition; the increase in 2-O sulfation above the level of 6S and NS and NA disaccharides is also consistent with ^{13}C NMR, with HSQC NMR, indicating the Δ-UA(2S)-GlcNS disaccharides are likely to be IdoA(2S)-GlcNS.

D1, although highly sulfated (~2.0 sulfates per disaccharide), was identified as being the least structurally comparable to Hp. Upon anion exchange of intact D1 chains primarily elute at ~1.5 M NaCl, although material can be identified at all salt concentrations. This initial study suggests that the sample has moderate levels of sulfation and is of similar size to the other samples and Hp (11,500 Da), though the average level of sulfates per disaccharide was found to be slightly lower than Hp (~2 vs 2.2). Although D1 by-product has fewer tri-sulfated disaccharides, the maintenance of an overall high level of sulfation could be due to a reduction in un-sulfated structures and an increase in all mono- and di-sulfated residues, compared to Hp. Taken together, the compositional analysis data suggest that these chains may have long domains of di-sulfated saccharides interspersed with mono-sulfated residues rather than unsulfated residues, with additional highly concentrated tri-sulfated sequences, as seen in Hp. This could account for a comparable level of sulfates per disaccharides but elution from anion exchange of lower salt concentrations than Hp. It is possible that the spatial distribution of the sulfate residues may also influence the anion exchange results. Analysis thus far indicates a high level of Δ-UA(2S)-GlcNS and, to a lesser extent, Δ-UA-GlcNS > Δ-UA(2S)-GlcNAc. This analysis can be narrowed by looking at the individual disaccharide structures and the primary increase in 2-O sulfation could be from the structure Δ-UA(2S)-GlcNS (9.4%). Typical of HS, HSQC NMR suggests that D1 contains a mixture of higher amounts IdoA(2S) vs GlcA(2S).

From the position of their procurement in the process, it could be suggested that the by-products would resemble the control Hp in the following order H>F1>D1>M1. However, based on the use of multiple techniques to elucidate their structure, the data suggests that although highly sulfated, D1 rather than M1 is the least comparable to Hp and M1 also appeared to be more similar to Hp than F1. After analysis of sulfation, the order of similarity to Hp is suggested to be H>M1>F1>D1. However, structural analysis has highlighted that all samples are unique and different to Hp in their proportion and probable patterns of sulfation. It also needs to be appreciated that this is a tentative assignment based on the comparison to one example of Hp.

Finally, F1 and D1 are obtained from the Hp production process at similar stages, and have average levels of sulfation similar to typical tissue HS chains. These two samples were

thus obtained in large quantities (~1-2 Kg) for continued work, so it is important to compare intact samples for later bioactivity studies. As previously discussed, ^{13}C NMR suggests that D1 contains more 2-O sulfation than F1 with comparable amounts of both 6-O and N-sulfation. Compositional analysis showed that, in fact, D1 contains more of all sulfate groups and an overall increase in sulfation, primarily due to a significant increase of the tri-sulfated disaccharide, Δ-UA(2S)-GlcNS(6S) (P=0.0004), resulting in overall increase in the levels of sulfation per disaccharide of D1.

In conclusion for continued work, although F1 and D1 are the closest in their location in the Hp production process and physical appearance, they have significantly different structural properties, the consequences of which will be explored in later Chapters when comparing the by-products in growth factor bioassays, side-effect studies and biological applications.

D1 and F1 have relatively low mono-GlcNAc content like Hp, however further work on these samples by selecting peaks from the anion exchange of the initial intact chains (Figure 3.5), may lead to sub fractionations with differing disaccharide compositions and chains with lower, more evenly distributed levels of sulfation to obtain more 'HS-like' material (Griffin *et al*., 1995).

Chapter 4- The Generation of By-Product Fractions

4.1 Aims

This Chapter describes multiple techniques used in order to refine the by-product material, with the goal of enabling more potent growth factor activation whilst maintaining a good yield of product, compared to the intact samples in following Chapters.

By-product samples were subjected to enzymatic digestion with heparinase III before being separated by gel filtration and strong anion exchange chromatography into oligosaccharide fractions. This process, which provides a good breadth of products, whilst maintaining a good yield of material, was used to produce material for further work in the following Chapters.

4.2 Introduction

It has been well researched and discussed that HS-protein interactions although not absolutely specific do, nevertheless, favour certain sized and sulfated oligosaccharides for binding of proteins and activation. It must be noted that the requirements for binding are a subset of those required for successful activation and therefore so are the oligosaccharide requirements. For example, it is thoroughly documented that the Hp pentasaccharide sequence, discussed previously, binds ATIII with high affinity thereby preventing coagulation; this has led to the exploitation of this sequence by pharmaceutical companies for use in patients. However, this interaction is most certainly not exclusive and other HS/Hp sequences have also been shown to bind ATIII (Brito *et al*., 2014). To date it is the only Hp/HS sequence that has been widely, although inaccurately, described as being 'specific' to a particular protein. The current theory suggests that successful initiation of such pathways is primarily due to the shape, conformational flexibility and spatial distribution of charged groups along the HS chain, enabling it to bind multiple ligands (Thunberg *et al*., 1980; Casu *et al*., 1988).

For example, HS oligosaccharides in a range of ~dp 8 with 6-O and 2-O sulfation are generally the smallest, relevant saccharides for FGF growth factor signalling (Walker *et al*., 1994). Although, smaller ~dp 6 oligosaccharides have been shown to bind but not activate growth factors. However, it has been suggested that a highly sulfated 6mer could lead to successful activation (Walker *et al.*, 1994). This research therefore builds the foundation for investigations into refining oligosaccharide mixtures for more specific growth factor activity.

4.2.1 Size Exclusion Chromatography

Size exclusion chromatography (SEC) is a well-documented technique for the separation of proteins and oligosaccharides. SEC separates material according to its hydrodynamic volume and, as per other methods, oligosaccharide products are detected by UV, using the wavelength 232 nm to detect the unsaturated double bond (Linhardt *et al.*, 1988; Ziegler and Zaia, 2006). As oligosaccharides pass along the column, those of smaller size have a longer elution path as they are able to pass through the pores in the beads, whereas larger chains are excluded from the pores, and subsequently elute earlier. The quality of separation is determined by the material being separated, the beads and the buffer used. For fractionating by-products partially digested by heparinase III, Superdex 30 (GE Healthcare, UK), a composite matrix of cross-linked dextran and agarose with pore sizes of around 24-44 µm, are effective. Previous work by Powell *et al.* (2010), Feyzi *et al.* (1997) and others have demonstrated that Superdex 30, provides good resolution for oligosaccharide separation, is very durable and offers high reproducibility. However, higher resolution of SEC separation has been shown with beads such as BioGel P10 and Sephadex 75, but these composites compress easily and therefore do not provide consistent run to run reproducibility (Vorup-Jensen *et al.*, 2007; Goger *et al.*, 2002; Lever *et al.*, 2007). The reproducibility of the beads can be indicated by noting run-to-run consistency of the void volumes of the column, for these beads the void volume is relatively large (~1/3 of total volume, see Figure 4.1).

4.2.2 Strong Anion Exchange Chromatography

Strong anion exchange chromatography (SAX) is a technique used to separate samples predominantly by charge. Other factors, such as the saccharide chains access to the surface area of the bead and saturation of the first layers of the beads may also play a role in determining elution. This is apparent in compositional analysis separation as disaccharides with the same charge elute at different times e.g. Δ-UA-GlcNS(6S), Δ-UA(2S)-GlcNS and Δ-UA(2S)-GlcNAc(6S) all contain 2 sulfate groups but their elution is distinct (see Figure 3.6). It is claimed by the manufacturer that the polymer beads are all spherical and the same size and shape (10 µm – ThemoFisher Scientific, UK), to ensure high resolution.

Similarly, to compositional analysis, products are first bound to the column containing positively charged Propac PA1 beads, the samples are then dissociated from the beads with increasing concentrations of salt. This technique is often used in parallel with SEC to refine oligosaccharides with the aim of selecting single structures, which can be characterised by techniques such as molecular spectroscopy (Tissot *et al.*, 2008).

4.3 Methods

4.3.1 Size Exclusion Chromatography

For analytical purposes beads are packed into a 16 mm by 16 cm column which allows good separation of material up to around 50 mg. During the production of large quantities of fractions, beads are packed into a 2.5 cm x 100 cm column, allowing high throughput of material. Buffer selection for proteins are based on the pI of the protein of interest, whereas for HS this is not much of a concern due to its high negative nature. It has been shown that ammonium bicarbonate (NH_4HCO_3) allows better resolution for distinguishing different sized oligosaccharides than separation by ddH_2O, so all SEC separations have subsequently been conducted in 0.5 M NH_4HCO_3 (Powell *et al.,* 2010).

4.3.1.1 Calibration of Size Exclusion Chromatography Column

10 mg of phenol red (0.5% liquid, Sigma Aldrich, UK) and blue dextran (Sigma Aldrich, UK) were mixed in a volume of 2 ml with ddH_2O. The dye was injected over a Superdex 30 packed in a 26 XK column (2.5 cm x 100 cm) at 0.5 ml/min.

The dyes were detected using absorbance values of 620 nm (blue dextran) and 560 nm (phenol red). Blue dextran has a very large molecular weight, $2x10^6$, therefore it is excluded from the column matrix passing straight through the column, and hence indicates the V_O of the column. Phenol red has a molecular weight of 354 g/mol, as a small molecule it is of similar size to a dp 2 and takes the longest path through the beads and is used to measure the V_t.

4.3.1.2 Heparinase III Digestion of By-Products

Enzymatically clean by-products (1 mg/ml) were digested in heparinase buffer (Chapter 2) with the equivalent of 2.5 U heparinase III (expression plasmids were a gift from Prof Liu, UNC Chapel Hill, NC, USA) at 37˚C, agitating for 24 hours with an additional 2.5 U heparinase III added after the first 6 hours.

The products of digestion were then separated according to size on a Superdex 30 column (diameter 2.5 cm x length 100 cm) and eluted with 0.5 M NH_4HCO_3 (ThermoFisher Scientific, UK) over a 16 hour programme at 0.5 ml/min. 1 ml fractions were collected on a 950-frac collector (GE Healthcare, UK) and grouped based on the degree of polymerisation, from dp 2-18+, digested fully to the capabilities of heparinase III. Undigested peaks were also collected for further digestion. Samples were rotary evaporated to reduce the volume and put through 4 cycles of freeze drying and resuspension to remove the NH_4HCO_3, and finally

weighed. This process was repeated until enough weighable material was obtained for the bioactivity studies.

4.3.1.3 Heparinase II Digestion of By-Products

The same protocol as heparinase III digestion was followed, substituting heparinase III enzyme for heparinase II (expression plasmids were a gift from Prof Liu, UNC Chapel Hill, NC, USA).

4.3.1.4 PAGE Separation of Digested By-Products

2-20 µg of each by-product fraction were fluorescently tagged by a saturated solution of 100 mg 4-amino napthalene 1,3 di-sulfonic acid in 500 µl formamide, incubated overnight at RT. The largest fraction was also loaded onto the gel with phenol red. This allowed the detection of the leading edge of the separation ~dp 2 to ensure that no sample was run off. These samples were loaded on to a 33% acrylamide gel (Chapter 2). For comparison of relative size, Hp standards from dp 2-18 were loaded as a ladder of standards. Oligosaccharides were separated on the gels at 250 V at 4°C for 3 hours, and imaged by UV in order to visualise the ladder (produced by Dr Y Ahmed (Liverpool University) by digestion and separation of Hp) and smaller fractions (1-2), before the gels were stained (1 hour, RT) with 0.08% Azure A and destained overnight with ddH_2O, generating images for the larger fractions. The cation stain Azure A provides poor staining of lower sulfated saccharides, hence the UV imaging of the smaller samples (Turnbull and Gallagher, 1988).

4.3.2 Strong Anion Exchange Chromatography of Heparinase III Digested Samples

Enzymatically clean by-products were digested in heparin lyase buffer (at 1 mg/ml) with the equivalent of 2.5 U heparinase III at 37˚C, agitating for 24 hours with an additional 2.5 U heparinase III after the first 6 hours.

50 mg of digested samples were then separated according to charge on a Dionex Propac PA1 semiprep 9x250 mm column (ThermoFisher Scientific, UK) and eluted using a linear 0-2 M NaCl gradient, over 60 mins. Oligosaccharides were detected by UV at 232 nm, samples were not collected, since this was an analytical exercise.

4.4 Results

4.4.1 Size Exclusion Chromatography Separation

4.4.1.2 Establishing V_o and V_t from Superdex 30 Chromatography

Frequently checking the void volume of the column gives some indication of the state of the beads, particularly if they have started to compress under pressure or the column has dried out and the beads have shrunk. As stated the void volume is known to be quite large (~1/3 of the total volume) indicated by the dyed glucose polymer, blue dextran (~$2x10^6$ g/mol) and was identified by absorbance at 620 nm at ~180 ml, whilst the V_t measured by the identification of phenol red (354 g/mol), absorbing at 560 nm and indicated that the total volume was ~510 ml (Figure 4.1).

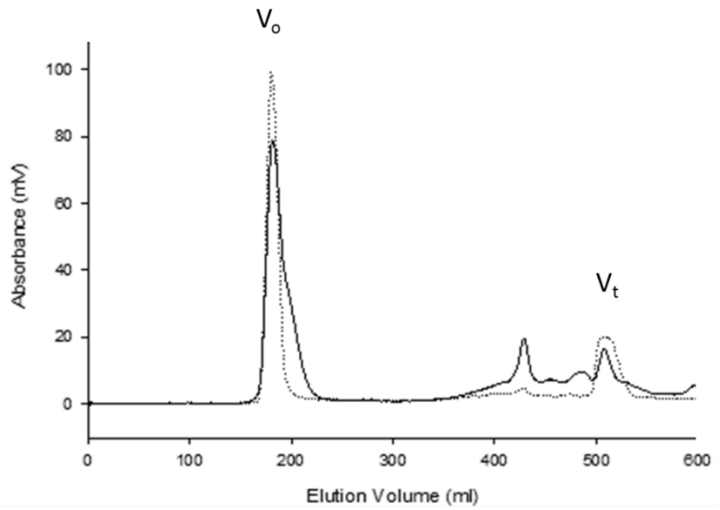

Figure 4.1- The Vo and Vt of Superdex beads in a 2.5cm x 100 cm column are identified using blue dextran and phenol red. A mixture of 10 mg of each blue dextran and phenol red were run under 0.5 ml/min in 0.5 M NH_4HCO_3, dyes were detected by UV at 560 nm —— and 620 nm ------.

4.4.1.3 Enzymatic Digestion of By-Products with Heparinase II

Heparinase II digests both sulfated and unsulfated residues along the chain and in principle should digest more than the other two enzymes (Linhardt *et al.*, 1990). However, not only was there a large amount of unseparated material remaining after digestion but the enzymes produced in the laboratory also gave a digestion profile showing a high degree of variability between repeat runs.

In general, the digestion gives rise to a number of different sized groups of oligosaccharides, with 6-7 distinct peaks (Figure 4.2). An estimate of molarity can be

established from SEC chromatographs due to the detection of a single double bond on each chain, however, this can only be a semi-quantitative estimation as different structures have the potential to have slightly altered extinction coefficients and therefore for large scale preparations weighing the material was deemed a better option (Powell *et al.*, 2010). It can be appreciated that only small amounts of material are produced for the smallest fractions and the majority remain as large oligosaccharides in an unresolved peak, due to the inability of heparinase III to digest these structures. Due to the quality of separation and the consistency between digestion (data not shown), heparinase II digestion and separation was not taken any further than this analytical step.

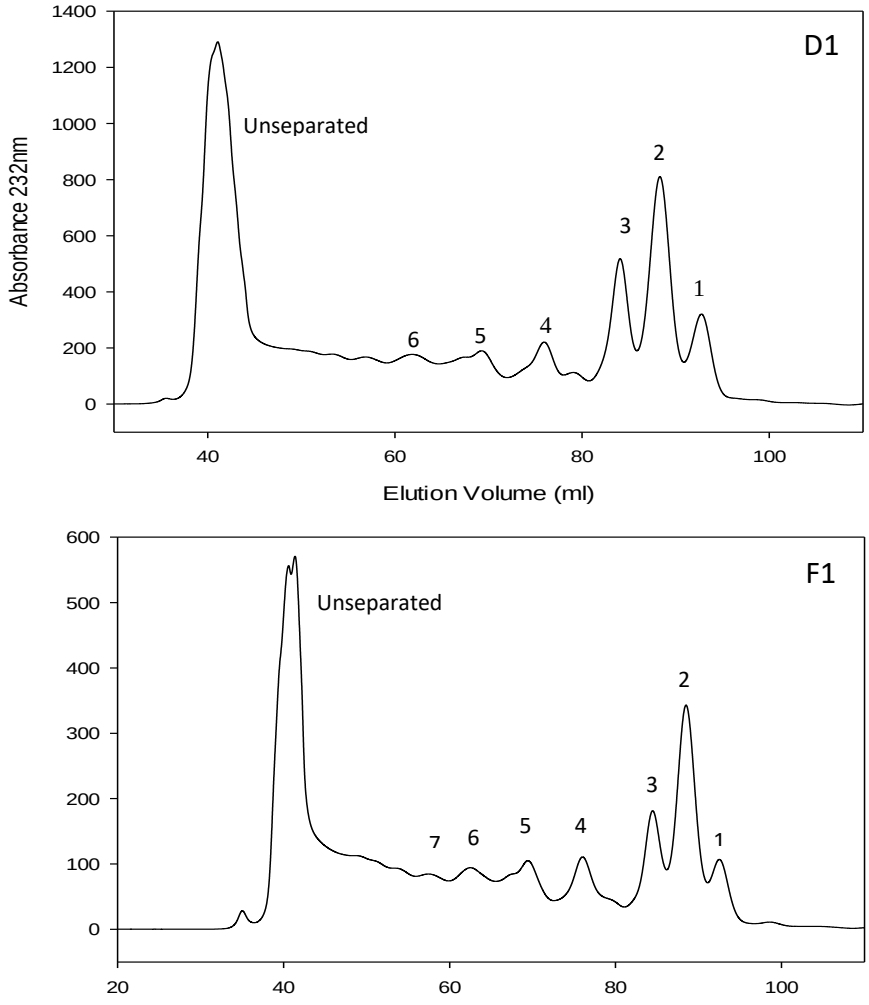

Figure 4.2- Products of digestion of D1 and F1 with heparinase II after separation by Superdex 30 beads show a wide range of sized fractions. 13 mg of D1 was fully digested with heparinase II. Products of digestion were separated on a 16 mm x 60 cm column with Superdex 30 beads (GE Healthcare, UK) using 0.5 M NH_4HCO_3 buffer. Products were detected by UV at 232 nm.

4.4.1.4 Enzymatic Digestion of By-Products with Heparinase III

Samples were digested to their fullest extent by heparinase III using a 24 hour incubation. All by-products (D1, F1 and M1) show substantial digestion and separation (Figure 4.3). However, by-product M1 was not as susceptible to heparinase III digestion as D1 and F1, which were both separated into ~11 distinguishable peaks, of which 8 were selected and freeze dried. For this reason M1 was discounted from further separation and analysis.

Digestion and separation were both highly reproducible and provided consistent amounts of material from run to run (Figure 4.4). F1 appeared to digest into smaller or unseparated fractions than D1, with over 60% of the material collected in fractions 1, 2 and unseparated. Around ~15% also digests to produce a mid-range size of fractions (peaks 3-8). Whilst a large proportion of D1 still eluted in the final unseparated fractions and ~20% eluted in the smallest fraction alone (peak 1). For the most part, all other fractions in both F1 and D1 were produced in similar milligram quantities (Figure 4.5).

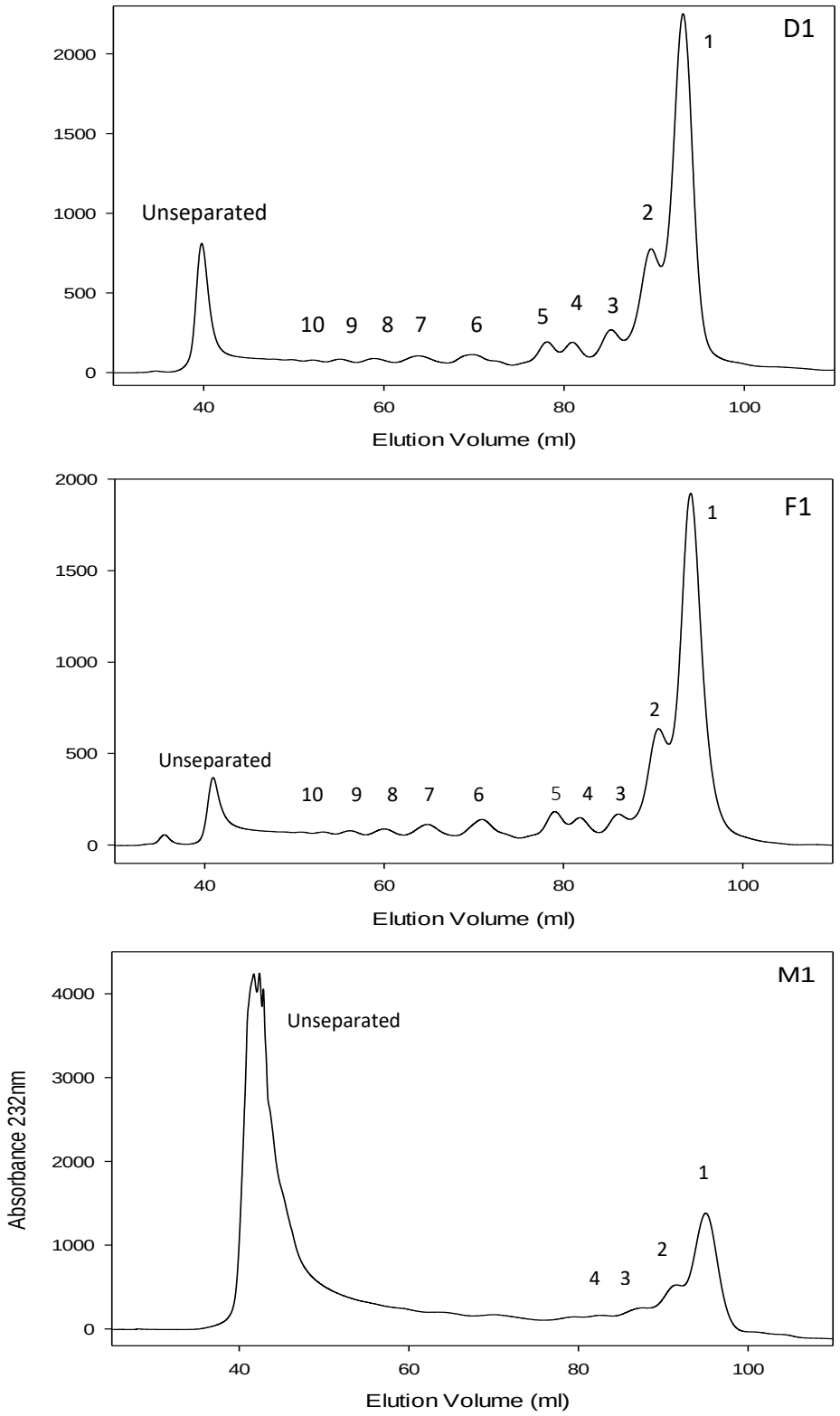

Figure 4.3- SEC Chromatographs of heparinase III digested material detected by UV absorbance at 232 nm. 200 mg of either D1, F1 or M1 were separated by Superdex 30 on a 16 mm x 60 cm column at 0.5 ml/min.

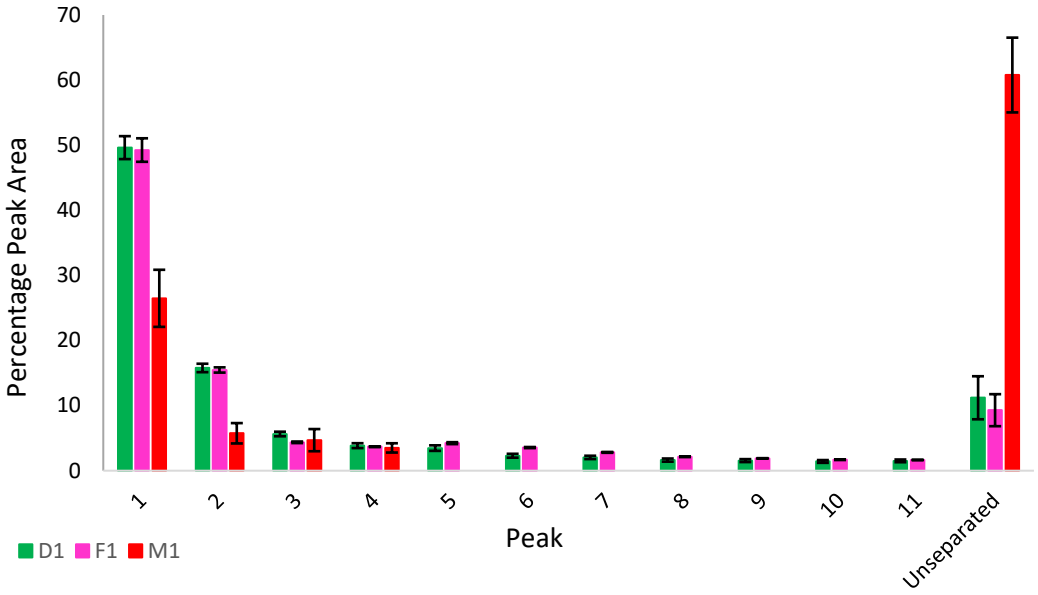

Figure 4.4- Products of digestion by heparinase III separated by Superdex 30 chromatography showed a wide range of sized products. 200 mg of samples (n=5) were fully digested with heparinase III and showed considerable run to run consistency.

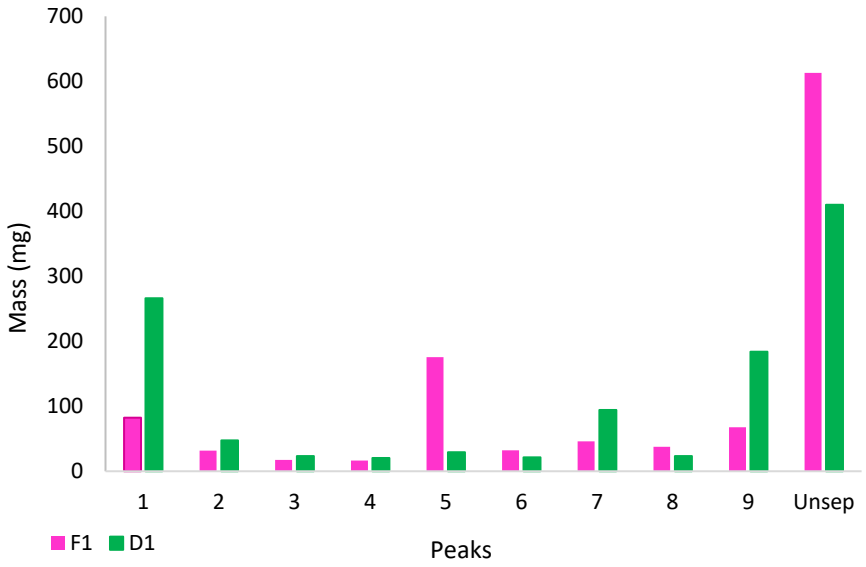

Figure 4.5- Mass of peaks selected and pooled from 1020mg of by-products D1 and F1, separated by size using Superdex 30 SEC. Peaks selected from multiple runs (Figure 4.3) were pooled and desalted using four rounds of freeze drying before being weighed.

4.4.1.4 Acrylamide Gel Separation of By-Products D1 and F1 Initially Separated by SEC after Heparinase III Digestion.

Eight oligosaccharide peaks of D1 and F1 from heparinase III separation by SEC (Figure 4.3 and 4.4) were collected and were sized by comparison with known standards on polyacrylamide gels (Figure 4.6). All of the peaks collected from the size exclusion separation showed a spread in the degree of polymerisation. However, most fractions showed a predominant size defined set of species (Table 4.1). Fraction 3-4 both contained the highest abundance of ~dp 6-8, which from the literature, are the smallest size for which growth factor activation would typically be successful (Guimond *et al.*, 1994; Walker *et al.*, 1994).

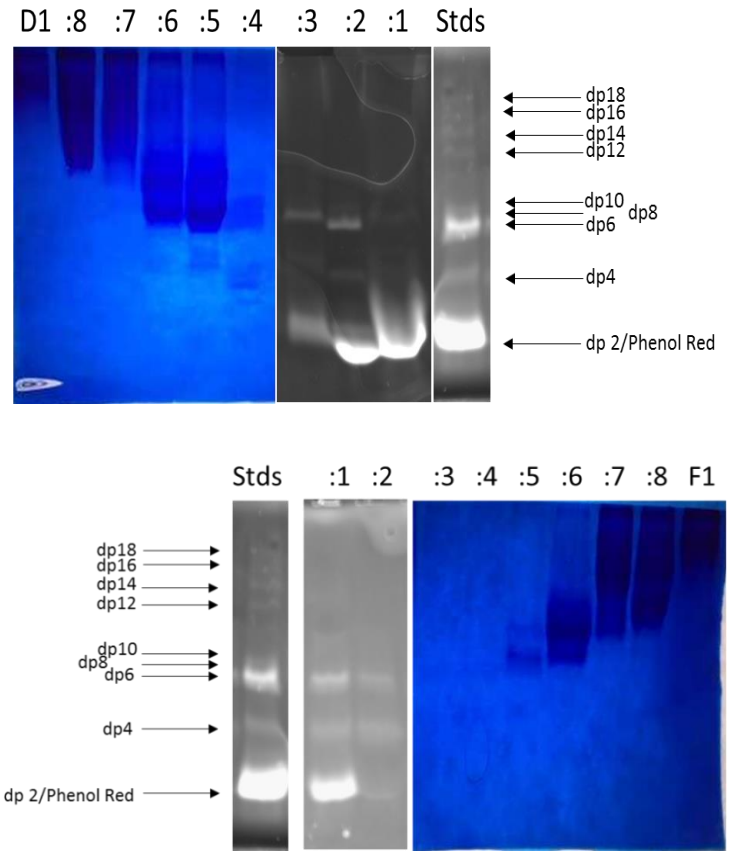

Figure 4.6 – PAGE gels of by-products D1 and F1 after digestion by heparinase III separated by SEC. After digestion with heparinase III and separation by Superdex 30, products of D1 (top) and F1 (bottom) were separated on a 33% acrylamide gel at 250 V for 3 hours. Known size standards were run for comparison. The grey lanes have been identified by UV after being fluorescently tagged, the blue lanes have been stained with Azure A. NB. Both of the grey and blue images have been taken from the same gel and all samples were treated the same, however they were imaged as described above.

Fraction	Degree of polymerisation
1	**2**, 4, 6
2	2, **4**, 6
3	2, 4, **6**
4	4, 6, **8**
5	6, 8, **10**, 12-18+
6	8, 10, **12**, 14-18+
7	**12, 14,** 16, 18+
8	12, 14, **16, 18**+
Intact	**18+**

Table 4.1- Estimated degree of polymerisation of fractions after heparinase III digestion and SEC separation. Highlighted in red are the size of oligosaccharides that are most abundant in each fraction, determined by the amounts identified on the PAGE gels, applied to both D1 and F1, as full quantification is not feasible (Figure 4.6).

4.4.2 Strong Anion Exchange Chromatography (SAX) of Heparinase III Digested Samples Resolves a Range of Oligosaccharide Products.

After identifying heparinase III digestion as the most reproducible digestion technique which produces the largest range of sized oligosaccharides, SAX was then used to separate these samples based on charge as a comparison to SEC.

D1 and F1 were separated using a 0-2 M NaCl gradient, over 60 minutes at 1 ml/min. Although there are multiple visible peaks, most of the sample elutes at a low salt concentration for both D1 and F1, suggesting that the products of heparinase III digestion contain low levels of sulfation (Figure 4.7). Broadly speaking, the SAX profile is consistent with data from the SEC profile, with high levels of early elution (lower sulfated and smaller oligosaccharides), tapering off to lower amounts of material with medium to high levels of sulfation, around 10% of the total. However, material eluting in the region of 30-40 mins would be moderately sulfated and therefore be expected to exhibit the most interesting bioactivity compared to its low or highly sulfated neighbours. Due to the lower throughput rate and the lower level of yield of material in the area of interest, SAX separation was only used for this analytical separation and not pursued further for preparative analysis.

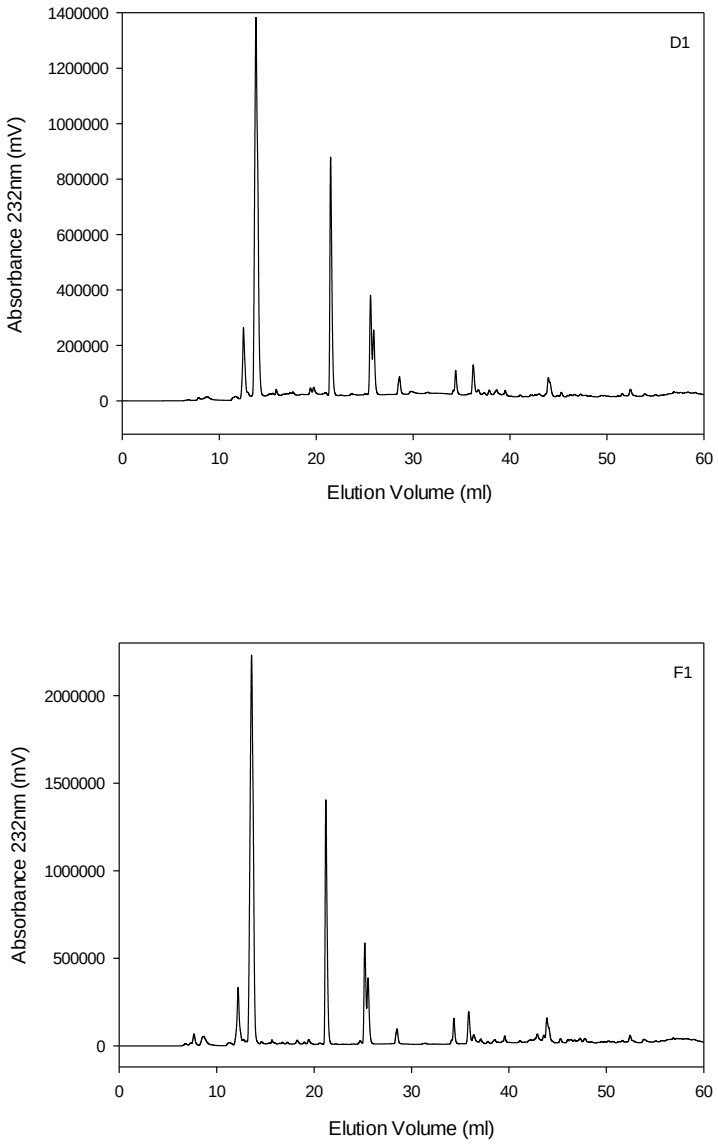

Figure 4.7 – SAX chromatographs of by-products D1 and F1 following digestion with heparinase III. 50 mgs of by-products from the digestion were separated using a 0-2 M NaCl gradient on a Dionex Propac PA1 semiprep 9x250 mm column, with detection by UV at 232 nm.

4.5 Discussion

Overall, this Chapter has highlighted that heparinase III was the most appropriate enzyme for digestion to produce large quantities of sulfated oligosaccharides for bioactivity studies in further Chapters. In comparison, heparinase I, would digest more highly sulfated oligosaccharide sequences based on its specificity and would show less variation in biological activity and is therefore unsuitable for further bioactivity testing in this thesis (Linhardt *et al.*, 1990). Heparinase II, did not provide as large a range of fractions and also produced significantly higher levels of undigested material compared to heparinase III (Figure 4.2).

SAX separation demonstrated a diverse range of oligosaccharide products from a digestion with heparinase III, though providing a profile consistent with the SEC separation. However, from previous work, the material likely to elicit the most diverse range of bioactivity are in the peaks which elute around 30-40 minutes (Powell *et al.,* 2010). From Figure 4.7, it can be seen that this material is also of low abundance in the sample and therefore this method of separation would increase the time taken to provide enough material for bioassays, as well as decreasing the overall useful yield from the initial starting material.

From the digestion of these products with heparinase III, it was evident that a range of sized fractions can be produced reliably for structures ranging from dp 2 to 18 by SEC (fractions 1-8) for both D1 and F1. These samples were collected and pooled together to provide more refined mixtures of similar sized oligosaccharides. From the literature, it was identified that moderately sulfated 6-8mers are the smallest bioactive oligosaccharides to initiate growth factor signalling (Guimond *et al.,* 1994; Walker *et al.,* 1994). For growth factor analysis in Chapter 5, it was hypothesised that the largest differences would be seen between the fractions that contain the largest amount of dp 6-8 (fractions 4-5), whereas significantly lower levels of activity would be expected in smaller fractions (1-3). However, size separation, although refining the intact by-products, is still a relatively crude preparation. For example, it has to be appreciated that a highly sulfated 6-mer will likely coelute with a low sulfated 8-mer, due to the additional sulfate group contents of the 6-mer resulting in them having similar hydrodynamic volumes to the 8-mer (Powell *et al.*, 2010). From the gels (Figure 4.6) it was evident that the smaller fractions (1-3) did have identifiable material of around dp 6, perhaps dp 8, although not in high abundance relative to other sizes in that fraction. It could be hypothesised that these fractions will consequently exhibit weak bioactivity.

Although a large range of fractions were produced successfully by SEC and could be tested in bioactivity assays described in the following Chapters, it must be noted that in

industry large scale anion exchange is the favoured route to obtaining refined groups of Hp chains or oligosaccharides, followed by size separation using membrane filtration. However, membrane filtration methods are not applicable for the scale of the products that have been separated in this Chapter and are more applicable to the Kg quantities of industry, as well as being a relatively crude method of size separation compared to the resolving capabilities of Superdex 30 beads. Additionally, SAX separation used in industry is also likely to incorporate beads of lower resolving capacity quality than the Propac PA1 beads available to us and thus give less SAX separation. However, SAX separation followed by SEC (or vice versa) using the equipment available in our laboratory, could lead to an enhanced refinement of the oligosaccharide mixtures. It would also reduce the yield of the final material, whilst increasing the cost. For this reason, SEC was utilised as the most efficient way to separate samples at a crude level, whilst maintaining a good yield of product for further studies.

Chapter 5- Bioassay Studies with Intact By-Products and Size Derived Fractions of D1 and F1

5.1 Aims

For successful growth factor activation HS typically needs to be able to bind the protein and in some cases also its receptor. The first aim of this Chapter is to report investigations into differences between the intact by-product samples and their ability to activate a range of growth factors, compared to Hp as a control. The second aim was to explore whether digesting and fractionating the intact material changes the bioactivity of the samples.

5.2 Introduction

As discussed in previous Chapters, HS plays a pivotal role in many protein interactions. Growth factors in particular often require HS to be available to make an activated ligand-receptor complex. Four main roles have been attributed to HS:GF binding: 1) sequestering the growth factor at the cell surface and thereby protecting it from degradation; 2) binding of growth factor ligand and activation of downstream pathway; 3) Inhibiting growth factor signalling; and 4) acting as a co-receptor for growth factors and receptors, which may also require direct interactions of receptors with HS (reviewed by Ornitz, 2000).

The most extensively researched growth factors to date are the FGF family. The HBS of all FGFs have now been mapped (Xu *et al*, 2012; Li *et al*., 2015). For the purpose of this thesis the focus will be on FGF2, as it was the growth factor used in the bioassays in this thesis. There are three distinct HBS on FGF2, these have been extensively characterised by multiple methods including; X-ray crystallography, NMR, the use of synthetic peptides and amino acid mutations (Faham *et al*., 1996; Thompson *et al*., 1994; Baird *et al*., 1988).

FGF2 adopts a β-trefoil structure, made up of antiparallel β-sheets (Eriksson *et al*., 1991; Zhang *et al*., 1991). Located within these sheets are several HBS, the canonical binding site (HBS1) has been shown to have the greatest affinity for HS/Hp. It consists of a cluster of positively charged residues with regions of peptides forming loops on the β-strands. These are primarily made up of positive arginine and lysine, and hydrogen bonding asparagine and glutamine amino acids. Two FGF2 molecules dimerize, with the primary binding sites on the top surface, forming a Hp binding cleft. Further loops adjacent to the primary HBS form secondary binding sites with other arginine and lysine amino acid residues, securing the two molecules and providing optimal positioning for receptor interaction (Ori *et al*., 2009; Plotnikov *et al*., 1999).

Binding of FGF2 and HS is suggested to be primarily facilitated by 2-O and N-sulfation of oligosaccharides being fully activated by dp 8 (Turnbull *et al*., 1992; Maccarana *et al*., 1993; Kreuger *et al*., 1999). Further N-sulfation and 6-O sulfation increases the strength of the FGF2:HS complex and is also required for the successful activation of the complete FGF2:FGFR1:HS complex (Lundin *et al*., 2000; Guimond *et al*., 1993; Sugaya *et al*., 2008). However, specificity is largely biased towards highly charged species of HS that have thus far been used for binding affinity studies. There is some argument for a more generalised sulfation density which can bind the growth factor just as successfully regardless of the proportions of specific sulfation domains (Jestrebova *et al*., 2006; Kreuger *et al*., 2006).

With productive FGF2-FGFR interactions having resulted in FGFR trans-phosphorylation, FGF2 signalling influences four main downstream pathways (see Figure 1.5). These include RAS-MAPK (by which many MAPK proteins are regulated); ERK 1/2, p38 and JNK; these result in inducing proliferation and survival of cells (reviewed by Ornitz and Itoh, 2015). Other pathways also induce cell survival and proliferation. For example, PI3K-AKT inhibits many pro-apoptotic effectors, promoting cell survival and AKT also induces activation of the mTOR complex and therefore proliferation (reviewed by Manning and Cantley, 2007). The third pathway, PLCϒ indirectly increases intracellular calcium and PKC, leading to an increase in mitogenesis and finally, STATs influence gene expression in cells inducing many events such as migration and tubule formation (reviewed by Ornitz and Itoh, 2015).

To date, less is known about the details of HS regulation of the other two growth factors explored in this Chapter, namely VEGF-A_{165} and PDGF-BB. VEGF-A_{165} is a splice form of VEGF containing 165 amino acids, which also contains a 44-aa sequence (exon 7) that has been shown to bind Hp. However, the presence of both exon 6 and 7, which are rich in arginine, are required to form a C-terminal HBS. In collaboration with lysine residues along the protein, a positive cluster is formed which interacts with HS (Stauffer *et al*., 2002).

Unlike FGFs, N- and 6-O sulfation are required for VEGF-A_{165} binding, with carboxylate and 2-O sulfate groups contributing to an increased binding strength (Robinson *et al*., 2006). Like FGF2, less specific sulfation arrangements of longer HS fragments, ~22mer, have been shown to activate the complex just as well. However, some shorter Hp fragments of ~dp 8 bind VEGF-A_{165}, and have been shown to be inhibitory for binding VEGFR-2 (Soker *et al*., 1994; reviewed by Koch *et al*., 2011).

Successful VEGFR phosphorylation, from the binding of VEGF-A_{165} and HS, leads to multiple downstream signalling events (Figure 1.6). PLCγ binds directly to a tyrosine residue on

the phosphorylated receptor, producing inositol 1,4,5-triphosphate which leads to an intracellular influx of Ca_2^+. Along with PLCγ, tyrosine 1213 of VEGFR also binds other SH2-containing proteins, GRB, Nck, SHP-2. Independent of these proteins, PI3K activation upon VEGFR phosphorylation leads to further downstream AKT activation and differentiation of cells. Other factors such as the stress kinase, p38 MAPK, as well as the proliferation pathway ERK1/2, are also activated (reviewed by Koch *et al*., 2011).

PDGF-BB, as discussed in Chapter 1, binds HS in a similar manner to VEGF, through antiparallel β-sheets. Within the sheets are three basic loop receptor HS binding residues. Optimum binding is supported by spaced N-sulfated residues with a further need for 6-O and to some extent 2-O sulfation to increase the binding strength. Whilst 2-O sulfation is not an absolute requirement, in HS with low levels of 6-O sulfation, increasing 2-O increases binding affinity, albeit not to the same extent (Abramsson *et al*. 2007; Feyzi *et al*., 1997; Schilling *et al*., 1998).

PDGFR activation by autophosphorylation after HS binding causes downstream tyrosine kinase activation through many SH2 domain proteins such as PI3K, as well as the independent PLCγ path, supporting survival and proliferation of cells, the activation of the receptor also signals its internalisation and degradation, thus ending its signalling. Unlike PDGFR-α, PDGFR-β also directly engages RasGAP, inactivating Ras (Engelman *et al*., 2006).

5.3 Methods

5.3.1 FGF2 Assay

BaF3 (B-lymphoid) cells transfected with a FGFR1c receptor (gifted by Dave Ornitz, Washington State University, USA) were grown to confluence in a T75 flask (ThermoFisher Scientific, UK) in normal growth media (BaF3-1c - Chapter 2). Cells were washed twice with normal growth medium by centrifugation and aspiration before being resuspended in an appropriate amount of normal growth medium ($1x10^4$/50µl per well) and plated in triplicate in a 96-well plate (CoStar, UK).

As controls for the experiment each of the following were added to the plate in 50 µl triplicates: 0.1 or 0.4 nM FGF2 (R&D Systems, UK) + assay media; 1 ng/ml IL-3 + assay media; 20 µg/ml Hp (Celsus, UK) or by-products + assay media; and assay media alone.

50 µl of assay media containing 0.4 nM FGF2 (intact by-products) or 0.1 nM FGF2 (fractions) was added to the plate in triplicate with the following concentrations of Hp or by-products: $1x10^5$, $3x10^4$, $1x10^4$, $3x10^3$, $1x10^3$, $3x10^2$, $1x10^2$ and 30 ng/ml.

Cells were incubated in test conditions at 37˚C in 5% CO_2 for 72 hours before adding 10 µl of 5 mg/ml 3-(4,5-dimethylthiazol-2-YI)-2,5-diphenyltetrazolium bromide (MTT, Sigma, UK) followed by a further 4 hour incubation. MTT is used to assess viable, metabolically active cells, producing a water soluble tetrazolium salt, which is yellow in colour; this is reduced in the mitochondria of metabolically active cells, through the action of dehydrogenase enzymes. This reaction produces an insoluble purple formazan due to cleavage of the tetrazolium ring. In order to assess the colour change, which was used as a measure of cell proliferation, formazan is solubilised with 100 µl of 10% SDS/0.01N HCL (Sigma-Aldrich, UK) per well and incubated overnight. Plates were read on a MultiScan Ex plate reader (ThermoFisher, UK) at 570 nm.

5.3.2 PDGF-BB Assay

NIH3T3 cells (ATCC, USA) were seeded at $2x10^4$ per well on a 24 well plate and allowed to adhere overnight in growth media (NIH3T3 – Chapter 2) at 37˚C in 5% CO_2. Normal media was aspirated off and replaced with starvation media, to sync the cell cycle, and incubated under the same conditions for 24 hours.

Cells in triplicate were exposed to the following conditions: starvation media (SM); growth media; SM + 20 µg/ml Hp/by-products; SM + 30 ng/ml PDGF-BB; and SM + 20 µg/ml

Hp/by-products and 30 ng/ml PDGF-BB (Peprotech, UK). Experimental conditions were applied at 48 and 72 hours after starvation, with fresh starvation media. After 48 hours in experimental conditions, the media was aspirated off and the DNA in the nucleus of cells were stained with 500 µl 0.5% crystal violet (Sigma-Aldrich, UK) in 20% methanol (ThermoFisher Scientific, UK) for 5 mins, washed twice with PBS (Gibco Lifesciences, UK) and 300µl 10% SDS was used to solubilise the stained cells and the absorbance of the wells read on an MultiScan Ex plate reader at 590 nm.

5.3.3 VEGF-A_{165} Assay

Human umbilical vein endothelial cells (HUVECs), at passage 6, were grown to confluence in a T75 flask in normal growth medium (HUVEC – Chapter 2). Cells were trypsinised using 1.5 ml of trypsin (Sigma, UK) per flask, counted and replated $3x10^5$ cells per well in a 6 well plate with 2 ml of normal growth media and left overnight to adhere.

Cells were washed twice in PBS and starved for 5 hours with endothelial media supplemented with 0.1% BSA, but lacking supplements or FBS. After starvation 10 µg/ml of Hp or by-products were added with 10 ng/ml of VEGF-A_{165}, and cells were returned to the incubator for 10 minutes.

After incubation plates were washed twice with PBS before cells were lysed on ice with 100 µl RIPA buffer (Chapter 2), containing protease and phosphatase inhibitors (Cell Signalling Technology, UK). Cells were scraped off and placed in an Eppendorf tube and allowed to mix via spinning at 4°C for 30 minutes in the RIPA buffer. Lysed cells were then centrifuged at 13200 RPM at 4°C for 20 minutes, and the supernatant was collected and frozen at -80°C.

Protein content was quantified using a standard Bicinchoninic acid assay (BCA) (reagents-ThermoFisher, UK) comparing the colour change to known BSA standards (2, 1.5, 1, 0.75, 0.5, 0.25, 0.125 and 0 mg/ml). A calibration curve was made from the standards and used to quantify protein content in the samples.

The results of the assay were visualised using a Western blot. 15 µg of protein per well was loaded onto 12% acrylamide gels (40% 37.5:1 bis-acrylamide:acrylamide - Sigma, UK) and the protein was separated for 1.5 hours at 160 V before being transferred onto a nitrocellulose membrane (Sigma, UK) for 2 hours and 100 V.

Membranes were blocked for an hour at room temperature with 5% BSA in TBST. Primary antibodies – anti-P-AKT^{Ser473} and anti-P-ERK 1/2 (Cell Signalling Technology, UK)

dilutions of 1:1000 and anti-Vinculin 1:10000 (Cell Signalling Technology, UK) to the blocking buffer and left agitating on the membrane overnight at 4°C.

Membranes were washed three times with Tris-buffered saline with tween (TBST) before an HRP IgG anti-rabbit secondary antibody (Cell Signalling Technology, UK) was added at 1:10000 and left agitating on the membrane for an hour at room temperature.

After the secondary incubation, membranes were washed with TBST (x3) followed by one wash with TBS before the membranes were then probed using an ECL kit (ThermoFisher, UK) and imaged using a QuantLaser (GE Healthcare, UK).

Image J was used to quantify the blots and data was normalised by total AKT and ERK (Cell Signalling Technology, UK) for intact samples, and Vinculin (Abcam, UK), for fractionated material.

Antibody	Dilution	Supplier/Cat No.
P-ERK 1/2	**1:1000**	CST/9101
P-AKT^{Ser473}	**1:1000**	CST/9271
Total ERK 1/2	**1:1000**	CST/9102
Total AKT	**1:1000**	CST/9272
Vinculin	**1:10000**	Abcam/129002
Rabbit Secondary	**1:10000**	CST/7074

Table 5.1 - A summary of antibody dilutions used for VEGF-A_{165} and by-product induced phosphorylation.

5.4 Results

5.4.1 Investigating the Effects of the Intact By-Products and Hp in Combination with FGF2 on Proliferation of BaF3-1c Cells

BaF3-1c, are B-lymphoid cells requiring IL-3 for proliferation and survival, which have been transfected with an FGFR1c receptor. These cells can respond to the presence of exogenous Hp/HS in the absence of IL-3, it is also important to note that the cells also do not produce endogenous HS and therefore this is a response from null. BaF3-1c cells were plated $1x10^4$ cells per well in a 96 well plate and used to establish activation of FGF2 signalling in the presence of Hp or by-product samples at concentrations from 0.03-100 μg/ml. Absorbance of the sample at 570 nm, after incubation with MTT was used as a proxy measure of cell proliferation.

From an initial assessment, all by-product samples stimulate proliferation in a concentration dependent manner, similar to the action of Hp (Figure 5.1). Minimal impact on cell proliferation is seen at the lowest concentration. The largest increase in proliferation was seen at concentrations between 3-30 μg/ml. All by-product samples showed significant changes in the induction of proliferation at several concentrations, when compared to Hp ($P<0.05$), particularly at 30 and 100 μg/ml (Figure 5.1B and Table 5.2).

Samples D1 and H showed substantially more activity at higher dilutions compared to that of Hp along the concentration curve (D1- 100, 30, 3, 0.1 and 0.03 μg/ml, H- 100, 30, 10, 0.3 and 0.1 μg/ml – Figure 5.1 and Table 5.2). This suggests that they were more able to activate the FGF2/R1c pathway compared to Hp. By-product M1, whilst having a significant increase in proliferation over Hp at multiple concentrations (3 μg/ml and to a lesser extent 100/30 μg/ml), overall appeared to have a similar activity to Hp. F1 is the least able to induce proliferation, albeit still having 3 concentrations with higher proliferation levels than Hp, 100, 30 and 0.3 μg/ml.

When comparing the two samples which are available in large batches, D1 and F1, D1 was considerably better at facilitating BaF3-1c cell proliferation at all concentrations than F1. The most notable difference was seen at the lower concentrations before the maximum rate of cell growth (0.03 and 0.1 μg/ml).

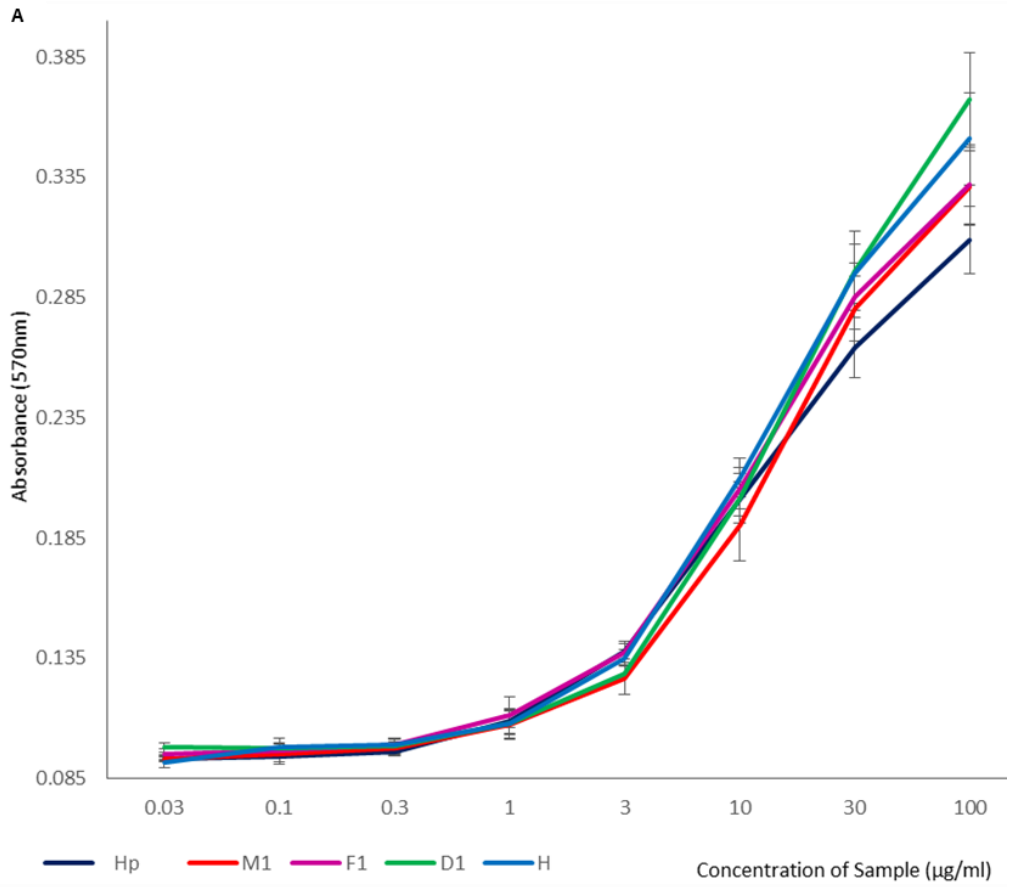

Figure 5.1 - Proliferation of BaF3-1c cells was induced Hp or by-products in response to FGF2. Cells were incubated in the presence of 0.4 nm FGF2 and a range of by-product samples or Hp control (0.03-100 µg/ml) for 72 hours. MTT was added to the wells with a further 4-hour incubation. The assay was stopped by addition of 10% SDS/0.01% HCl and incubated overnight. Absorbance of samples was read at 570 nm. Panel A - the whole concentration curve, Panel B – magnified view of 1-100 µg/ml (n=triplicate of 3 biological repeats (9)).

Concentration (µg/ml)	M1	F1	D1	H
100	0.002	0.002	<0.0001	<0.0001
30	0.005	0.0006	<0.0001	<0.0001
10	-	-	-	0.01
3	<0.0001	-	0.002	-
1	-	-	-	-
0.3	-	0.0006	-	0.009
0.1	-	-	0.002	0.003
0.03	-	-	<0.0001	-

Table 5.2- P values for by-products compared to Hp for FGF2 induced proliferation of BaF3-1c cells. The mean and standard error for each sample was calculated. Multiple t-tests (p=0.05, n=3) were carried out for all repeats, at all concentrations and samples were compared to Hp. The p values are represented in the table, - represents non-significant results, an increase above Hp and a decrease below Hp.

5.4.2 Investigating the Impact of Heparinase III Digestion and Size Separation on FGF2 Induced Proliferation of BaF3-1c Cells

By-products D1 and F1 were digested with heparinase III and separated by size. As discussed in Chapter 3, heparinase III cuts at the low sulfated regions of the chain, thereby producing a good range of products, especially when then separated by size. This initial refinement aimed to investigate differences in biological activity compared to the parental material, with a view to potential, future rigorous refinement to produce fractions tailored to specific growth factors.

Fraction D1

Size fractionated products were tested to investigate whether their biological activity was affected by digestion with heparinase III and size separation when compared to the intact parental material. As discussed in Chapter 1, polysaccharides ranging in sizes ~dp 6 have been shown to induce FGF2 signalling. To date a preferential moderately sulfated octasaccharide showed optimum activity, which is then maintained up to ~dp 14 (Walker *et al*., 1994).

D1 was fractionated into 8 peaks, ranging in size from dp 2 – dp 18+ (Table 4.1). Initially, the results showed a spread in size dependent increase in FGF2/FGFR1c/HS induced proliferation (Figure 5.2). Multiple t-tests were used to compare the intact material to each of the fractionated by-products at concentrations of 0.03-100 µg/ml (p=0.05). The larger fractions, 5-8, showed no significant differences at any concentration compared to the control intact material. The smaller fractions (1-4) showed similar activity to the intact material at the slowest rates of growth at either end of the concentration range. However, interestingly they

show some appreciable differences in the middle of the concentration range (3 and 10 µg/ml), where the greatest dose-dependent increases in rate of cell proliferation occurred (p=0.05, Table 5.3).

Fraction F1

F1, similarly to D1, was fractioned into 8 peaks, which were than used to treat BaF3-1c cells as described above. Multiple t-tests were used to compare the intact material to each of the fractions at concentrations from 0.03-100 µg/ml. F1 showed more significantly different changes in activity than D1. At lower concentrations (0.3 and 1 µg/ml), the largest fractions (F1:7 and :8) showed a significant increase in activity compared to the intact parental material. However, this was counteracted by a larger spread of small material showing a significant decrease in ability to induce proliferation at mid-high concentrations (~3-100 µg/ml – Table 5.4).

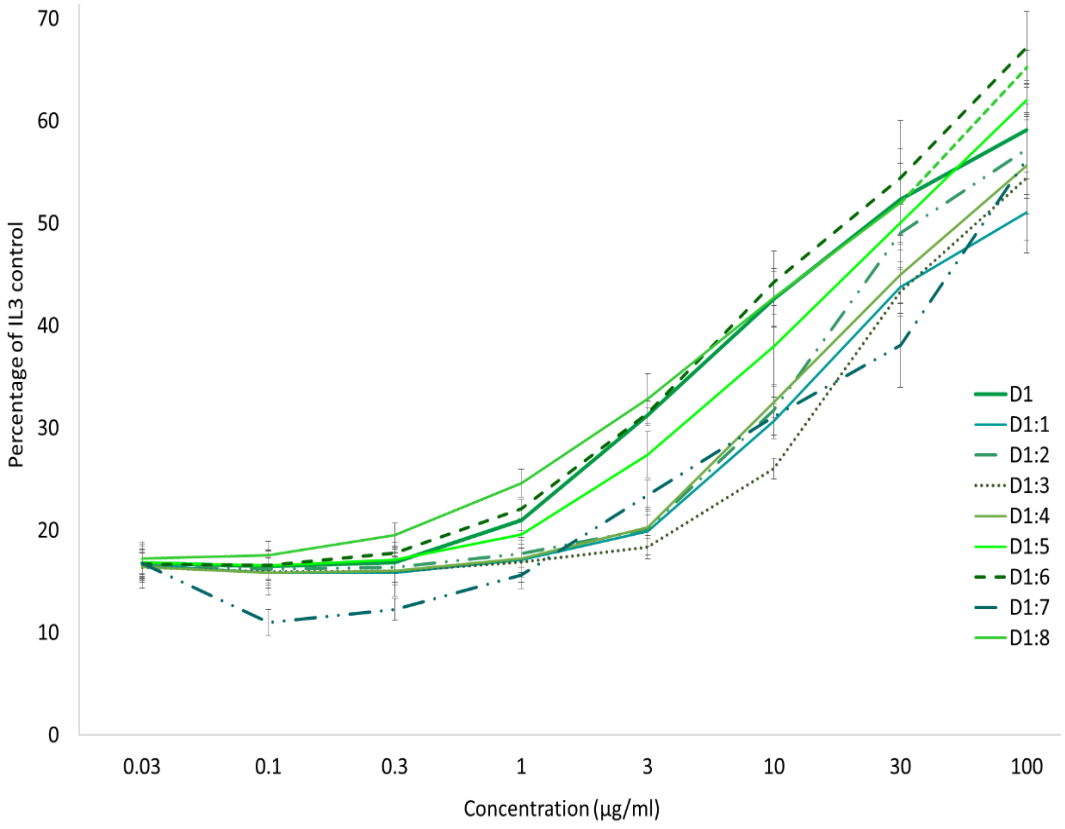

Figure 5.2- Proliferation of BaF3-1c cells induced by D1 and size fractionated products, in response to FGF2. Cells were incubated at 37°C, 5% CO_2 in the presence of 0.1 nm FGF2 and a range 0.03-100 µg/ml D1/fractions for 72 hours. 5 µl of 5 mg/ml MTT were added to each of the wells with a further 4 hour incubation. The assay was stopped by addition of 10% SDS/0.01% HCl and incubated overnight, absorbance was read at 570 nm (n=triplicate of 3 biological repeats (9)).

Concentration (µg/ml)	D1:1	D1:2	D1:3	D1:4
3	0.002	0.004	0.0007	0.001
10	0.01	0.04	0.005	0.03

Table 5.3 – P values for results of fractionated D1 products which show a significant decrease in activity compared to intact D1 for FGF2 induced BaF3-1c cell proliferation. Multiple t-tests for each concentration were used to compare the fractionated material to the intact (p=0.05, n=3)

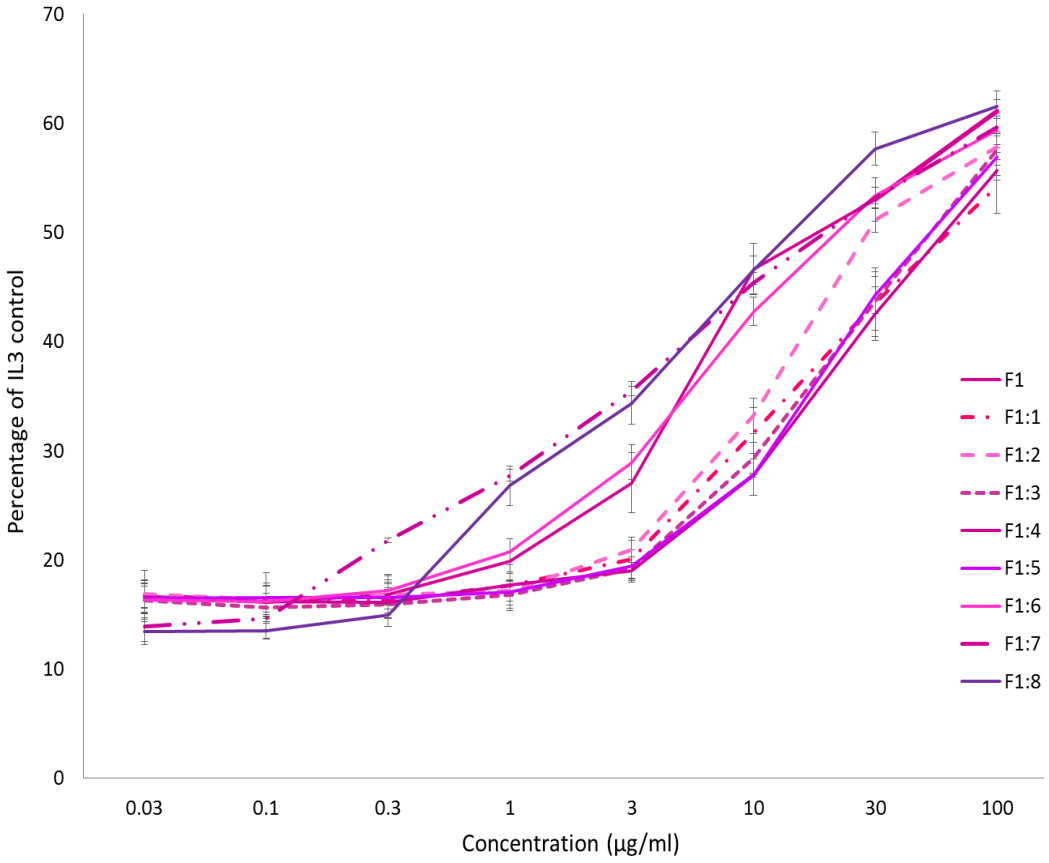

Figure 5.3- Proliferation of BaF3-1c cells induced by F1 and size fractionated products in response to FGF2. Cells were incubated at 37°C, 5% CO_2 in the presence of 0.1 nm FGF2 and a range 0.03-100 µg/ml F1/fractions for 72 hours. 5 µl of 5 mg/ml MTT were added to each of the wells with a further 4 hour incubation. The assay was stopped by addition of 10% SDS/0.01% HCl and incubated overnight, absorbance was read at 570 nm (n=triplicate of 3 biological repeats (9)).

Concentration (µg/ml)	F1:1	F1:2	F1:3	F1:4	F1:5	F1:7	F1:8
0.3	-	-	-	-	-	0.008	-
1	-	-	-	-	-	0.002	0.003
3	-	-	-	0.05	-	-	-
10	0.005	0.009	0.003	0.001	0.003	-	-
30	0.03	-	0.05	0.03	0.03	-	-
100	0.04	-	-	0.05	-	-	-

Table 5.4 – P values for the results of fractionated F1 products that show a significant change in activity compared to intact F1 of FGF2 induced BaF3-1c cell proliferation. Multiple t-tests for each concentration were used to compare the fractionated material to the intact (p=0.05, n=3)

5.4.3 Investigating the Impact of By-Products and Hp in Combination with PDGF-BB on NIH3T3 Cell Proliferation

NIH3T3 rat dermal fibroblast cells were used as they are a fast growing, robust established cell line, which can be used as a target for PDGF-BB induced proliferation. They were plated at $2x10^4$ per well in a 24 well plate, cells were left to adhere for 24 hours, following this starvation media was added and the cells were incubated for a further 24 hours. At 48 and 72 hours cells were treated with 30 ng/ml PDGF-BB and 20 µg/ml of Hp or by-products. These concentrations were selected after initial preliminary testing (data not shown). The assay was finished at 96 hours, at which point the cells were stained with 0.5% crystal violet, washed with PBS and solubilised with 10% SDS. Absorbance was read at 590 nm and used as an indicator of cell proliferation.

When evaluating the results, significant variation across biological repeats was noted for the results of PDGF-BB and by-product/Hp in combination (data not shown). Therefore, statistics were completed on triplicates within one experimental repeat for all samples and the trend across 3 biological repeats are discussed below. The by-product samples alone did not elicit any increase in cell proliferation above the starvation media control (~0.4 AU Average). T-tests were used to compare samples in combination with PDGF-BB to PDGF-BB alone and also to Hp as a control (p=0.05). All of the samples combined with PDGF-BB showed a significant increase in NIH3T3 cell proliferation when compared to PDGF-BB alone (except for one biological repeat of H, Figure 5.4). Sample M1 appeared to induce the highest level of cell proliferation in all biological repeats and showed a statistical increase in two repeats compared

to Hp (p=0.03 and 0.003). The general trend of the intact material across all three repeats suggests that M1 was the most potent at inducing PDGF-BB driven proliferation, H produced only one case out of 3 biological replicates that showed statistical significance when compared to Hp, suggesting it may be slightly better. Finally, D1 and F1 showed no significant difference across all three repeats. There was also no significant difference seen across all repeats between D1 and F1 PDGF-BB induced proliferation (Figure 5.4).

5.4.4 Investigating the Impact of Heparinase III Digestion and Size Separation of By-Products D1 and F1, on PDGF-BB Induced Proliferation of NIH3T3 Cells

Size separated fractions were also compared to the intact parental material for both D1 and F1 to investigate whether the heparinase III digestion of the by-products produced samples exhibiting different biological activities. For both, t-tests showed that none of the 8 fractions have a greater effect on cell proliferation than the intact, parental material. All samples showed either a statistically similar or possibly reduced level of proliferation compared to the parental material. The most noticeable pattern amongst the fractionated material was the effect that both of the largest fractions (D1 (7 and 8) and F1 (8)) maintain a statistically lower level of proliferation across all three biological repeats.

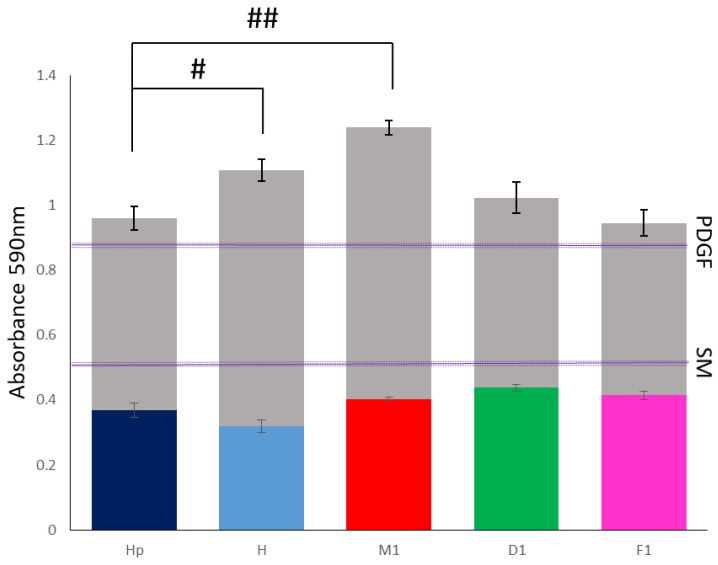

Figure 5.4- NIH3T3 cells show increased proliferation when media is supplemented with Hp or by-product samples in response to PDGF-BB. $2x10^4$ cells were plated per well in a 24 well plate and starved for 24 hours. At a further 24 and 48 hours the starvation media was supplemented with 20 µg/ml Hp or by-products and 30 ng/ml PDGF-BB. Cells were stained with 0.5% crystal violet and solubilised with 10% SDS. Coloured bars represent samples alone, grey + colour bars represent samples in combination with PDGF-BB. T-tests were used to evaluate statistical significance in triplicate and trends were compared across three biological replicates (p=0.05). NB- # indicates the number of repeats which show a statistical increase when compared to Hp. PDGF and starvation media (SM) alone show both the mean and SEM.

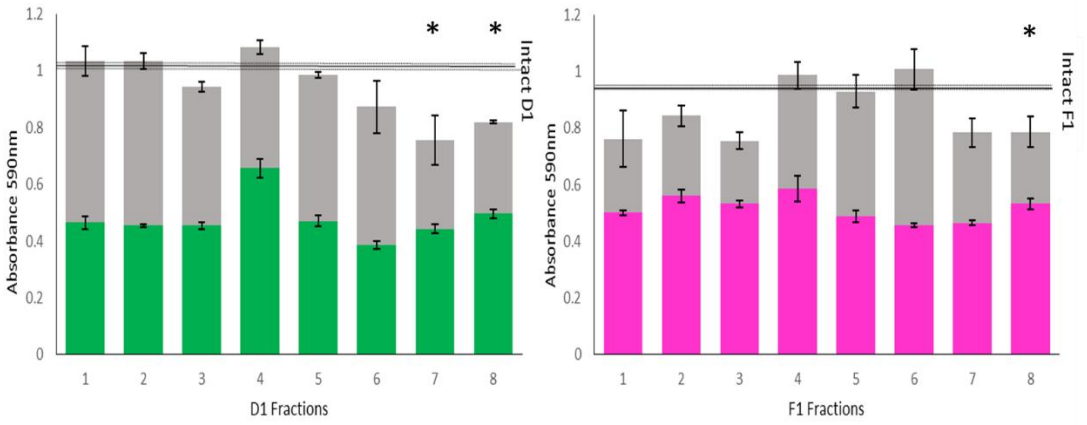

Figure 5.5- By-product samples D1 and F1 digested with heparinase III and separated by size, show equal or reduced PDGF-BB driven NIH3T3 cell proliferation compared to the intact parental material. $2x10^4$ cells were plated per well, starved for 24 hours. At a further 24 and 48 hours the starvation media was supplemented with 20 µg/ml Hp or by-products and 30 ng/ml PDGF-BB. Cells were stained with 0.5% crystal violet and solubilised with 10% SDS. Coloured bars represent samples alone, grey + colour bars represent samples in combination with PDGF-BB. T-tests were used to evaluate statistical significance in triplicate and trends were compared across three biological replicates (p=0.05), * indicates a significant decrease, vs parental material, in proliferation on all biological repeats.

5.4.5 Investigating Phosphorylation of ERK 1/2 and AKT^{Ser473} in Primary HUVECs, After Incubation with VEGF-A_{165}, in the Presence of Hp or By-Products

Primary human umbilical vein endothelial cells at passage 6 were plated at $3x10^5$ cells in a 6 well plate. for 10 mins, further incubation led to a decrease in ERK1/2 phosphorylation (Appendix D.2). Cells were lysed and proteins were separated by electrophoresis and subjected to Western blotting, to investigate phosphorylation of ERK1/2 and AKT^{Ser473} by specific antibody detection. Measurement of phosphorylation of the receptor was undertaken, however, the results were very inconsistent, with large amounts of non-specific signalling (Appendix D.1). An increase in cell number was required to acquire enough protein. However, this led to cell stacking and eventual tubule formation in the wells, suggesting that the cells were cultured under improper growth conditions. Along with the added problem of growing enough cells whilst maintaining a low passage number, led to alternative measurements of downstream phosphorylation events being explored. Cells were left to settle overnight before being starved in serum free media for 5 hours and treated with 10 ng/ml VEGF-A_{165} and/or 10 µg/ml of Hp or by-products

Comparison of ERK1/2 activation with all by-products and Hp show a large increase in phosphorylation over the VEGF-A_{165} control (Figure 5.6). As the trend of both ERK 1 (44 kDa) and ERK 2 42 kDa) are the same for each sample, the analysis of the two are combined in the quantitative output (Figure 5.6 - Panel B) By-products or Hp without VEGF-A_{165} did not elicit a

greater response than starvation media alone. When comparing to Hp and VEGF-A_{165}, the levels of phosphorylation of all the by-products appeared to be greatly reduced. F1, as the least sulfated sample, appeared to be the least able to activate the ERK pathway potentially leading to less cell proliferation than the other samples.

Interestingly, the trend observed for the activation of AKT^{Ser473} appeared to follow a different pattern to that of ERK. Sample H showed the highest level of AKT^{Ser473} phosphorylation, with D1 showing a similar increase to that of Hp. F1 and M1 appeared to show no difference in their ability to activate the pathway, with both having lower activity than Hp (Figure 5.7).

D1 elicits more phosphorylation of both ERK 1/2 and AKT^{Ser473} than F1 in both Western analyses, also supporting the other findings that these responses are both favoured by more highly sulfated saccharides.

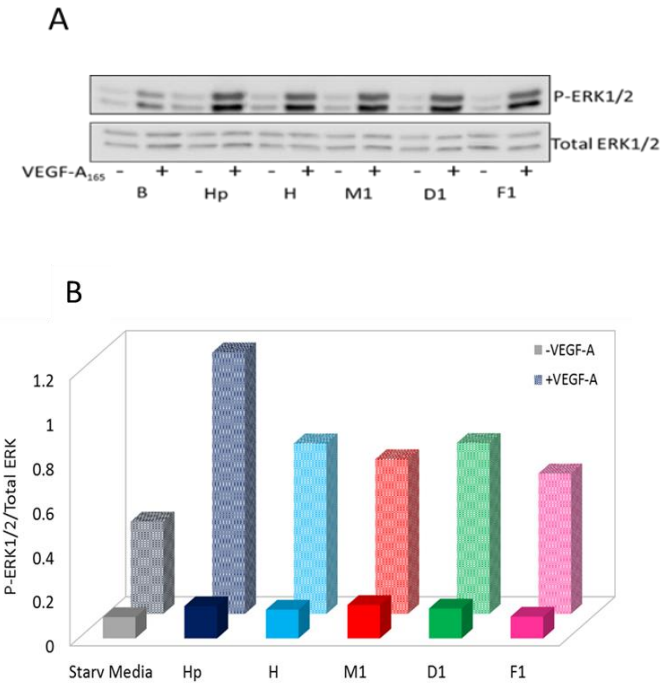

Figure 5.6 – Phosphorylation of ERK1/2 detected by Western blot analysis of HUVECs treated with Hp and by-products and/or VEGF-A_{165}. 3x10^5 cells were plated, starved for 5 hours and treated with 10 ng/ml VEGF-A_{165} and/or 10 µg/ml Hp/by-products for 10 mins. Cells were lysed and 15 µg of protein separated on a 12% gel. After transfer, membranes were incubated with P-ERK1/2 (1:1000) and a rabbit secondary (1:10000). Membranes were washed and incubated with ECL and imaged by chemiluminescence (Panel A). All samples show an increase in activation when compared to VEGF-A_{165} alone. Hp appeared to show the greatest level of ERK1/2 phosphorylation (Panel B, n=1).

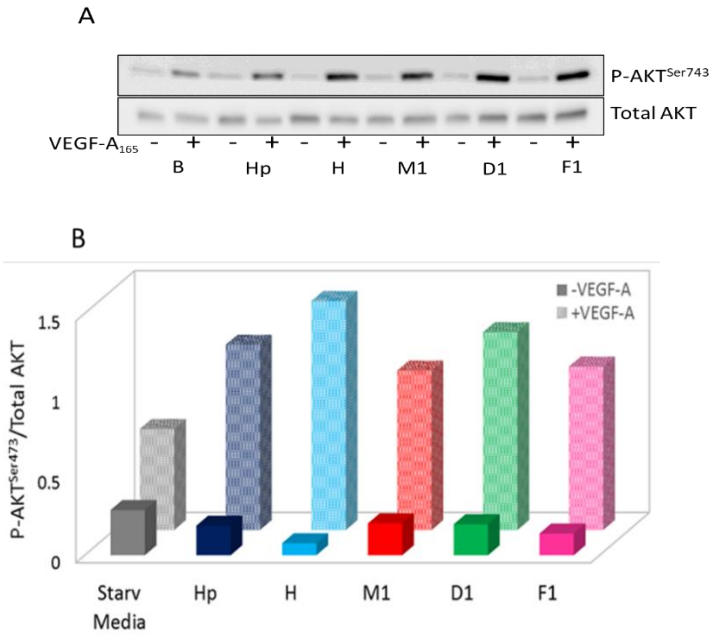

Figure 5.7 - Phosphorylation of AKT^{Ser473} 473 detected by Western blot analysis of HUVECs treated with Hp and by-products and/or VEGF-A$_{165}$. 3x10^5 cells were plated, starved for 5 hours and treated with 10 ng/ml VEGF-A$_{165}$ and/or 10 µg/ml Hp/by-products for 10 mins. Cells were lysed and 15 µg of protein separated on a 12% gel. After transfer, membranes were incubated with AKT^{Ser473} (1:1000) and a rabbit secondary (1:10000). Membranes were washed and incubated with ECL and imaged by chemiluminescence (Panel A). Sample H and D1 show the largest phosphorylation of AKT^{Ser473} of the samples (Panel B, n=1).

5.4.6 Investigating Phosphorylation of ERK 1/2 and AKT^{Ser473} in Primary HUVECs, After Incubation with VEGF-A$_{165}$ in the Presence of D1/F1 By-Products Digested with Heparinase III and Separated According to size

Size separated fractions were also tested for their ability to initiate ERK1/2 and AKT^{Ser473} signalling in HUVECs and the change compared to intact parental by-product material. All of the D1 size fractionations appeared to show a decrease in phosphorylation of AKT^{Ser473} when compared to the intact material, with a trend towards less activity in the larger fractions, agreeing with the data from the intact, parental material, with H being the smallest but most active by-product. Interestingly, the larger fractions generally produced greater responses of the ERK pathway compared to intact D1 (Figure 5.8).

Fractionated F1 appeared to show a different trend to that of D1, where all of the size separated fractions, exhibited a decrease in phosphorylation of ERK 1/2 compared to the parental, intact material (the largest fraction has similar activity). However, the larger fractions of F1 (5 and 7) did elicit an increase in activity of AKT^{Ser473} compared to the smaller factions and

slightly more than the intact control, suggesting that an increase in size and therefore sulfation leads to an increase in activity (Figure 5.9).

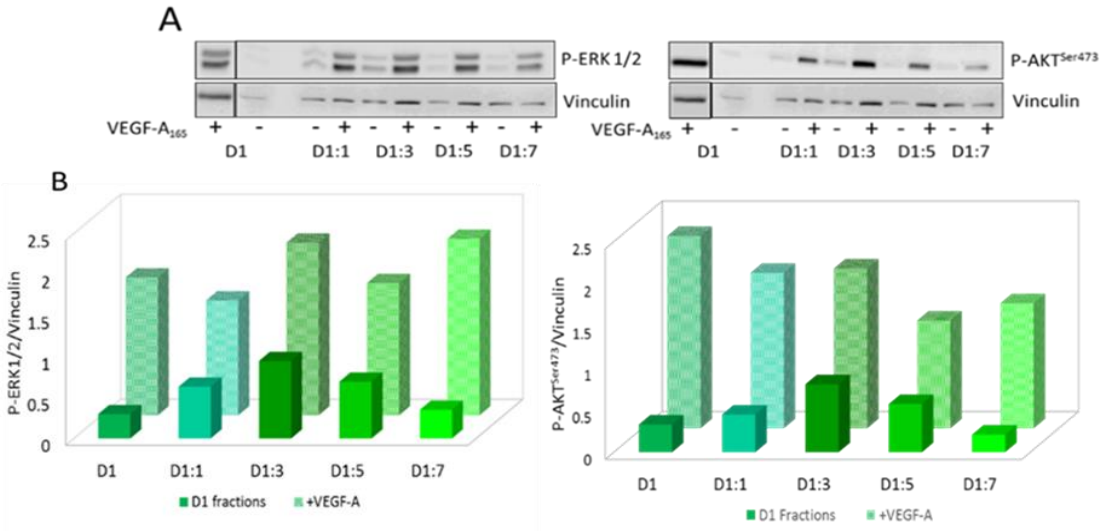

Figure 5.8 - Phosphorylation of ERK1/2 and AKT^{Ser473} detected by Western blot analysis of HUVECs treated with D1 and its sized fractions and/or VEGF-A$_{165}$. 3x10^5 cells were, starved for 5 hours and treated with 10 ng/ml VEGF-A$_{165}$ and/or 10 µg/ml fractionated by-products for 10 mins. Cells were lysed and 15 µg of protein separated on a 12% gel. After transfer, membranes were incubated with P-ERK 1/2 and P-AKT^{Ser473} (1:1000), Vinculin (1:10000) and a rabbit secondary (1:10000). Membranes were washed and were incubated with ECL and imaged by chemiluminescence. The larger fractions appear to show an increase in ERK phosphorylation compared to the intact control, whilst none of the fractions activated the AKT^{Ser473} pathway as greatly as intact D1. Panel A, Western blot analysis, Panel B, quantification of Western blot (n=1).

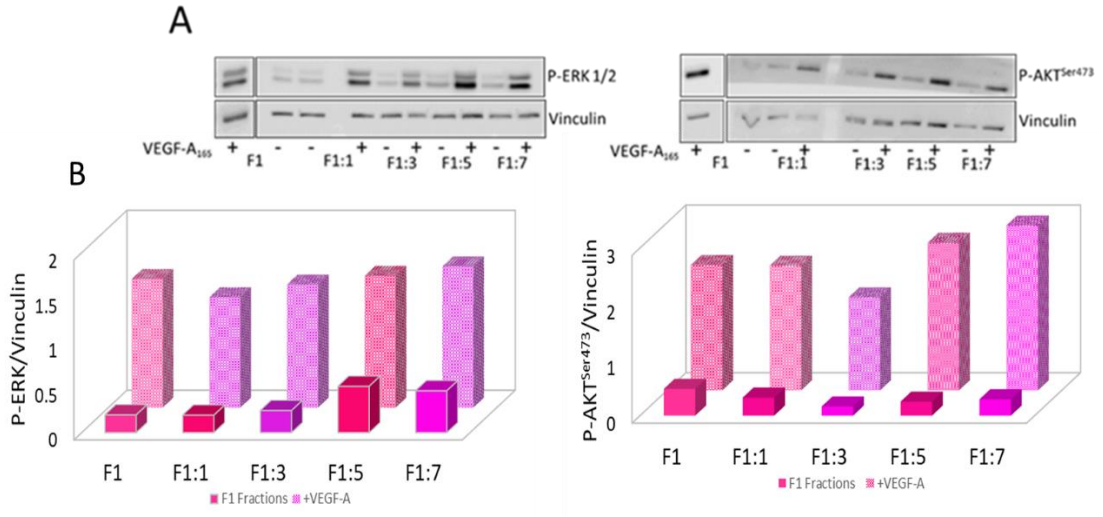

Figure 5.9 - Phosphorylation of ERK1/2 and AKT^{Ser473} detected by Western blot analysis of HUVECs treated with intact F1 and its sized fractions and/or VEGF-A$_{165}$. 3x10^5 cells were, starved for 5 hours and treated with 10 ng/ml VEGF-A$_{165}$ and/or 10 µg/ml fractionated by-products for 10 mins. Cells were lysed and 15 µg of protein separated on a 12% gel. After transfer, membranes were incubated with P-ERK 1/2 and P-AKT^{Ser473} (1:1000), Vinculin (1:10000) and a rabbit secondary (1:10000). Membranes were washed and were incubated with ECL and imaged by chemiluminescence. Whilst most of the fractions show comparable activity to the parental intact control, the smallest fractionated product showed a decrease in ERK phosphorylation. The larger two fractions appear to show an increase in activity above all other fractions and intact material for AKT^{Ser473}. Panel A, Western blot analysis, Panel B, quantification of Western blot (n=1).

5.5 Discussion

A general comparison of the biological activities of the by-products with the three growth factors suggests that all by-products showed appreciable differences compared to Hp in terms of activation of particular signalling pathways. By scoring the by-products 1-5 (least to most active) on the basis of how well they induce growth factor activity in each assay, the samples can be ranked in the order H>D1>M1>F1. This order also correlates with decreasing levels of sulfation, as discussed in Chapter 3. However, looking more in depth, this trend only appeared to hold for the lowest sulfated by-product, F1. In this case it appeared to be the least active in both PDGF-BB and VEGF-A_{165} activation and only showed an increase above Hp with FGF2 at the most extreme concentrations (where the lowest rate of proliferation occurs).

FGF2 signalling

The results of the proliferation assays with BaF3-1c cells, showed that FGF2 favours the highly sulfated sample H and D1 at more concentrations, than both the other by-products and Hp. The structural difference across the samples appeared to show some structure-activity correlations. Those containing more di- and tri-sulfated saccharides, H and D1, are more potent for FGF2 activation than the next most active sample (M1), when compared to Hp. Both H and D1 also contained a higher abundance of 6-O sulfation compared to M1, which is known to be vital for orchestrating the dimerization of FGFR and binding to FGF2 (Pye *et al.*, 1998). Interestingly, H also showed a higher level of 2-O sulfation, shown to be important for dimerization and binding of FGF2 (Guglier *et al.,* 2008). Although all three showed comparable levels of N-sulfation, together, this evidence strongly supports the relevance of increased levels of 6-O and 2-O sulfation for successful binding, activation and therefore FGF2-induced proliferation of BaF3-1c cells. Whilst H has comparable overall sulfation to Hp, and similar amounts of 2-O and 6-O sulfation, it must be noted that, on average, by-product H had a much smaller chain length than Hp. Chains being smaller on average would not only increase the presence of single chains in the same concentration of solution compared to longer Hp, but could also favour binding of the growth factor and receptor on these particular cells. The expression of the receptors on the cell surface of BaF3-1c is far greater in number than on endogenously expressing cells. Hp being larger would be more likely to sequester FGF2 at the cell surface next to a receptor binding site that it is also blocking, due to its overall length, preventing successful activation of those receptors, whilst rendering the bound growth factor inactive.

From the digestion of D1 and F1, size separation of the by-products strongly suggests that, unless added in excess at high concentrations, oligosaccharides below ~dp 8-10 are far less active than intact chains. Only minimal differences dependent on sulfation were noted at this level of refinement (F1 fractions 1-5 have significantly lower activity than the intact, compared to 1-4 of D1 – Table 5.3 and 5.4), but any fractions larger than this optimum binding size had comparable activity compared to the intact, parental control.

PDGF-BB signalling

In contrast, proliferation of NIH3T3 cells induced by activation of PDGF signalling presents a very different pattern of response to by-products than that of FGF2 signalling. Whilst F1 was still the least active by-product, the amount of proliferation induced by F1 also corresponded closely to Hp and D1 in these assays. By-product M1 appeared to induce the greatest degree of proliferation, followed by H. These two by-products both had similar levels of N- and 6-O sulfation, which were similar to that of Hp (Chapter 3- Figure 3.8). However, M1 and H also both had greater amounts of GlcNAc residues and thus possibly NA domains, which could potentially provide spaces between regions of N- and 6-O sulfation, which have been shown to be optimal for PDGF activation (Abramsson *et al*. 2007; Feyzi *et al*., 1997; Schilling *et al*., 1998).

Size separated fractions of D1 and F1 did not appear to greatly change PDGF-BB driven cell proliferation, suggesting that the size of these by-products was less important than the sulfation. This theory was also supported by the size differences and relative activity of the two most active by-products (H ~8800 Da, M1 ~11500 Da) and relatively similar activity.

VEGF-A_{165} Signalling

For activation of VEGF-A_{165} induced ERK1/2 phosphorylation, Hp, as the most sulfated polysaccharide appeared to be more successful at initiating activation than the by-products. Results for ERK1/2 activation also suggest that there was no particular sulfation patterns for the sugar which are favoured for successful phosphorylation events. However, the overall level of activity does correlate with the level of sulfation, Hp being the most sulfated and most potent activator of ERK1/2 followed by H>M1>D1>F1 (Figures 3.9 and 5.6). AKT^{Ser743} activation also favoured the highly sulfated by-products, however, like FGF2 signalling, it appeared to favour the smallest by-product sample, H. Size also appeared to have the largest influence with fractionated D1 and F1 activity. Whilst none of the fractionated material reached the level of the parental intact D1, it can be tentatively suggested that the larger fractions of F1 have a

greater level of activation than the smaller fractions. Overall these results suggested VEGF signalling favours highly sulfated, mid-size oligosaccharides for optimal activity.

General comments

The PDGF-BB and the VEGF-A_{165} activity were induced in cells which produce endogenous Hp and growth factors. It is important to note that the activity based on these assays are due to exogenous Hp activity above that of the base level produced by the cells naturally. HUVECs in particular, as a sensitive primary cell line, also require the addition of Hp into the normal growth media, although this was absent from the starvation media. During this project HUVECs were grown in culture in several types of media, including mixtures of Hams F12 and DMEM, with differing concentrations of Hp and serum. However, this led to a drastic decrease in cell proliferation (data not shown) and the subsequent inability to complete the assay. Both the VEGF-A_{165} and PDGF-BB assays could be established in cell lines such as BaF cells, where their receptor is transfected onto the cell membrane and no endogenous Hp is produced. This would reduce the background of the control conditions and give results purely based on the growth factor-saccharide interaction. On the other hand, like the BaF3-1c cells and FGF2 activity, the abundance of receptors at the cell surface of these cells are more than would typically occur naturally. It could be suggested that there would be some changes in the activity profile of polysaccharides when switching to a naturally derived cell line where receptors are less frequent and there is competition for the saccharides.

In conclusion, the structure-activity investigation of all by-products, in combination with several growth factors agrees with previous work on Hp/HS by many other groups. However, the extent of the difference in biological activity observed in the parental intact material compared to Hp and the influence of size and sulfation of these previously unknown structures is interesting. In particular, FGF2 and PDGF-BB assays suggests that the growth factors do indeed have preferential sulfation patterns and sizes of oligosaccharides for optimal activity. Whilst all of the by-products show a good level of biological activity, H and D1 in particular showed a substantial increase in growth factor driven cellular responses in multiple assays above that of Hp. The size fractionation of D1 and F1 also showed some interesting activity and even at this level of refinement we could possibly select better oligosaccharides for specific growth factor activity. For example, fractions of at least ~dp 6-8, such as fraction 7/8, would reduce PDGF-BB interaction whilst not affecting either FGF2 or VEGF-A_{165} activity, whereas FGF2 activity could be minimised by selecting smaller fractions (1-4) without significantly impacting PDGF-BB and VEGF-A_{165} activity. This suggests that the by-products may

be of use in further understanding protein-HS interactions. However, these responses could be explored in more detail and in different cell lines to establish a clearer idea of the relationship between growth factor activation and the by-products.

Chapter 6- Side Effects and Biological Applications of By-Products

6.1 Aims

The aim of studies described in this final results Chapter was to explore the possible of off-target activities of the by-products, with a view to their potential therapeutic applications. This was accomplished by comparing the anticoagulant activities of the sample, the main purpose of current Hp drugs, and possible toxic effects on cells. The purpose of these assays was to ascertain the samples' levels of some potential undesirable off-target effects, which would be detrimental for any therapeutic use.

A further aim in this Chapter was to explore the possibility of the by-products in protecting neural cells from apoptosis when they are infected with Zika virus. Although mechanisms underlying how Hp reduces apoptosis and protects neuroblast cells is unknown, it has been suggested that there may be a role for Hp in the reduction of apoptotic signalling and thus apoptotic death (Ghezzi *et al.,* 2017). Therefore, a desirable outcome would be to obtain by-products which possessed both low toxicity, low anticoagulant activity and the ability to inhibit cell death following Zika virus infection.

6.2 Introduction

As discussed in Chapter 1, the principle purpose of pharmaceutical Hp is to function as an anticoagulant. However, for other applications it is not an advantageous property, therefore the anticoagulant properties of the by-products needs to be tested. There are several points along the coagulation pathway where Hp can disrupt the successful production of a fibrin clot and this can be tested by partial thromboplastin (PT) and activated partial thromboplastin time assays (APTT) (Figure 1.4).

PT is a synthetic substitute for the protein thromboplastin. It reflects the extrinsic and common pathways, including factors II, V, VII and X. The assay assesses the integrity of these pathways and thereby Hp's ability to disrupt it, this output was assessed by the time taken for blood to clot (Korsen-Bengsten, 1971). APTT also monitors the ability of a clot to form due to factors affected by Hp, however, in this case, in the intrinsic and common pathways. The APTT assay is able to monitor more factors than PT including; VIII, IX, XI, XII and fibrinogen, making it a more sensitive assay (Reviewed by Chee and Greaves, 2003).

Testing the inhibition of factors IIa and Xa in the coagulation cascade (Figure 1.4) was also possible and it is something that should be explored for these samples in the future. For

this thesis, a global approach was taken to understand the abilities of the by-products to interfere in the coagulation pathway in general.

As well as monitoring the anticoagulant activity of the by-products, cell toxicity is another undesirable effect. The ability to measure the viability of the cells with increasing concentrations of sample up to and beyond likely therapeutic doses was paramount to assess the potential toxic effect the compounds may have *in vivo.*

There are four common ways of determining the viability of cells; LDH, MTT, neutral red and protein assays.

The LDH assay measures the level of lactate dehydrogenase in the extracellular medium. LDH (lactate dehydrogenase) is released from compromised cell membranes and is an indicator of irreversible cell death. The assay is quick and highly reproducible (Decker and Lohmann-Matthes, 1988).

MTT is also a colourimetric assay, however, it assesses viable cells as opposed to those that are dying, unlike LDH. As described in Chapter 3 (5.2i), MTT is cleaved to form an insoluble purple formazan by metabolically active cells (Mossman, 1983).

Neutral red allows a direct representation of living cells, where it is taken up and concentrated in the lysosomes of living cells (Haugen & Hensten-Petterson, 1978).

Finally, the Bradford protein assay measures the protein content of cells after treating and washing them. This is a prediction of toxicity as living cells are hypothesised to have a higher total protein content than dead ones.

6.3 Methods

6.3.1 Partial Thromboplastin

25 µl of prewarmed by-products or ddH_2O, control, were combined with 50 µl of prewarmed normal human control plasma (Technoclone, Austria). These were incubated in a Thrombostat$^+$ (Behnk Electronik, Germany) for 30 secs at 37°C. 50µl of prewarmed Thromborel S (Siemens, UK) was added and the time taken for the assay to either coagulate or reach 120 secs (at which point recording ceased if no coagulation had occurred), was recorded.

A concentration curve of Hp, M1, D1, F1 and H was made using 10-fold dilutions from 1 mg/ml – 0.01 ng/ml. From this, log IC_{50} results were calculated. Using these results, further concentrations were selected to repeat the assay, enabling accurate IC_{50}s. For Hp and H concentrations of 0.1, 0.01, 0.08, 0.06, 0.04, 0.02 and 0.01 mg/ml and for F1, M1 and D1 1, 0.8, 0.6, 0.4, 0.2 and 0.1 mg/ml were used.

6.3.2 Activated Partial Thromboplastin

50 µl of prewarmed normal human control plasma was preincubated with 25 µl of by-product sample or ddH_2O control and 50 µl of HemosIL SynthAsil APTT reagent (IL, Italy) for 2 mins at 37°C in a Thrombostat$^+$. To this 25 µl 50mM $CaCl_2$ was added and the time taken for the sample to coagulate was recorded. At 120 secs, if no coagulation had occurred, the assay was stopped.

A concentration curve of Hp, M1, D1, F1 and H was made using 10-fold dilutions from 1 mg/ml – 0.01 ng/ml. From this, log IC_{50} results were calculated. Using these results, further concentrations were selected to repeat the assay, enabling accurate IC_{50}s. For Hp, D1, H and F1 concentrations of 10, 8, 6, 4, 2 and 1 µg/ml and M1 0.1, 0.08, 0.06, 0.04, 0.02, 0.01 mg/ml were used.

6.3.3 LDH- Cytotoxicity Assay

An LDH assay kit was purchased from Abcam (UK) and the manufacturer's protocol followed; preliminary testing for cell number and incubation time established the final protocol below.

$6x10^4$ HUVECs cells were seeded using 100 µl in normal growth media (HUVEC media, Chapter 2), in a 96 well plate. Cells were incubated overnight at 37°C/5% CO_2 with the following conditions;

Background control – 100 µl media with no cells

Low control – 100 µl cells

High control – 100 µl cells with 10 µl cell lysis solution (for the increase in volume, 11 µl of supernatant was taken for the next stage).

Test conditions – 100 µl cells with 1, 0.3, 0.1, 0.03, 0.01, 0.003, 0.001 and 0.0003 mg/ml of either Hp or the by-products.

After incubation cells were centrifuged at 600 g for 10 minutes to precipitate cells and cell debris. 10 µl of supernatant (11 µl high control) were transferred into a new 96 well plate.

100 µl LDH reaction mix was added to each well and incubated for 30 mins at room temperature and absorbance read at 450 nm on a MultiScan Ex plate reader.

6.4 Results

6.4.1 Activated Partial Thromboplastin & Partial Thromboplastin of Intact By-Products

Prior to digestion and separation, all samples were tested for their ability to prevent coagulation; this was achieved by investigating their effects globally, on intrinsic and extrinsic factors involved in the cascade.

As previously discussed, PT measures the effect of Hp and its related products on their ability to disrupt extrinsic factors, such as factors II, V, X and fibrinogen. During the investigation 120 seconds was selected as a cut off time of the experiment, this being the recommended point at which, if coagulation has not occurred, it was unlikely to do so. A dose dependent protocol was established for each sample based on the results from an initial screening of concentrations from 0.1 mg/ml-0.01 ng/ml of 8 concentrations at 10-fold increments, in triplicate. From this, a further 5 concentrations per sample were selected to give a good range of results. IC_{50}s for each sample were calculated from a log graph (Figure 6.1).

The results suggested, by Dunnett's multiple comparison test, samples D1, F1, and M1 were significantly less able to prevent coagulation ($p=0.05$) when compared to Hp. M1 required a substantially higher concentration of material to inhibit coagulation than the other samples, 0.42 mg/ml. D1 and F1 had similar results, 0.15 and 0.21 mg/ml respectively. H required far less material than all other samples to inhibit coagulation, 0.08 mg/ml. Statistical testing suggested that PT results of sample H were not significantly different to the IC_{50} concentration of Hp ($p=0.02$, Table 6.1).

APTT is a more global assay for investigating intrinsic factors which can be inhibited by Hp and other related products, such as factors II, V, X and fibrinogen. In the same manner as a PT assay, an initial screening of concentrations from 0.1 mg/ml-0.01 ng/ml allowed 5 further concentrations to be selected to enable a good range of results for statistical comparison. The IC_{50}'s for each sample were calculated from a log graph (Figure and Table 6.1).

IC_{50} results, by Dunnett's multiple comparison test, suggest that all samples were significantly less able to disrupt coagulation when compared to Hp ($p=0.05$). D1, F1 and H had reasonably similar IC_{50} results, 7 µg/ml H and D1, 8 µg/ml F1. Although these were the closest to the IC_{50} of Hp, 4 µg/ml, they are still a significantly higher concentration, almost 1.5 fold, than that which was required for Hp to prevent coagulation. Again, like PT, the APTT assay showed that M1 appeared to have the lowest ability to inhibit coagulation, requiring a much higher IC_{50} concentration, 22 µg/ml.

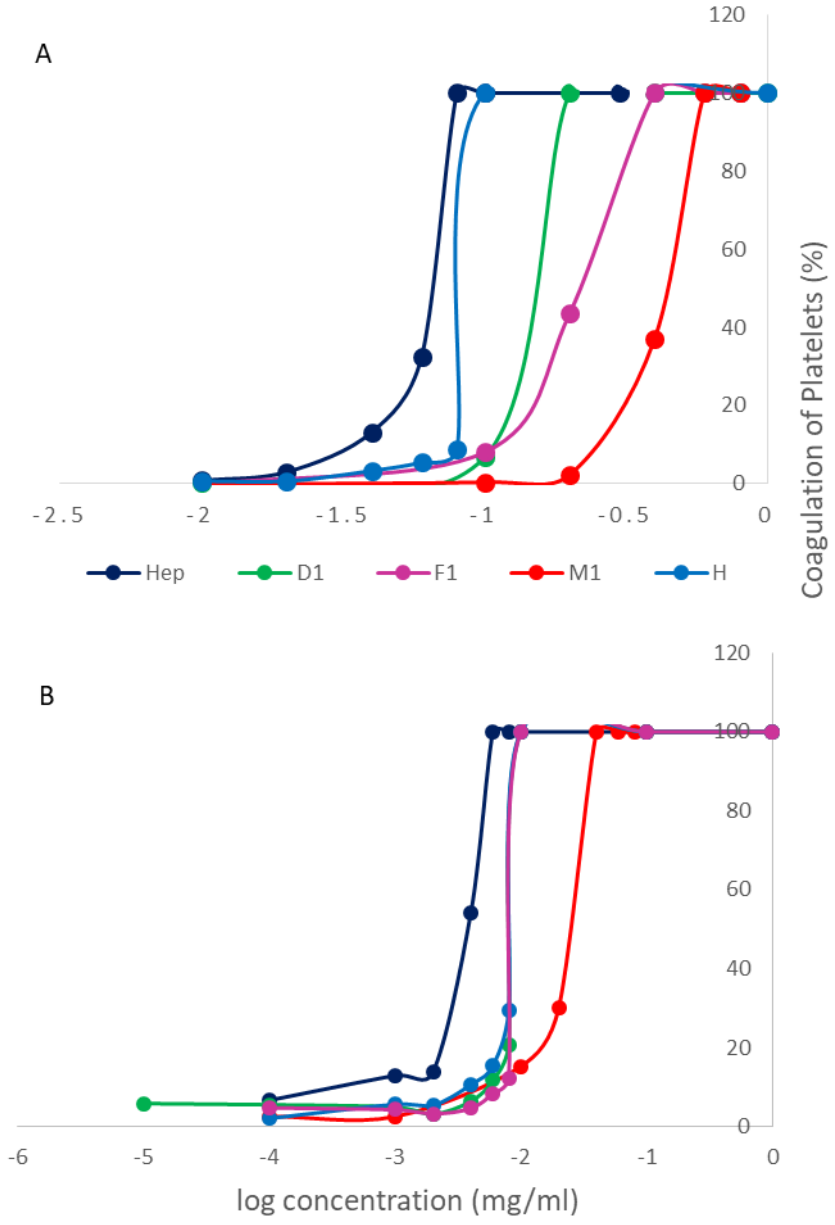

Figure 6.1- Log IC_{50} graphs representing the anticoagulant activity of the by-products and Hp. Assays were measured by PT and APTT assays, as Hp can influence factors associated with prothrombin, preventing coagulation. Samples were incubated with prewarmed normal control human plasma and either APTT or PT reagents added and time taken for samples to coagulate was measured by a thrombostat+ system in seconds, 120 secs was the stopping point for any samples not yet coagulated (graphs were plotted from the means of n=3).

Sample	Hp	D1	F1	H	M1
PT mg/ml	0.064	0.15	0.21	0.08	0.42
APTT mg/ml	0.0038	0.0073	0.0075	0.0074	0.022

Table 6.1 – IC_{50} results for PT and APTT of by-products and Hp. IC_{50}s were calculated from the log graph above in Figure 6.1. Results are given in mg/ml, highlighted in red are results that are not significantly different to Hp determined by multiple t-tests (p=0.05, n=3).

6.4.2 Toxicity Testing of Intact By-Products

It was important to establish whether the samples can affect the viability of cells *in vitro* and by proxy their susceptibility to damage cells, tissues and organs *in vivo*. This will ultimately determine their overall suitability for therapeutic use. An LDH assay was used to assess cell viability. The release of LDH into the cell media suggests that the cell membrane was compromised and therefore the cells are unable to survive. The by-product samples and Hp were added to cells at concentrations from 3 ng/ml to 1 mg/ml in normal growth media and incubated for 24 hours. LDH reaction mixture was added according to manufacturer's instructions and left to develop for around 30 mins. The high control was established by adding lysis solution to the media, which breaks up the cell membrane and releases a large proportion of LDH from the cells.

All samples, including Hp, showed relatively low levels of toxicity. At lower concentrations (<0.03 mg/ml) all samples had the ability to induce cell survival over and above normal growth media. H, although peaking at 0.1 mg/ml above all samples, overall appeared to be the most able to reduce normal cell death below 0.03 mg/ml (p=0.01) and has the lowest toxic effect at the highest concentration, 1 mg/ml.

An increase in LDH release above the low control was seen in all samples above 0.03 mg/ml. However, at every concentration tested, all samples showed significantly less LDH release than the lysis (high) control. F1 has the highest overall release of LDH of the samples at 1 mg/ml, but this was still significantly reduced when compared to the high control (p=0.02). Owing to the low level of toxicity observed with all samples, the comparison of the samples to Hp showed very few results which were significantly different, only H at concentrations of 1, 0.001 and 0.003 mg/ml showed a significant decrease in the release of LDH when compared to Hp.

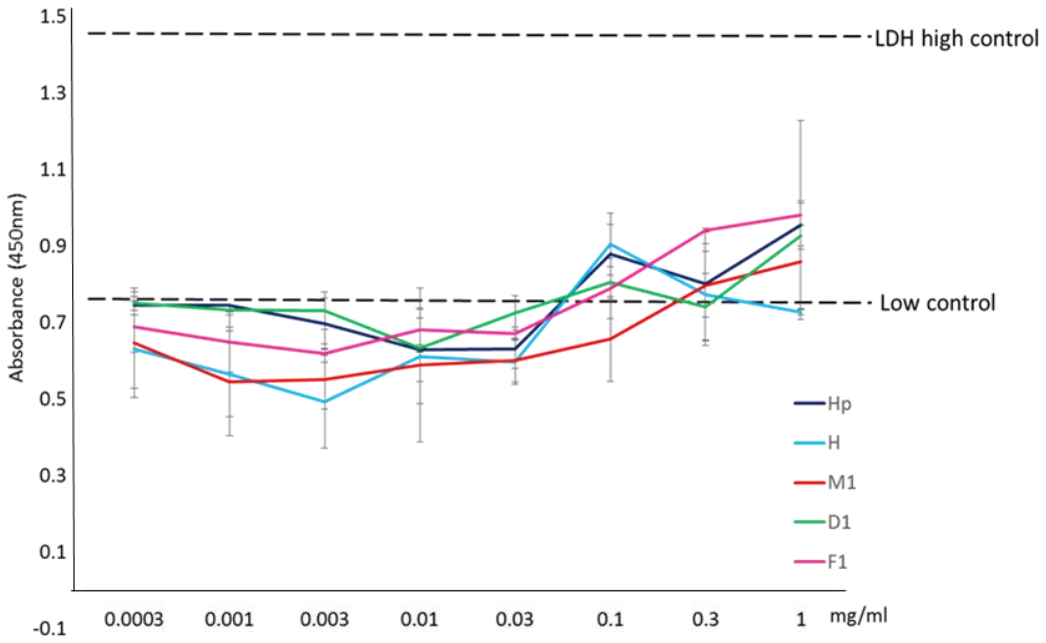

Figure 6.2 – Toxicity of the by-product samples and Hp measured by LDH release. 1 mg/ml-3ng/ml of Hp and by-product samples were added in culture to 6x10^4 HUVECs per well in a 96 well plate and incubated for 24 hours at 37°C/5% CO_2. To the high control, 10 µl of lysis buffer was added to 3 wells, whilst the low control recorded cells in media alone. Cells were spun at 600g for 10 mins and 10µl of supernatant removed and added to 100 µl of LDH reaction mixture. Plates were left to incubate at RT for ~30 mins before the release of LDH was measured on a plate reader at 450 nm. The mean and SEM of the results were calculated for each sample minus the absorbance for media alone. Multiple t-tests were carried out on the by-product samples versus Hp ($p<0.05$, n=2), and when compared to Hp, only sample H at 1 mg/ml, 1 and 3 ng/ml reduced cell death significantly, although all were significantly lower than the high control.

6.4.3 Zika Virus Assay of Intact By-Products

As described previously, in normal viral function, HS has been shown to bind to the protein envelope and facilitate the internalisation of members of the Flavivirus family (Avirutnan *et al.*, 1998). However, more recently Hp has been shown to reduce apoptosis of Zika infected neuroblasts (Ghezzi *et al.*, 2017). Currently a small study with a group in Milan, has been undertaken to see if, like Hp, the by-product samples have the ability to reduce viral associated apoptosis of neuroblast spheres in culture.

Neuroblasts spheres (human neural progenitor cells, obtained from reprogrammed human pluripotent stem cells) were seeded at 1x10^4 in a 96 well plate and were left for 1 hour to stabilize. Compounds were added to the plate at 5, 50 or 100 µg/ml for 4 hours, after which the cells were infected with INMI-1, the more recently discovered Brazilian strain of Zika and the supernatant collected 6 days post infection. Along with monitoring the levels of adenylate kinase (Figure 6.3), a marker of apoptosis released when the cell membrane was damaged, the cells were also imaged at 6 days post infection, as they have a very distinctive morphology

when infected with the virus (Figure 6.4). Cell debris breaking off and surrounding the spheres was frequently seen in infected cells, this causes the neuroblast spheres to look less rounded in appearance, with poorly defined edges.

After incubating neuroblast spheres with the by-product samples at all concentrations, showed a large reduction in the release of adenylate kinase compared to the infected control, INMI-1. However, D1 at 50 and 100 µg/ml was shown to be at least as effective Hp and probably more potent. At these concentrations, the by-product was not only able to greatly reduce cell death compared to the infected control but also reduce the adenylate kinase concentrations when compared to the normal growth media control. This suggests that not only was this by-product potentially better at reducing apoptosis than Hp in infected cells, but that it may also reduce general apoptosis in the normal cell cycle. As seen in Figure 6.4, all treated cells maintain a healthier morphology than those infected with Zika.

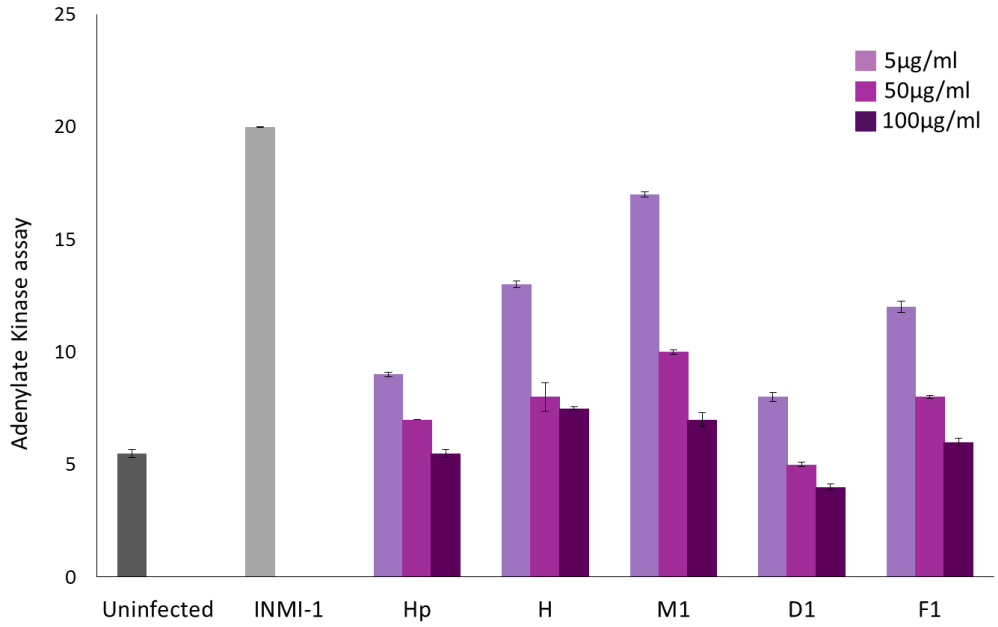

Figure 6.3 – Effects of by-products on adenylate kinase levels recorded as an indication of apoptosis in cells infected with Zika virus. Raw data was collected by Dr Vicenzi (Milan) and the graph produced by the thesis author. Neuroblast spheres were preincubated with by-products and a heparin control for 4 hours before being infected with INMI-1 Brazilian strain of Zika. Supernatant, from the cells was collected 6 days post infection and the level of adenylate kinase assessed. D1 greatly reduces adenylate kinase levels compared to not only the Zika infected control and all cells treated with Hp/by-products, but also the normal healthy control (n=3).

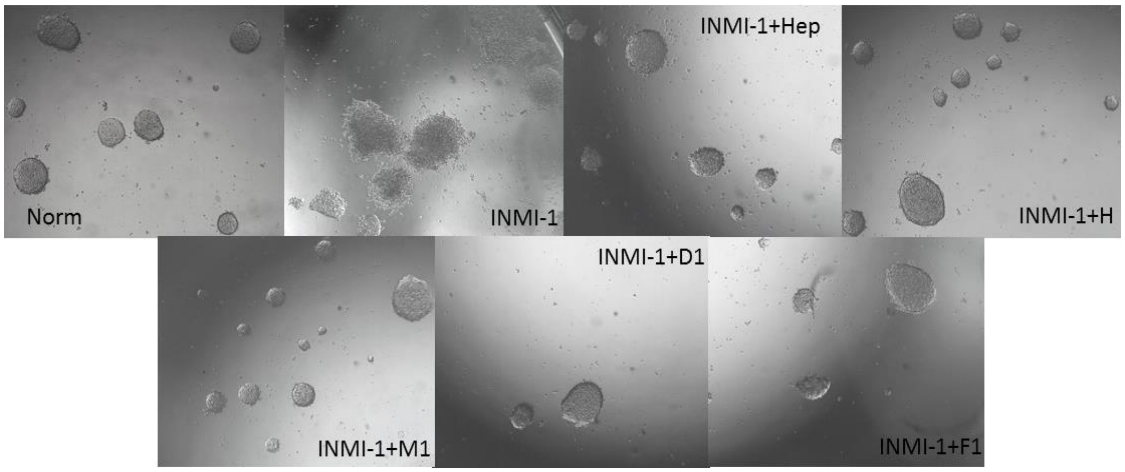

Figure 6.4- Effect of the by-products on phenotype of cells infected with Zika virus 6 days post infection. Cells were photographed 6 days post infection. Cell death typically causes an increase in cell debris, with the spheres of cells losing their defined edges and becoming less rounded. With the addition of heparin or by-products the cells maintain a similar phenotype to the uninfected 'Norm' control.

6.5 Discussion

It is the position and number of different sulfate substitution patterns along the HS chain which give the polysaccharide its diverse bioactivities. As the by-product samples contain a diverse range of sulfation patterns, it could be hypothesised that all the samples could potentially have off target, undesirable effects, which could make them unsuitable as potential therapeutics. This Chapter has described studies aimed at assessing the suitability of the by-products for further *in vitro/vivo* testing, by measuring the key off targets effects of anticoagulation and toxicity. Finally, the by-products were tested for their ability to reduce cell death in neuroblast spheres infected with Zika virus, as an example of a potential biological application.

The results of the anticoagulant and toxicity investigations suggest that the by-products may indeed be suitable for therapeutic use. All samples show low anticoagulant properties, which may be surprising considering the highly sulfated nature of some of the by-products.

M1, in particular, showed the lowest anticoagulant activity of all the samples, in both the APTT and PT assay, it required the highest concentration of sample to inhibit coagulation and was the most significantly different to Hp. As well as its low anticoagulation properties, M1 showed no deleterious effects on the viability of cells when added in concentrations up to 1 mg/ml (a very high level that is at least 10-fold higher than any expected *in vivo* usage levels). At lower concentrations, up to ~0.2 mg/ml, the sample not only maintains cell viability but also reduces the level of LDH released significantly beyond that of the low growth media control, indicating that M1 actively induces cell survival. From these assays, it could be suggested that M1 has the best potential as a therapeutic agent due to its low anticoagulant and toxic effects. However, when applied to Zika infected cells, M1 was the least able to reduce adenylate kinase release and therefore reduce cell death of the neuroblast spheres. At its highest concentration (100 µg/ml), the levels of adenylate kinase are still greatly above that of the normal uninfected control, suggesting that for this disease model, it was the least suitable of all the by-products.

H requires the lowest concentration of material to induce anticoagulant activity, particularly in the PT assay and it was not significantly different to the concentration required for Hp to inhibit coagulation. However, the APTT assay results were not significantly different to by-products D1 and F1 but were significantly lower than the concentration of Hp, it could be suggested that H exerts its effects on factors involved in the extrinsic coagulation pathway rather than intrinsic factors. Despite its moderate anticoagulant activity, H seems to exhibit the

lowest overall release of LDH in the toxicity assay, although it did peak slightly at 0.1 mg/ml. It was the only sample that showed a significant reduction in LDH release when compared to Hp, at multiple concentrations. These results suggested that, although H had low toxic effects on cells, it may have limited use in therapeutic studies as it could potentially induce high levels of anticoagulation, comparative to that of Hp, *in vivo*. Like M1, H has been shown not to be the most suitable sample in the Zika infection model, as it was unable to reduce levels of adenylate kinase to control levels.

Both D1 and F1 could have potential for therapeutic studies, as they both showed similar low levels of anticoagulant activity, which are significantly below that of Hp. However, F1 may be less favourable as it showed the highest level of LDH release, although this was still significantly lower than the high LDH control ($p=0.02$).

It could be suggested that D1 was the sample to continue investigating at this stage, for further Zika studies, as not only does it have low levels of anticoagulation and toxicity, it was also able to greatly reduce the levels of adenylate kinase release at all concentrations compared to the other by-products and Hp. At 50 and 100 µg/ml it was able to reduce the levels of adenylate kinase below normal uninfected control, the latter being substantially reduced. Together the results suggest that at 50 µg/ml D1 could greatly reduce cell death associated with Zika infection, to the same level as the normal uninfected control, whilst having little to no impact on toxic cell death and limited anticoagulation activity (no PT evidence at this level but some APTT).

Overall, these results suggest that the by-product samples would likely, produce only limited adverse effects, as they cause almost no damage to cells *in vitro*, possibly leading to minimal effects *in vivo* on whole tissues/organs. However, beyond this, they also have positive results in culture combating cell death associated with Zika virus. In order to gain a better understanding of the role these samples could play as a therapeutic for Zika virus infection, more studies into understanding the mechanisms by which Hp/HS prevents viral associated apoptosis needs to be explored.

Chapter 7- Concluding Remarks & Future Directions

Heparin and heparan sulfate are complex chains of repeating disaccharides of glucuronic/iduronic acid and glucosamine residues. It was the sulfation of these disaccharides at the 2 position of glucuronic/iduronic acid, the 6- and N-sulfation and rarely 3-O sulfation of glucosamine and the pattern at which they are present along the chain that ultimately determines the biological activity of these polysaccharides. In the first experimental Chapter of this thesis 4 by-products from the production of Hp were purified and characterised using multiple techniques. Compositional analysis and NMR of the by-products led to the conclusion that each of them is unique in their structure, and clearly different from Hp and each other. Whilst Hp had the highest level of tri-sulfated disaccharides, leading to it having an increase average number of sulfates per disaccharide (~2.2), 3 of the other by-products also contained high levels of average sulfation, H and D1 with ~2.0, with M1 at sulfates per disaccharide ~1.8 and finally F1 at around ~1.6. This suggests that the latter by-products, was the most HS-like. To increase the diversity of available structures, whilst also further separating and refining them, Chapter 4 discussed the possibility of producing more selective protein binders whilst maintaining comparatively equal or better activity to the parental material. This was achieved by digestion with heparinase III and separation by charge and size. In Chapter 5, the bioactivity of the intact, parental material for each by-product compared to each other, as well as the size fractionated material, were investigated to determine if the differences in structure translated to differences in bioactivity. The Chapter established that sample H, being highly sulfated and containing the smallest intact chains, elicited the strongest potency for activity in FGF2 signalling in BaF3-1c cells. Possibly because of the large number of receptors on the surface of the cells it was favoured above Hp. However, separating D1 and F1 into size fractions showed that there was a level of tolerance at which activity in the log growth rate agreed with previous literature, oligosaccharides below ~dp 6 were significantly less able to induce proliferation than the intact material. Interestingly, D1 being more highly sulfated resulted in a fraction one lower in size than F1 being able to induce comparable proliferation to the intact material (D1:5 vs F1:6). Following this it was identified that H and this time M1 elicited an increase in PDGF-BB driven NIH3T3 proliferation. Both by-products contained a higher level of N-sulfation compared to the other by-products and more NA residues than Hp. No increase in proliferation was seen with size separation of D1 and F1, however, the larger fractions did show an overall decrease in their PDGF-BB driven proliferation. Finally, VEGF-A_{165} also showed preference to sample H and Hp for promotion of AKT^{Ser473} and ERK1/2 phosphorylation, respectively. Size separation demonstrated some correlation with F1 having an increase in chain length, equating to an increase in phosphorylation events, but this was not the case for the higher sulfated D1. Overall, growth factor analysis suggested that generally by-product H was the most potent,

most likely due to its highly sulfated nature but smaller intact chain length; and that size fractionation of D1 and F1 oligosaccharides at this level of refinement already show promising results for creating sub-fractions with more selective protein-HS interactions measured at the functional level. For example, whilst the activity for each growth factor was not generally improved over the parental material, selecting smaller sizes fractions such as 7/8, would reduce PDGF-BB activity whilst not affecting either FGF2 or VEGF-A activation. Conversely selecting smaller 1:5 fractions would reduce FGF2 activity without impacting significantly on PDGF-BB and VEGF-A_{165}, at these given concentrations. Importantly in Chapter 6, all the by-products show a marked reduction in their anticoagulant potential shown through APTT and PT assays, which test the integrity of many factors of the coagulation pathway. All samples, including Hp, show minimal cell toxicity up to high concentrations (1mg/ml) and below ~0.05mg/ml induce cell survival beyond that of the low media only control. This suggests they have favourable properties as potential therapeutics. Finally, all by-products, especially D1, show exciting capabilities in reducing neural progenitor cell death associated with Zika virus and have strong prospects in being able to be explored for therapeutic use, as well as studying the mechanisms underpinning this disease.

This thesis has highlighted several promising applications for these by-products. As described previously the biggest issue facing exploitation of protein-HS interactions is the structural complexity of HS, which has led to the somewhat arduous task of trying to link specific HS sequences with protein binding sites and activities. This has revealed that the relationship between the two is largely based on charge disposition, geometry and chain flexibility (Thunberg *et al*., 1980; Casu *et al*., 1988). These investigations have often called for the production of simple saccharides as starting blocks for these investigations, which make the experiments expensive. Furthermore, due to the possibility of innumerable combinations of disaccharides along a chain the conclusions of these studies are biased towards the structures tested. As previously mentioned, the process of producing GAGs for research or pharmaceutical purposes is expensive, this is primarily due to the loss of yield at each stage of the production from both natural and synthetic processes. The drive for profitability has the potential to cause problems with companies trying to increase their revenue, and the most notorious consequence of this is the introduction of contaminants to the products, particularly in Hp production, as occurred in 2008. The level of these contaminants has been shown to be introduced up to and in some cases beyond that to which they are permitted e.g. oversulfated chondroitin sulfate (Kishimoto *et al.*, 2008; Guerrini *et al.*, 2008; Zhang *et al.*, 2008). Similarly, chemical modifications of HS structures to achieve a desirable amount of product can also lead

to inconsistencies and large variation between batches (Mulloy *et al.*, 2016). This can have a detrimental knock-on effect to the cohesiveness of scientific research between not only experiments in a single laboratory but also the comparison of results obtained by others.

This thesis has explored the previously uncharacterised HS products from waste material derived from the production process of Hp to provide a structurally defined, economical selection of bioactive oligosaccharides with low off target side-effects, which may have potential use in therapeutic research. The purification and characterisation of these by-products has identified that they are structurally different to Hp in regard to the sulfation within the chain, becoming more Hp-like, the closer the by-product was removed to the end of the process. Consequently, this led to different levels of biodiversity in the growth factor assays between the by-products, suggesting that further exploration could be undertaken to discover stronger partners of protein-by-product binding/activity. Furthermore, the refinement of the by-products described in Chapter 4, showed another level of diversity can be achieved when looking at protein-by-product interactions; refinement of these by-products by incorporating the SAX and SEC methods sequentially, in either order, could possibly lead to the discovery of sub-fractions with more potent growth factor bioactivities. However, whilst the selection of more refined oligosaccharides would be useful in the discovery of better binding partners, it must be noted that increasing the level of refinement will drastically reduce the yield recovered at each step and therefore the by-products could potentially lose their economic value as a practicable source of Hp/HS. Future work should take this into consideration and a balance between refinement and cost should be monitored. For example, an initial level of refinement could be achieved before digestion, from the weak anion exchange step at the beginning of Chapter 3. Following work from Griffin *et al.* (1995), where by-products were separated by weak anion exchange to investigate the broad level of sulfation in intact chains (Figure 3.5), peaks from each salt elution could be selected prior to digestion and their structure determined by compositional analysis and NMR to increase the diversity of HS saccharides available before further refinement.

Currently HS is sold at a considerable price (e.g. Sigma, £529/mg and Celsus, £195/mg Celsus on 6/12/17); in comparison, the by-products can be purchased at ~£500-1000 per Kg for the crude material. This thesis described a ~15-18% recovery of Hp/HS saccharides with low costs involved in the enzymatic clean-up and the DEAE recovery (Figure 3.3). These by-products therefore contain Hp/HS saccharides at a cost well below commercial price, and have the added advantage that the oligosaccharide mixtures have been structurally analysed, providing

extra information but also reassurance for research groups that might be interested in purchasing them. These results were based on 4 by-products that were used in this thesis, having also tested a further 3 by-products and discounted them due to a poor yield of Hp/HS. Since there is also the possibility of more waste products being removed between F1 and H (Figure 3.1), it is evident that through the manufacturing of Hp, tonnes of useful material are being discarded and seen as having no commercial/research value. However, this thesis has demonstrated that these by-products contain a high yield of bioactive saccharides, which could potentially offer a significant source of revenue to commercial manufacturers, initially in the smaller research reagents market and possibly in the longer term as natural product therapeutics.

Furthermore, an example of the potential use of these by-products in therapeutic applications was highlighted in the final results Chapter. The low level of anticoagulant potential and cell toxicity is an exciting prospect for the exploration of these by-products in many biological roles, coupled with the promising activity shown in three different growth factors assays demonstrated in this thesis. These alone could suggest the by-products may be beneficial in wound healing, muscle and blood vessel regeneration, as well as many other processes which depend on FGF2, PDGF-BB, VEGF-A_{165} activation. However, at this level of refinement the by-products may not be suitable for therapeutics as they will most certainly be interacting with multiple growth factors simultaneously. This pan-activity could be an advantage in some applications, but further refinement may lead to interesting bioactive fractions which could possibly have more targeted therapeutic potential. In addition, as the by-products are already being produced because of the production of Hp, there would be no immediate additional demand on the number of pigs sourced. However, the by-products as they stand are already an ideal source for continued discovery in scientific research into potential therapeutic actions of HS, as well as being used to understand disease mechanisms.

The possibilities for future investigations into the understanding of Zika virus are numerous. Since its association with HS/Hp is only a recent area of interest, much is still unknown about the mechanisms underpinning the attenuation of Zika virus. It has been suggested that Hp reduces the level of CASP-3, leading to a reduction in apoptotic cell death. However, to date whilst Flaviviruses have been shown to induce CASP-3 dependent apoptosis, studies of Zika virus have yet to link infection conclusively with this pathway (Olmo *et al.*, 2017). Whilst the mechanism by which this occurs is still not understood, by-products, in particular D1, have the potential to be used to explore apoptosis in Zika infection, as well as CASP-3

signalling, and the mechanisms by which the introduction of exogenous saccharides effects the cells stress response. CASP-3 is unlikely to be the only signalling pathway in which Hp/HS is involved in the mechanism of cell stress when neural progenitor cells are infected with Zika virus. Interestingly, Aid *et al.*, 2017 looked at expression of proteins in the cerebral spinal fluid of infected rhesus monkeys and showed cellular stress responses from many other signalling factors including; NOX1, ROS1 and several members of the HIF and NFκB family. This paper also described the extracellular matrix components; PDGF receptors A, B, HSPG2 and a range of FGFs being downregulated in the CSF of Zika infected monkeys. Therefore, it would be interesting to explore the addition of HS saccharides in combination with PDGF/FGFs on the effects of cell survival and stress.

Whilst Hp does not reduce the viral burden of human cells, in fact HS has been implicated in enabling the internalisation of some Flaviviruses into cells, which also allows the survival and replication of the virus (Ghezzi *et al.*, 2017). Investigations into the mechanisms by which internalisation occurs, specifically if certain sulfation patterns of HS are favoured for the internalisation of these viruses, could potentially lead to the development of therapeutic HS saccharides which could hamper or block the infection of the cells by the virus. Whilst there is still much left to explore in regards to the virus and the human host, there is even less known about the insect host. HS chains have been isolated in the Anopheles mosquito during infection and transmission of the malarial parasite (Sinnis *et al.*, 2007). Owing to the importance of HS saccharides being discovered in the role of infection of the human host from members of the Flavivirus family, there is also a strong possibility that HS may also play a role in Zika virus infecting the insect mosquito host.

In conclusion, four Hp by-products have been purified and investigated using multiple rigorous techniques to fully describe their structure and have also shown promising bioactivity with many growth factors, as well as containing low levels of anticoagulant activity and cell toxicity. This suggests that they may be a low-cost source of Hp/HS for research, as well as being useful in bioactivity studies involving HS-protein interactions and finally for further understanding the mechanisms underpinning Zika virus infection in both human and insect hosts.

References

Abdayem, R., Formanek, F., Minondo, A.M., Potter, A. & Haftek, M. (2016) 'Cell surface glycans in the human stratum corneum: distribution and depth -related changes', *Exp Dermatol*, vol. 19, no. 10, p. 13070.

Abramsson, A., Kurup, S., Busse, M., Yamada, S., Lindblom, P., Schallmeiner, E., Stenzel, D., Sauvaget, D., Ledin, J., Ringvall, M., Landegren, U., Kjellen, L., Bondjers, G., Li, J.P., Lindahl, U., Spillmann, D., Betsholtz, C. & Gerhardt, H. (2007) 'Defective N-sulfation of heparan sulfate proteoglycans limits PDGF-BB binding and pericyte recruitment in vascular development', *Genes Dev.*, vol. 21, no. 3, pp. 316-331.

Aid, M., Abbink, P., Larocca, R.A., Boyd, M., Nityanandam, R., Nanayakkara, O., Martinot, A.J., Moseley, E.T., Blass, E., Borducchi, E.N., Chandrashekar, A., Brinkman, A.L., Molloy, K., Jetton, D., Tartaglia, L.J., Liu, J., Best, K., Perelson, A.S., De La Barrera, R.A., Lewis, M.G. & Barouch, D.H. (2017) 'Zika Virus Persistence in the Central Nervous System and Lymph Nodes of Rhesus Monkeys', *Cell.*, vol. 169, no. 4, pp. 610-620.e614.

Aikawa, J., Grobe, K., Tsujimoto, M. & Esko, J.D. (2001) 'Multiple isozymes of heparan sulfate/heparin GlcNAc N-deacetylase/GlcN N-sulfotransferase. Structure and activity of the fourth member, NDST4', *J Biol Chem.*, vol. 276, no. 8, pp. 5876-5882.

Arungundram, S., Al-Mafraji, K., Asong, J., Leach, F.E., Amster, I.J., Venot, A., Turnbull, J.E. & Boons, G.J. (2009) 'Modular Synthesis of Heparan Sulfate Oligosaccharides for Structure-Activity Relationship Studies', *J Am Chem Soc.*, vol. 131, no. 47, pp. 17394-17405.

Avirutnan, P., Malasit, P., Seliger, B., Bhakdi, S. & Husmann, M. (1998) 'Dengue virus infection of human endothelial cells leads to chemokine production, complement activation, and apoptosis', *J Immunol.*, vol. 161, no. 11, pp. 6338-6346.

Bai, X. & Esko, J.D. (1996) 'An animal cell mutant defective in heparan sulfate hexuronic acid 2-O-sulfation', *J Biol Chem.*, vol. 271, no. 30, pp. 17711-17717.

Baird, A., Schubert, D., Ling, N. & Guillemin, R. (1988) 'Receptor- and heparin-binding domains of basic fibroblast growth factor', *Proc Natl Acad Sci U S A.*, vol. 85, no. 7, pp. 2324-2328.

Basilico, C. & Moscatelli, D. (1992) 'The FGF family of growth factors and oncogenes', *Adv Cancer Res*, vol. 59, pp. 115-165.

Bauer, K.A. (2001) 'Fondaparinux sodium: a selective inhibitor of factor Xa', *Am J Health Syst Pharm.*, vol. 58, no. Suppl 2, pp. S14-17.

Bennett, S.P., Griffiths, G.D., Schor, A.M., Leese, G.P. & Schor, S.L. (2003) 'Growth factors in the treatment of diabetic foot ulcers', *Br J Surg.*, vol. 90, no. 2, pp. 133-146.

Bernfield, M., Kokenyesi, R., Kato, M., Hinkes, M.T., Spring, J., Gallo, R.L. & Lose, E.J. (1992) 'Biology of the syndecans: a family of transmembrane heparan sulfate proteoglycans', *Annu Rev Cell Biol*, vol. 8, pp. 365-393.

Blixt, O. & Razi, N. (2006) 'Chemoenzymatic synthesis of glycan libraries', *Methods Enzymol*, vol. 415, pp. 137-153.

Brito, A.S., Cavalcante, R.S., Palhares, L.C., Hughes, A.J., Andrade, G.P., Yates, E.A., Nader, H.B., Lima, M.A. & Chavante, S.F. (2014) 'A non-hemorrhagic hybrid heparin/heparan sulfate with anticoagulant potential', *Carbohydr Polym.*, vol. 99:372-8., no.

Bruns, A.F., Bao, L., Walker, J.H. & Ponnambalam, S. (2009) 'VEGF-A-stimulated signalling in endothelial cells via a dual receptor tyrosine kinase system is dependent on co-ordinated trafficking and proteolysis', *Biochem Soc Trans.*, vol. 37, no. Pt 6, pp. 1193-1197.

Burke, D., Wilkes, D., Blundell, T.L. & Malcolm, S. (1998) 'Fibroblast growth factor receptors: lessons from the genes', *Trends Biochem Sci.*, vol. 23, no. 2, pp. 59-62.

Busse, M., Feta, A., Presto, J., Wilen, M., Gronning, M., Kjellen, L. & Kusche-Gullberg, M. (2007) 'Contribution of EXT1, EXT2, and EXTL3 to heparan sulfate chain elongation', *J Biol Chem.*, vol. 282, no. 45, pp. 32802-32810.

Canales, A., Angulo, J., Ojeda, R., Bruix, M., Fayos, R., Lozano, R., Gimenez-Gallego, G., Martin-Lomas, M., Nieto, P.M. & Jimenez-Barbero, J. (2005) 'Conformational flexibility of a synthetic glycosylaminoglycan bound to a fibroblast growth factor. FGF-1 recognizes both the (1)C(4) and (2)S(O) conformations of a bioactive heparin-like hexasaccharide', *J Am Chem Soc.*, vol. 127, no. 16, pp. 5778-5779.

Carlsson, P. & Kjellen, L. (2012) 'Heparin biosynthesis', *Handb Exp Pharmacol*, no. 207, pp. 23-41.

Carlsson, P., Presto, J., Spillmann, D., Lindahl, U. & Kjellen, L. (2008) 'Heparin/heparan sulfate biosynthesis: processive formation of N-sulfated domains', *J Biol Chem.*, vol. 283, no. 29, pp. 20008-20014.

Carmeliet, P. & Collen, D. (1999) 'Role of vascular endothelial growth factor and vascular endothelial growth factor receptors in vascular development', *Curr Top Microbiol Immunol*, vol. 237, pp. 133-158.

Casu, B., Grazioli, G., Razi, N., Guerrini, M., Naggi, A., Torri, G., Oreste, P., Tursi, F., Zoppetti, G. & Lindahl, U. (1994) 'Heparin-like compounds prepared by chemical modification of capsular polysaccharide from E. coli K5', *Carbohydr Res.*, vol. 263, no. 2, pp. 271-284.

Casu, B., Petitou, M., Provasoli, M. & Sinay, P. (1988) 'Conformational flexibility: a new concept for explaining binding and biological properties of iduronic acid-containing glycosaminoglycans', *Trends Biochem Sci.*, vol. 13, no. 6, pp. 221-225.

Chee, Y.L. & Greaves, M. (2003) 'Role of coagulation testing in predicting bleeding risk', *Hematol J*, vol. 4, no. 6, pp. 373-378.

Chen, Y., Maguire, T., Hileman, R.E., Fromm, J.R., Esko, J.D., Linhardt, R.J. & Marks, R.M. (1997) 'Dengue virus infectivity depends on envelope protein binding to target cell heparan sulfate', *Nat Med.*, vol. 3, no. 8, pp. 866-871.

Cifonelli, J.A. & King, J. (1972) 'The distribution of 2-acetamido-2-deoxy-D-glucose residues in mammalian heparins', *Carbohydr Res.*, vol. 21, no. 2, pp. 173-186.

Dalrymple, N. & Mackow, E.R. (2011) 'Productive dengue virus infection of human endothelial cells is directed by heparan sulfate-containing proteoglycan receptors', *J Virol.*, vol. 85, no. 18, pp. 9478-9485.

Dawes, J. (1988) 'Measurement of the affinities of heparins, naturally occurring glycosaminoglycans, and other sulfated polymers for antithrombin III and thrombin', *Anal Biochem.*, vol. 174, no. 1, pp. 177-186.

De Donatis, A., Comito, G., Buricchi, F., Vinci, M.C., Parenti, A., Caselli, A., Camici, G., Manao, G., Ramponi, G. & Cirri, P. (2008) 'Proliferation versus migration in platelet-derived growth factor signaling: the key role of endocytosis', *J Biol Chem.*, vol. 283, no. 29, pp. 19948-19956.

Deakin, J.A. & Lyon, M. (2008) 'A simplified and sensitive fluorescent method for disaccharide analysis of both heparan sulfate and chondroitin/dermatan sulfates from biological samples', *Glycobiology.*, vol. 18, no. 6, pp. 483-491.

Decker, T. & Lohmann-Matthes, M.L. (1988) 'A quick and simple method for the quantitation of lactate dehydrogenase release in measurements of cellular cytotoxicity and tumor necrosis factor (TNF) activity', *J Immunol Methods.*, vol. 115, no. 1, pp. 61-69.

Dempsey, L.A., Brunn, G.J. & Platt, J.L. (2000) 'Heparanase, a potential regulator of cell-matrix interactions', *Trends Biochem Sci.*, vol. 25, no. 8, pp. 349-351.

Driguez, P.A., Potier, P. & Trouilleux, P. (2014) 'Synthetic oligosaccharides as active pharmaceutical ingredients: lessons learned from the full synthesis of one heparin derivative on a large scale', *Nat Prod Rep.*, vol. 31, no. 8, pp. 980-989.

Dulaney, S.B. & Huang, X. (2012) 'Strategies in synthesis of heparin/heparan sulfate oligosaccharides: 2000-present', *Adv Carbohydr Chem Biochem*, vol. 67:95-136., no. doi, pp. 10.1016/B1978-1010-1012-396527-396521.300003-396526.

Eming, S.A. & Hubbell, J.A. (2011) 'Extracellular matrix in angiogenesis: dynamic structures with translational potential', *Exp Dermatol.*, vol. 20, no. 7, pp. 605-613.

Engelman, J.A., Luo, J. & Cantley, L.C. (2006) 'The evolution of phosphatidylinositol 3-kinases as regulators of growth and metabolism', *Nat Rev Genet.*, vol. 7, no. 8, pp. 606-619.

Eriksson, A.E., Cousens, L.S., Weaver, L.H. & Matthews, B.W. (1991) 'Three-dimensional structure of human basic fibroblast growth factor', *Proc Natl Acad Sci U S A.*, vol. 88, no. 8, pp. 3441-3445.

Esko, J.D. & Lindahl, U. (2001) 'Molecular diversity of heparan sulfate', *J Clin Invest.*, vol. 108, no. 2, pp. 169-173.

Esko, J.D., Stewart, T.E. & Taylor, W.H. (1985) 'Animal cell mutants defective in glycosaminoglycan biosynthesis', *Proc Natl Acad Sci U S A.*, vol. 82, no. 10, pp. 3197-3201.

Esko, J.D. & Zhang, L. (1996) 'Influence of core protein sequence on glycosaminoglycan assembly', *Curr Opin Struct Biol.*, vol. 6, no. 5, pp. 663-670.

Evanko, S.P., Tammi, M.I., Tammi, R.H. & Wight, T.N. (2007) 'Hyaluronan-dependent pericellular matrix', *Adv Drug Deliv Rev*, vol. 59, no. 13, pp. 1351-1365.

Faham, S., Hileman, R.E., Fromm, J.R., Linhardt, R.J. & Rees, D.C. (1996) 'Heparin structure and interactions with basic fibroblast growth factor', *Science.*, vol. 271, no. 5252, pp. 1116-1120.

Faham, S., Linhardt, R.J. & Rees, D.C. (1998) 'Diversity does make a difference: fibroblast growth factor-heparin interactions', *Curr Opin Struct Biol.*, vol. 8, no. 5, pp. 578-586.

Ferrara, N. (2004) 'Vascular endothelial growth factor: basic science and clinical progress', *Endocr Rev.*, vol. 25, no. 4, pp. 581-611.

Feyzi, E., Lustig, F., Fager, G., Spillmann, D., Lindahl, U. & Salmivirta, M. (1997) 'Characterization of heparin and heparan sulfate domains binding to the long splice variant of platelet-derived growth factor A chain', *J Biol Chem.*, vol. 272, no. 9, pp. 5518-5524.

Folkman, J., Klagsbrun, M., Sasse, J., Wadzinski, M., Ingber, D. & Vlodavsky, I. (1988) 'A heparin-binding angiogenic protein--basic fibroblast growth factor--is stored within basement membrane', *Am J Pathol.*, vol. 130, no. 2, pp. 393-400.

Fu, L., Suflita, M. & Linhardt, R.J. (2015) 'Bioengineered heparins and heparan sulfates', *Adv Drug Deliv Rev*, vol. 10, no. 15, pp. 00258-00256.

Funderburgh, J.L. (2002) 'Keratan sulfate biosynthesis', *IUBMB Life.*, vol. 54, no. 4, pp. 187-194.

Fuster, M.M. & Wang, L. (2010) 'Endothelial heparan sulfate in angiogenesis', *Prog Mol Biol Transl Sci*, vol. 93:179-212., no.

Gallagher, J.T., Lyon, M. & Steward, W.P. (1986) 'Structure and function of heparan sulphate proteoglycans', *Biochem J.*, vol. 236, no. 2, pp. 313-325.

Gallagher, J.T. & Walker, A. (1985) 'Molecular distinctions between heparan sulphate and heparin. Analysis of sulphation patterns indicates that heparan sulphate and heparin are separate families of N-sulphated polysaccharides', *Biochem J.*, vol. 230, no. 3, pp. 665-674.

Garcia-Olivas, R., Hoebeke, J., Castel, S., Reina, M., Fager, G., Lustig, F. & Vilaro, S. (2003) 'Differential binding of platelet-derived growth factor isoforms to glycosaminoglycans', *Histochem Cell Biol.*, vol. 120, no. 5, pp. 371-382.

Garcia-Olivas, R., Vilaro, S., Reina, M. & Castel, S. (2007) 'PDGF-stimulated cell proliferation and migration of human arterial smooth muscle cells. Colocalization of PDGF isoforms with glycosaminoglycans', *Int J Biochem Cell Biol*, vol. 39, no. 10, pp. 1915-1929. Epub 2007 May 1925.

Germain, S., Monnot, C., Muller, L. & Eichmann, A. (2010) 'Hypoxia-driven angiogenesis: role of tip cells and extracellular matrix scaffolding', *Curr Opin Hematol.*, vol. 17, no. 3, pp. 245-251.

Germi, R., Crance, J.M., Garin, D., Guimet, J., Lortat-Jacob, H., Ruigrok, R.W., Zarski, J.P. & Drouet, E. (2002) 'Heparan sulfate-mediated binding of infectious dengue virus type 2 and yellow fever virus', *Virology.*, vol. 292, no. 1, pp. 162-168.

Ghatak, S., Maytin, E.V., Mack, J.A., Hascall, V.C., Atanelishvili, I., Moreno Rodriguez, R., Markwald, R.R. & Misra, S. (2015) 'Roles of Proteoglycans and Glycosaminoglycans in Wound Healing and Fibrosis', *Int J Cell Biol*, vol. 2015:834893., no.

Ghezzi, S., Cooper, L., Rubio, A., Pagani, I., Capobianchi, M.R., Ippolito, G., Pelletier, J., Meneghetti, M.C., Lima, M.A., Skidmore, M.A., Broccoli, V., Yates, E.A. & Vicenzi, E. (2017) 'Heparin prevents Zika virus induced-cytopathic effects in human neural progenitor cells', *Antiviral Res.*, vol. 140:13-17., no.

Gingis-Velitski, S., Zetser, A., Kaplan, V., Ben-Zaken, O., Cohen, E., Levy-Adam, F., Bashenko, Y., Flugelman, M.Y., Vlodavsky, I. & Ilan, N. (2004) 'Heparanase uptake is mediated by cell membrane heparan sulfate proteoglycans', *J Biol Chem.*, vol. 279, no. 42, pp. 44084-44092.

Goger, B., Halden, Y., Rek, A., Mosl, R., Pye, D., Gallagher, J. & Kungl, A.J. (2002) 'Different affinities of glycosaminoglycan oligosaccharides for monomeric and dimeric interleukin-8: a model for chemokine regulation at inflammatory sites', *Biochemistry.*, vol. 41, no. 5, pp. 1640-1646.

Griffin, C.C., Linhardt, R.J., Van Gorp, C.L., Toida, T., Hileman, R.E., Schubert, R.L., 2nd & Brown, S.E. (1995) 'Isolation and characterization of heparan sulfate from crude porcine intestinal mucosal peptidoglycan heparin', *Carbohydr Res.*, vol. 276, no. 1, pp. 183-197.

Guerrini, M., Beccati, D., Shriver, Z., Naggi, A., Viswanathan, K., Bisio, A., Capila, I., Lansing, J.C., Guglieri, S., Fraser, B., Al-Hakim, A., Gunay, N.S., Zhang, Z., Robinson, L., Buhse, L., Nasr, M., Woodcock, J., Langer, R., Venkataraman, G., Linhardt, R.J., Casu, B., Torri, G. & Sasisekharan, R. (2008) 'Oversulfated chondroitin sulfate is a contaminant in heparin associated with adverse clinical events', *Nat Biotechnol.*, vol. 26, no. 6, pp. 669-675.

Guglier, S., Hricovini, M., Raman, R., Polito, L., Torri, G., Casu, B., Sasisekharan, R. & Guerrini, M. (2008) 'Minimum FGF2 binding structural requirements of heparin and heparan sulfate oligosaccharides as determined by NMR spectroscopy', *Biochemistry.*, vol. 47, no. 52, pp. 13862-13869.

Guimond, S., Maccarana, M., Olwin, B.B., Lindahl, U. & Rapraeger, A.C. (1993) 'Activating and inhibitory heparin sequences for FGF-2 (basic FGF). Distinct requirements for FGF-1, FGF-2, and FGF-4', *J Biol Chem.*, vol. 268, no. 32, pp. 23906-23914.

Guimond, S.E. & Turnbull, J.E. (1999) 'Fibroblast growth factor receptor signalling is dictated by specific heparan sulphate saccharides', *Curr Biol.*, vol. 9, no. 22, pp. 1343-1346.

Habuchi, H., Tanaka, M., Habuchi, O., Yoshida, K., Suzuki, H., Ban, K. & Kimata, K. (2000) 'The occurrence of three isoforms of heparan sulfate 6-O-sulfotransferase having different specificities for hexuronic acid adjacent to the targeted N-sulfoglucosamine', *J Biol Chem.*, vol. 275, no. 4, pp. 2859-2868.

Harmer, N.J., Ilag, L.L., Mulloy, B., Pellegrini, L., Robinson, C.V. & Blundell, T.L. (2004) 'Towards a resolution of the stoichiometry of the fibroblast growth factor (FGF)-FGF receptor-heparin complex', *J Mol Biol.*, vol. 339, no. 4, pp. 821-834.

Haugen, E. & Hensten-Pettersen, A. (1978) 'In vitro cytotoxicity of periodontal dressings', *J Dent Res.*, vol. 57, no. 3, pp. 495-499.

Hellberg, C., Ostman, A. & Heldin, C.H. (2010) 'PDGF and vessel maturation', *Recent Results Cancer Res*, vol. 180:103-14., no.

Hellstrom, M., Kalen, M., Lindahl, P., Abramsson, A. & Betsholtz, C. (1999) 'Role of PDGF-B and PDGFR-beta in recruitment of vascular smooth muscle cells and pericytes during embryonic blood vessel formation in the mouse', *Development.*, vol. 126, no. 14, pp. 3047-3055.

Herr, A.B., Ornitz, D.M., Sasisekharan, R., Venkataraman, G. & Waksman, G. (1997) 'Heparin-induced self-association of fibroblast growth factor-2. Evidence for two oligomerization processes', *J Biol Chem.*, vol. 272, no. 26, pp. 16382-16389.

Hilgard, P. & Stockert, R. (2000) 'Heparan sulfate proteoglycans initiate dengue virus infection of hepatocytes', *Hepatology.*, vol. 32, no. 5, pp. 1069-1077.

Hiratsuka, S., Maru, Y., Okada, A., Seiki, M., Noda, T. & Shibuya, M. (2001) 'Involvement of Flt-1 tyrosine kinase (vascular endothelial growth factor receptor-1) in pathological angiogenesis', *Cancer Res.*, vol. 61, no. 3, pp. 1207-1213.

Hiratsuka, S., Minowa, O., Kuno, J., Noda, T. & Shibuya, M. (1998) 'Flt-1 lacking the tyrosine kinase domain is sufficient for normal development and angiogenesis in mice', *Proc Natl Acad Sci U S A.*, vol. 95, no. 16, pp. 9349-9354.

Hsieh, P.H., Thieker, D.F., Guerrini, M., Woods, R.J. & Liu, J. (2016) 'Uncovering the Relationship between Sulphation Patterns and Conformation of Iduronic Acid in Heparan Sulphate', *Sci Rep.*, vol. 6:29602., no.

Hu, B.Y., Du, Z.W., Li, X.J., Ayala, M. & Zhang, S.C. (2009) 'Human oligodendrocytes from embryonic stem cells: conserved SHH signaling networks and divergent FGF effects', *Development.*, vol. 136, no. 9, pp. 1443-1452.

Hu, G., Shao, M., Gao, X., Wang, F. & Liu, C. (2017) 'Probing cleavage promiscuity of heparinase III towards chemoenzymatically synthetic heparan sulfate oligosaccharides', *Carbohydr Polym.*, vol. 173:276-285., no.

Hubbard, A.R., Jennings, C.A. & Barrowcliffe, T.W. (1984) 'Anticoagulant properties in vitro of heparan sulphates', *Thromb Res.*, vol. 35, no. 5, pp. 567-576.

Huntington, J.A., McCoy, A., Belzar, K.J., Pei, X.Y., Gettins, P.G. & Carrell, R.W. (2000) 'The conformational activation of antithrombin. A 2.85-A structure of a fluorescein derivative reveals an electrostatic link between the hinge and heparin binding regions', *J Biol Chem.*, vol. 275, no. 20, pp. 15377-15383.

Ishihara, M., Tyrrell, D.J., Stauber, G.B., Brown, S., Cousens, L.S. & Stack, R.J. (1993) 'Preparation of affinity-fractionated, heparin-derived oligosaccharides and their effects on selected biological activities mediated by basic fibroblast growth factor', *J Biol Chem.*, vol. 268, no. 7, pp. 4675-4683.

Itoh, N. & Ornitz, D.M. (2004) 'Evolution of the Fgf and Fgfr gene families', *Trends Genet.*, vol. 20, no. 11, pp. 563-569.

Jastrebova, N., Vanwildemeersch, M., Lindahl, U. & Spillmann, D. (2010) 'Heparan sulfate domain organization and sulfation modulate FGF-induced cell signaling', *J Biol Chem.*, vol. 285, no. 35, pp. 26842-26851.

Kan, M., Wu, X., Wang, F. & McKeehan, W.L. (1999) 'Specificity for fibroblast growth factors determined by heparan sulfate in a binary complex with the receptor kinase', *J Biol Chem.*, vol. 274, no. 22, pp. 15947-15952.

Kato, T., Nakano, S., Kogure, K., Sasaki, H., Koiwai, K., Yamasaki, Y. & Katagiri, T. (1992) 'The binding of basic fibroblast growth factor to ischaemic neurons in the rat', *Neuropathol Appl Neurobiol.*, vol. 18, no. 3, pp. 282-290.

Kim, S.Y., Zhao, J., Liu, X., Fraser, K., Lin, L., Zhang, X., Zhang, F., Dordick, J.S. & Linhardt, R.J. (2017) 'Interaction of Zika Virus Envelope Protein with Glycosaminoglycans', *Biochemistry.*, vol. 56, no. 8, pp. 1151-1162.

Kishimoto, T.K., Viswanathan, K., Ganguly, T., Elankumaran, S., Smith, S., Pelzer, K., Lansing, J.C., Sriranganathan, N., Zhao, G., Galcheva-Gargova, Z., Al-Hakim, A., Bailey, G.S., Fraser, B., Roy, S., Rogers-Cotrone, T., Buhse, L., Whary, M., Fox, J., Nasr, M., Dal Pan, G.J., Shriver, Z., Langer, R.S., Venkataraman, G., Austen, K.F., Woodcock, J. & Sasisekharan, R. (2008) 'Contaminated heparin associated with adverse clinical events and activation of the contact system', *N Engl J Med.*, vol. 358, no. 23, pp. 2457-2467.

Koch, S., Tugues, S., Li, X., Gualandi, L. & Claesson-Welsh, L. (2011) 'Signal transduction by vascular endothelial growth factor receptors', *Biochem J.*, vol. 437, no. 2, pp. 169-183.

Korsan-Bengtsen, K. (1971) 'Routine tests as measures of the total intrinsic blood clotting potential. A comparison of whole blood clotting time (WBCT), recalcification time of citrated plasma (RTST), partial thromboplastin time (PTT), and activated partial thromboplastin time (APTT)', *Scand J Haematol*, vol. 8, no. 5, pp. 359-368.

Kreuger, J., Prydz, K., Pettersson, R.F., Lindahl, U. & Salmivirta, M. (1999) 'Characterization of fibroblast growth factor 1 binding heparan sulfate domain', *Glycobiology.*, vol. 9, no. 7, pp. 723-729.

Kreuger, J. and Kjellén, L. (2012). 'Heparan sulfate biosynthesis: regulation and variability', *Journal of Histochemistr and Cytochemistry*., vol. 60, no 12, pp. 898-907.

Kreuger, J., Spillmann, D., Li, J.P. & Lindahl, U. (2006) 'Interactions between heparan sulfate and proteins: the concept of specificity', *J Cell Biol.*, vol. 174, no. 3, pp. 323-327.

Kuberan, B., Lech, M.Z., Beeler, D.L., Wu, Z.L. & Rosenberg, R.D. (2003) 'Enzymatic synthesis of antithrombin III-binding heparan sulfate pentasaccharide', *Nat Biotechnol.*, vol. 21, no. 11, pp. 1343-1346.

Kusche-Gullberg, M., Eriksson, I., Pikas, D.S. & Kjellen, L. (1998) 'Identification and expression in mouse of two heparan sulfate glucosaminyl N-deacetylase/N-sulfotransferase genes', *J Biol Chem.*, vol. 273, no. 19, pp. 11902-11907.

Laforest, M.D., Colas-Linhart, N., Guiraud-Vitaux, F., Bok, B., Bara, L., Samama, M., Marin, J., Imbault, F. & Uzan, A. (1991) 'Pharmacokinetics and biodistribution of technetium 99m labelled standard heparin and a low molecular weight heparin (enoxaparin) after intravenous injection in normal volunteers', *Br J Haematol.*, vol. 77, no. 2, pp. 201-208.

Lam, K., Rao, V.S. & Qasba, P.K. (1998) 'Molecular modeling studies on binding of bFGF to heparin and its receptor FGFR1', *J Biomol Struct Dyn.*, vol. 15, no. 6, pp. 1009-1027.

Lapierre, F., Holme, K., Lam, L., Tressler, R.J., Storm, N., Wee, J., Stack, R.J., Castellot, J. & Tyrrell, D.J. (1996) 'Chemical modifications of heparin that diminish its anticoagulant but preserve its heparanase-inhibitory, angiostatic, anti-tumor and anti-metastatic properties', *Glycobiology.*, vol. 6, no. 3, pp. 355-366.

Leconte, I., Fox, J.C., Baldwin, H.S., Buck, C.A. & Swain, J.L. (1998) 'Adenoviral-mediated expression of antisense RNA to fibroblast growth factors disrupts murine vascular development', *Dev Dyn.*, vol. 213, no. 4, pp. 421-430.

Lee, E. & Lobigs, M. (2008) 'E protein domain III determinants of yellow fever virus 17D vaccine strain enhance binding to glycosaminoglycans, impede virus spread, and attenuate virulence', *J Virol.*, vol. 82, no. 12, pp. 6024-6033.

Lever, R., Lo, W.T., Faraidoun, M., Amin, V., Brown, R.A., Gallagher, J. & Page, C.P. (2007) 'Size-fractionated heparins have differential effects on human neutrophil function in vitro', *Br J Pharmacol.*, vol. 151, no. 6, pp. 837-843.

Li, X., Wang, C., Xiao, J., McKeehan, W.L. & Wang, F. (2016) 'Fibroblast growth factors, old kids on the new block', *Semin Cell Dev Biol*, vol. 6, no. 15, pp. 30028-30028.

Li, Y., Sun, C., Yates, E.A., Jiang, C., Wilkinson, M.C. & Fernig, D.G. (2016) 'Heparin binding preference and structures in the fibroblast growth factor family parallel their evolutionary diversification', *Open Biol.*, vol. 6(3). no. pii, p. rsob.150275.

Liang, Q., Luo, Z., Zeng, J., Chen, W., Foo, S.S., Lee, S.A., Ge, J., Wang, S., Goldman, S.A., Zlokovic, B.V., Zhao, Z. & Jung, J.U. (2016) 'Zika Virus NS4A and NS4B Proteins Deregulate Akt-mTOR Signaling in Human Fetal Neural Stem Cells to Inhibit Neurogenesis and Induce Autophagy', *Cell Stem Cell.*, vol. 19, no. 5, pp. 663-671.

Lima, M.A., Viskov, C., Herman, F., Gray, A.L., de Farias, E.H., Cavalheiro, R.P., Sassaki, G.L., Hoppensteadt, D., Fareed, J. & Nader, H.B. (2013) 'Ultra-low-molecular-weight heparins: precise structural features impacting specific anticoagulant activities', *Thromb Haemost.*, vol. 109, no. 3, pp. 471-478.

Lin, X., Buff, E.M., Perrimon, N. & Michelson, A.M. (1999) 'Heparan sulfate proteoglycans are essential for FGF receptor signaling during Drosophila embryonic development', *Development.*, vol. 126, no. 17, pp. 3715-3723.

Lin, X., Wei, G., Shi, Z., Dryer, L., Esko, J.D., Wells, D.E. & Matzuk, M.M. (2000) 'Disruption of gastrulation and heparan sulfate biosynthesis in EXT1-deficient mice', *Dev Biol.*, vol. 224, no. 2, pp. 299-311.

Lindahl, P. & Betsholtz, C. (1998) 'Not all myofibroblasts are alike: revisiting the role of PDGF-A and PDGF-B using PDGF-targeted mice', *Curr Opin Nephrol Hypertens.*, vol. 7, no. 1, pp. 21-26.

Lindahl, U., Couchman, J., Kimata, K. & Esko, J.D. 'Proteoglycans and Sulfated Glycosaminoglycans' (2015).

Lindahl, U., Thunberg, L., Backstrom, G., Riesenfeld, J., Nordling, K. & Bjork, I. (1984) 'Extension and structural variability of the antithrombin-binding sequence in heparin', *J Biol Chem.*, vol. 259, no. 20, pp. 12368-12376.

Linhardt, R.J. & Gunay, N.S. (1999) 'Production and chemical processing of low molecular weight heparins', *Semin Thromb Hemost*, vol. 25, no. Suppl 3, pp. 5-16.

Linhardt, R.J., Loganathan, D., al-Hakim, A., Wang, H.M., Walenga, J.M., Hoppensteadt, D. & Fareed, J. (1990) 'Oligosaccharide mapping of low molecular weight heparins: structure and activity differences', *J Med Chem.*, vol. 33, no. 6, pp. 1639-1645.

Linhardt, R.J., Rice, K.G., Kim, Y.S., Lohse, D.L., Wang, H.M. & Loganathan, D. (1988) 'Mapping and quantification of the major oligosaccharide components of heparin', *Biochem J.*, vol. 254, no. 3, pp. 781-787.

Liu, J. & Linhardt, R.J. (2014) 'Chemoenzymatic synthesis of heparan sulfate and heparin', *Nat Prod Rep.*, vol. 31, no. 12, pp. 1676-1685.

Liu, R., Xu, Y., Chen, M., Weiwer, M., Zhou, X., Bridges, A.S., DeAngelis, P.L., Zhang, Q., Linhardt, R.J. & Liu, J. (2010) 'Chemoenzymatic design of heparan sulfate oligosaccharides', *J Biol Chem.*, vol. 285, no. 44, pp. 34240-34249.

Lokeshwar, V.B., Huang, S.S. & Huang, J.S. (1990) 'Intracellular turnover, novel secretion, and mitogenically active intracellular forms of v-sis gene product in simian sarcoma virus-transformed cells. Implications for intracellular loop autocrine transformation', *J Biol Chem.*, vol. 265, no. 3, pp. 1665-1675.

Lord, M.S., Cheng, B., Tang, F., Lyons, J.G., Rnjak-Kovacina, J. & Whitelock, J.M. (2016) 'Bioengineered human heparin with anticoagulant activity', *Metab Eng.*, vol. 38:105-114., no.

Lundin, L., Larsson, H., Kreuger, J., Kanda, S., Lindahl, U., Salmivirta, M. & Claesson-Welsh, L. (2000) 'Selectively desulfated heparin inhibits fibroblast growth factor-induced mitogenicity and angiogenesis', *J Biol Chem.*, vol. 275, no. 32, pp. 24653-24660.

Lustig, F., Hoebeke, J., Simonson, C., Ostergren-Lunden, G., Bondjers, G., Ruetchi, U. & Fager, G. (1999) 'Processing of PDGF gene products determines interactions with glycosaminoglycans', *J Mol Recognit.*, vol. 12, no. 2, pp. 112-120.

Maccarana, M., Casu, B. & Lindahl, U. (1993) 'Minimal sequence in heparin/heparan sulfate required for binding of basic fibroblast growth factor', *J Biol Chem.*, vol. 268, no. 32, pp. 23898-23905.

Maccarana, M., Sakura, Y., Tawada, A., Yoshida, K. & Lindahl, U. (1996) 'Domain structure of heparan sulfates from bovine organs', *J Biol Chem.*, vol. 271, no. 30, pp. 17804-17810.

Malavaki, C.J., Roussidis, A.E., Gialeli, C., Kletsas, D., Tsegenidis, T., Theocharis, A.D., Tzanakakis, G.N. & Karamanos, N.K. (2013) 'Imatinib as a key inhibitor of the platelet-derived growth factor receptor mediated expression of cell surface heparan sulfate proteoglycans and functional properties of breast cancer cells', *FEBS J.*, vol. 280, no. 10, pp. 2477-2489.

Markovic-Mueller, S., Stuttfeld, E., Asthana, M., Weinert, T., Bliven, S., Goldie, K.N., Kisko, K., Capitani, G. & Ballmer-Hofer, K. (2017) 'Structure of the Full-length VEGFR-1 Extracellular Domain in Complex with VEGF-A', *Structure.*, vol. 25, no. 2, pp. 341-352.

McCormick, C., Duncan, G., Goutsos, K.T. & Tufaro, F. (2000) 'The putative tumor suppressors EXT1 and EXT2 form a stable complex that accumulates in the Golgi apparatus and catalyzes the synthesis of heparan sulfate', *Proc Natl Acad Sci U S A.*, vol. 97, no. 2, pp. 668-673.

Meneghetti, M.C., Hughes, A.J., Rudd, T.R., Nader, H.B., Powell, A.K., Yates, E.A. & Lima, M.A. (2015) 'Heparan sulfate and heparin interactions with proteins', *J R Soc Interface.*, vol. 12, no. 110, p. 0589.

Merry, C.L., Bullock, S.L., Swan, D.C., Backen, A.C., Lyon, M., Beddington, R.S., Wilson, V.A. & Gallagher, J.T. (2001) 'The molecular phenotype of heparan sulfate in the Hs2st-/- mutant mouse', *J Biol Chem.*, vol. 276, no. 38, pp. 35429-35434.

Migliorini, E., Thakar, D., Kuhnle, J., Sadir, R., Dyer, D.P., Li, Y., Sun, C., Volkman, B.F., Handel, T.M., Coche-Guerente, L., Fernig, D.G., Lortat-Jacob, H. & Richter, R.P. (2015) 'Cytokines and growth factors cross-link heparan sulfate', *Open Biol.*, vol. 5(8). no.

Mikami, T. & Kitagawa, H. (2013) 'Biosynthesis and function of chondroitin sulfate', *Biochim Biophys Acta.*, vol. 1830, no. 10, pp. 4719-4733.

Mohammadi, M., Olsen, S.K. & Goetz, R. (2005) 'A protein canyon in the FGF-FGF receptor dimer selects from an a la carte menu of heparan sulfate motifs', *Curr Opin Struct Biol.*, vol. 15, no. 5, pp. 506-516.

Monneau, Y., Arenzana-Seisdedos, F. & Lortat-Jacob, H. (2015) 'The sweet spot: how GAGs help chemokines guide migrating cells', *J Leukoc Biol*, vol. 23, pp. 3MR0915-0440R.

Mossman, B.T. (1983) 'In vitro approaches for determining mechanisms of toxicity and carcinogenicity by asbestos in the gastrointestinal and respiratory tracts', *Environ Health Perspect.*, vol. 53, pp. 155-161.

Mourier, P.A., Herman, F., Sizun, P. & Viskov, C. (2016) 'Analytical comparison of a US generic enoxaparin with the originator product: The focus on comparative assessment of antithrombin-binding components', *J Pharm Biomed Anal.*, vol. 129:542-550., no.

Muller, Y.A., Li, B., Christinger, H.W., Wells, J.A., Cunningham, B.C. & de Vos, A.M. (1997) 'Vascular endothelial growth factor: crystal structure and functional mapping of the kinase domain receptor binding site', *Proc Natl Acad Sci U S A.*, vol. 94, no. 14, pp. 7192-7197.

Mulloy, B., Forster, M.J., Jones, C., Drake, A.F., Johnson, E.A. & Davies, D.B. (1994) 'The effect of variation of substitution on the solution conformation of heparin: a spectroscopic and molecular modelling study', *Carbohydr Res.*, vol. 255, pp. 1-26.

Mulloy, B., Hogwood, J. & Gray, E. (2010) 'Assays and reference materials for current and future applications of heparins', *Biologicals.*, vol. 38, no. 4, pp. 459-466.

Mulloy, B., Wu, N., Gyapon-Quast, F., Lin, L., Zhang, F., Pickering, M.C., Linhardt, R.J., Feizi, T. & Chai, W. (2016) 'Abnormally High Content of Free Glucosamine Residues Identified in a Preparation of Commercially Available Porcine Intestinal Heparan Sulfate', *Anal Chem.*, vol. 88, no. 13, pp. 6648-6652.

Multhaupt, H.A. & Couchman, J.R. (2012) 'Heparan sulfate biosynthesis: methods for investigation of the heparanosome', *J Histochem Cytochem.*, vol. 60, no. 12, pp. 908-915.

Nadanaka, S., Kitagawa, H. & Sugahara, K. (1998) 'Demonstration of the immature glycosaminoglycan tetrasaccharide sequence GlcAbeta1-3Galbeta1-3Galbeta1-4Xyl on recombinant soluble human alpha-thrombomodulin. An oligosaccharide structure on a "part-time" proteoglycan', *J Biol Chem.*, vol. 273, no. 50, pp. 33728-33734.

Nieto, L., Canales, A., Fernandez, I.S., Santillana, E., Gonzalez-Corrochano, R., Redondo-Horcajo, M., Canada, F.J., Nieto, P., Martin-Lomas, M., Gimenez-Gallego, G. & Jimenez-Barbero, J. (2013) 'Heparin modulates the mitogenic activity of fibroblast growth factor by inducing dimerization of its receptor. a 3D view by using NMR', *Chembiochem.*, vol. 14, no. 14, pp. 1732-1744.

Nunnelee, J.D. (1997) 'Low-molecular-weight heparin', *J Vasc Nurs.*, vol. 15, no. 3, pp. 94-96.

Okajima, T., Fukumoto, S., Furukawa, K. & Urano, T. (1999) 'Molecular basis for the progeroid variant of Ehlers-Danlos syndrome. Identification and characterization of two mutations in galactosyltransferase I gene', *J Biol Chem.*, vol. 274, no. 41, pp. 28841-28844.

Oldberg, A., Heldin, C.H., Wasteson, A., Busch, C. & Hook, M. (1980) 'Characterization of a platelet endoglycosidase degrading heparin-like polysaccharides', *Biochemistry.*, vol. 19, no. 25, pp. 5755-5762.

Olmo, I.G., Carvalho, T.G., Costa, V.V., Alves-Silva, J., Ferrari, C.Z., Izidoro-Toledo, T.C., da Silva, J.F., Teixeira, A.L., Souza, D.G., Marques, J.T., Teixeira, M.M., Vieira, L.B. & Ribeiro, F.M. (2017) 'Zika Virus Promotes Neuronal Cell Death in a Non-Cell Autonomous Manner by Triggering the Release of Neurotoxic Factors', *Front Immunol.*, vol. 8:1016., no.

Olsson, A.K., Dimberg, A., Kreuger, J. & Claesson-Welsh, L. (2006) 'VEGF receptor signalling - in control of vascular function', *Nat Rev Mol Cell Biol.*, vol. 7, no. 5, pp. 359-371.

Ono, K., Hattori, H., Takeshita, S., Kurita, A. & Ishihara, M. (1999) 'Structural features in heparin that interact with VEGF165 and modulate its biological activity', *Glycobiology.*, vol. 9, no. 7, pp. 705-711.

Ori, A., Free, P., Courty, J., Wilkinson, M.C. & Fernig, D.G. (2009) 'Identification of heparin-binding sites in proteins by selective labeling', *Mol Cell Proteomics.*, vol. 8, no. 10, pp. 2256-2265.

Ornitz, D.M. (2000) 'FGFs, heparan sulfate and FGFRs: complex interactions essential for development', *Bioessays.*, vol. 22, no. 2, pp. 108-112.

Ornitz, D.M. & Itoh, N. (2015) 'The Fibroblast Growth Factor signaling pathway', *Wiley Interdiscip Rev Dev Biol.*, vol. 4, no. 3, pp. 215-266.

Parenti, G., Meroni, G. & Ballabio, A. (1997) 'The sulfatase gene family', *Curr Opin Genet Dev.*, vol. 7, no. 3, pp. 386-391.

Pedersen, L.C., Tsuchida, K., Kitagawa, H., Sugahara, K., Darden, T.A. & Negishi, M. (2000) 'Heparan/chondroitin sulfate biosynthesis. Structure and mechanism of human glucuronyltransferase I', *J Biol Chem.*, vol. 275, no. 44, pp. 34580-34585.

Pellegrini, L., Burke, D.F., von Delft, F., Mulloy, B. & Blundell, T.L. (2000) 'Crystal structure of fibroblast growth factor receptor ectodomain bound to ligand and heparin', *Nature.*, vol. 407, no. 6807, pp. 1029-1034.

Pennock, S. & Kazlauskas, A. (2012) 'Vascular endothelial growth factor A competitively inhibits platelet-derived growth factor (PDGF)-dependent activation of PDGF receptor and subsequent signaling events and cellular responses', *Mol Cell Biol.*, vol. 32, no. 10, pp. 1955-1966.

Petitou, M., Duchaussoy, P., Driguez, P.A., Herault, J.P., Lormeau, J.C. & Herbert, J.M. (1999) 'New synthetic heparin mimetics able to inhibit thrombin and factor Xa', *Bioorg Med Chem Lett.*, vol. 9, no. 8, pp. 1155-1160.

Pisconti, A., Bernet, J.D. & Olwin, B.B. (2012) 'Syndecans in skeletal muscle development, regeneration and homeostasis', *Muscles Ligaments Tendons J.*, vol. 2, no. 1, pp. 1-9. Print 2012 Jan.

Plante, O.J., Palmacci, E.R. & Seeberger, P.H. (2001) 'Automated solid-phase synthesis of oligosaccharides', *Science.*, vol. 291, no. 5508, pp. 1523-1527.

Plotnikov, A.N., Schlessinger, J., Hubbard, S.R. & Mohammadi, M. (1999) 'Structural basis for FGF receptor dimerization and activation', *Cell.*, vol. 98, no. 5, pp. 641-650.

Pomin, V.H. (2016) 'Paradigms in the structural biology of the mitogenic ternary complex FGF:FGFR:heparin', *Biochimie*, vol. 2, no. 16, pp. 30106-30107.

Powell, A.K., Ahmed, Y.A., Yates, E.A. & Turnbull, J.E. (2010) 'Generating heparan sulfate saccharide libraries for glycomics applications', *Nat Protoc.*, vol. 5, no. 5, pp. 821-833.

Prabhu, A., Venot, A. & Boons, G.J. (2003) 'New set of orthogonal protecting groups for the modular synthesis of heparan sulfate fragments', *Org Lett.*, vol. 5, no. 26, pp. 4975-4978.

Pratt, C.W. & Church, F.C. (1991) 'Antithrombin: structure and function', *Semin Hematol.*, vol. 28, no. 1, pp. 3-9.

Prydz, K. (2015) 'Determinants of Glycosaminoglycan (GAG) Structure', *Biomolecules.*, vol. 5, no. 3, pp. 2003-2022.

Pye, D.A., Vives, R.R., Turnbull, J.E., Hyde, P. & Gallagher, J.T. (1998) 'Heparan sulfate oligosaccharides require 6-O-sulfation for promotion of basic fibroblast growth factor mitogenic activity', *J Biol Chem.*, vol. 273, no. 36, pp. 22936-22942.

Quinn, T.P., Peters, K.G., De Vries, C., Ferrara, N. & Williams, L.T. (1993) 'Fetal liver kinase 1 is a receptor for vascular endothelial growth factor and is selectively expressed in vascular endothelium', *Proc Natl Acad Sci U S A.*, vol. 90, no. 16, pp. 7533-7537.

Rider, C.C. & Mulloy, B. (2017) 'Heparin, Heparan Sulphate and the TGF-beta Cytokine Superfamily', *Molecules.*, vol. 22(5). no. pii, p. E713.

Ringvall, M., Ledin, J., Holmborn, K., van Kuppevelt, T., Ellin, F., Eriksson, I., Olofsson, A.M., Kjellen, L. & Forsberg, E. (2000) 'Defective heparan sulfate biosynthesis and neonatal lethality in mice lacking N-deacetylase/N-sulfotransferase-1', *J Biol Chem.*, vol. 275, no. 34, pp. 25926-25930.

Robinson, C.J., Mulloy, B., Gallagher, J.T. & Stringer, S.E. (2006) 'VEGF165-binding sites within heparan sulfate encompass two highly sulfated domains and can be liberated by K5 lyase', *J Biol Chem.*, vol. 281, no. 3, pp. 1731-1740.

Rolny, C., Spillmann, D., Lindahl, U. & Claesson-Welsh, L. (2002) 'Heparin amplifies platelet-derived growth factor (PDGF)- BB-induced PDGF alpha -receptor but not PDGF beta -receptor tyrosine phosphorylation in heparan sulfate-deficient cells. Effects on signal transduction and biological responses', *J Biol Chem*, vol. 277, no. 22, pp. 19315-19321.

Rudd, T.R., Preston, M.D. & Yates, E.A. (2017) 'The nature of the conserved basic amino acid sequences found among 437 heparin binding proteins determined by network analysis', *Mol Biosyst.*, vol. 13, no. 5, pp. 852-865.

Rudd, T.R., Uniewicz, K.A., Ori, A., Guimond, S.E., Skidmore, M.A., Gaudesi, D., Xu, R., Turnbull, J.E., Guerrini, M., Torri, G., Siligardi, G., Wilkinson, M.C., Fernig, D.G. & Yates, E.A. (2010) 'Comparable stabilisation, structural changes and activities can be induced in FGF by a variety of HS and non-GAG analogues: implications for sequence-activity relationships', *Org Biomol Chem.*, vol. 8, no. 23, pp. 5390-5397.

Rudd, T.R. & Yates, E.A. (2012) 'A highly efficient tree structure for the biosynthesis of heparan sulfate accounts for the commonly observed disaccharides and suggests a mechanism for domain synthesis', *Mol Biosyst.*, vol. 8, no. 5, pp. 1499-1506.

Ruhrberg, C., Gerhardt, H., Golding, M., Watson, R., Ioannidou, S., Fujisawa, H., Betsholtz, C. & Shima, D.T. (2002) 'Spatially restricted patterning cues provided by heparin-binding VEGF-A control blood vessel branching morphogenesis', *Genes Dev.*, vol. 16, no. 20, pp. 2684-2698.

Saksela, O., Moscatelli, D., Sommer, A. & Rifkin, D.B. (1988) 'Endothelial cell-derived heparan sulfate binds basic fibroblast growth factor and protects it from proteolytic degradation', *J Cell Biol.*, vol. 107, no. 2, pp. 743-751.

Sarkar, A. & Desai, U.R. (2015) 'A Simple Method for Discovering Druggable, Specific Glycosaminoglycan-Protein Systems. Elucidation of Key Principles from Heparin/Heparan Sulfate-Binding Proteins', *PLoS One.*, vol. 10, no. 10, p. e0141127..

Sasarman, F., Maftei, C., Campeau, P.M., Brunel-Guitton, C., Mitchell, G.A. & Allard, P. (2015) 'Biosynthesis of glycosaminoglycans: associated disorders and biochemical tests', *J Inherit Metab Dis*, vol. 21, p. 21.

Schilling, D., Reid, I.J., Hujer, A., Morgan, D., Demoll, E., Bummer, P., Fenstermaker, R.A. & Kaetzel, D.M. (1998) 'Loop III region of platelet-derived growth factor (PDGF) B-chain mediates binding to PDGF receptors and heparin', *Biochem J.*, vol. 333, no. Pt 3, pp. 637-644.

Schlessinger, J., Plotnikov, A.N., Ibrahimi, O.A., Eliseenkova, A.V., Yeh, B.K., Yayon, A., Linhardt, R.J. & Mohammadi, M. (2000) 'Crystal structure of a ternary FGF-FGFR-heparin complex reveals a dual role for heparin in FGFR binding and dimerization', *Mol Cell.*, vol. 6, no. 3, pp. 743-750.

Schworer, R., Zubkova, O.V., Turnbull, J.E. & Tyler, P.C. (2013) 'Synthesis of a targeted library of heparan sulfate hexa- to dodecasaccharides as inhibitors of beta-secretase: potential therapeutics for Alzheimer's disease', *Chemistry.*, vol. 19, no. 21, pp. 6817-6823.

Senay, C., Lind, T., Muguruma, K., Tone, Y., Kitagawa, H., Sugahara, K., Lidholt, K., Lindahl, U. & Kusche-Gullberg, M. (2000) 'The EXT1/EXT2 tumor suppressors: catalytic activities and role in heparan sulfate biosynthesis', *EMBO Rep.*, vol. 1, no. 3, pp. 282-286.

Senger, D.R., Ledbetter, S.R., Claffey, K.P., Papadopoulos-Sergiou, A., Peruzzi, C.A. & Detmar, M. (1996) 'Stimulation of endothelial cell migration by vascular permeability factor/vascular endothelial growth factor through cooperative mechanisms involving the alphavbeta3 integrin, osteopontin, and thrombin', *Am J Pathol.*, vol. 149, no. 1, pp. 293-305.

Seyrek, E., Dubin, P.L. & Henriksen, J. (2007) 'Nonspecific electrostatic binding characteristics of the heparin-antithrombin interaction', *Biopolymers.*, vol. 86, no. 3, pp. 249-259.

Sheng, J., Xu, Y., Dulaney, S.B., Huang, X. & Liu, J. (2012) 'Uncovering biphasic catalytic mode of C5-epimerase in heparan sulfate biosynthesis', *J Biol Chem.*, vol. 287, no. 25, pp. 20996-21002.

Shimada, K. & Ozawa, T. (1985) 'Evidence that cell surface heparan sulfate is involved in the high affinity thrombin binding to cultured porcine aortic endothelial cells', *J Clin Invest.*, vol. 75, no. 4, pp. 1308-1316.

Shriver, Z. & Sasisekharan, R. (2015) 'Capillary electrophoretic analysis of isolated sulfated polysaccharides to characterize pharmaceutical products', *Methods Mol Biol*, vol. 1229:161-71., no.

Sinnis, P., Coppi, A., Toida, T., Toyoda, H., Kinoshita-Toyoda, A., Xie, J., Kemp, M.M. & Linhardt, R.J. (2007) 'Mosquito heparan sulfate and its potential role in malaria infection and transmission', *J Biol Chem.*, vol. 282, no. 35, pp. 25376-25384.

Skidmore, M.A., Guimond, S.E., Dumax-Vorzet, A.F., Atrih, A., Yates, E.A. & Turnbull, J.E. (2006) 'High sensitivity separation and detection of heparan sulfate disaccharides', *J Chromatogr A.*, vol. 1135, no. 1, pp. 52-56.

Skidmore, M.A., Guimond, S.E., Dumax-Vorzet, A.F., Yates, E.A. & Turnbull, J.E. (2010) 'Disaccharide compositional analysis of heparan sulfate and heparin polysaccharides using UV or high-sensitivity fluorescence (BODIPY) detection', *Nat Protoc.*, vol. 5, no. 12, pp. 1983-1992.

Smeds, E., Feta, A. & Kusche-Gullberg, M. (2010) 'Target selection of heparan sulfate hexuronic acid 2-O-sulfotransferase', *Glycobiology.*, vol. 20, no. 10, pp. 1274-1282.

Soker, S., Goldstaub, D., Svahn, C.M., Vlodavsky, I., Levi, B.Z. & Neufeld, G. (1994) 'Variations in the size and sulfation of heparin modulate the effect of heparin on the binding of VEGF165 to its receptors', *Biochem Biophys Res Commun.*, vol. 203, no. 2, pp. 1339-1347.

Stauffer, M.E., Skelton, N.J. & Fairbrothe, W.J. (2002) 'Refinement of the solution structure of the heparin-binding domain of vascular endothelial growth factor using residual dipolar couplings', *J Biomol NMR.*, vol. 23, no. 1, pp. 57-61.

Stein, I., Neeman, M., Shweiki, D., Itin, A. & Keshet, E. (1995) 'Stabilization of vascular endothelial growth factor mRNA by hypoxia and hypoglycemia and coregulation with other ischemia-induced genes', *Mol Cell Biol.*, vol. 15, no. 10, pp. 5363-5368.

Stenzel, D., Nye, E., Nisancioglu, M., Adams, R.H., Yamaguchi, Y. & Gerhardt, H. (2009) 'Peripheral mural cell recruitment requires cell-autonomous heparan sulfate', *Blood.*, vol. 114, no. 4, pp. 915-924.

Sterner, E., Masuko, S., Li, G., Li, L., Green, D.E., Otto, N.J., Xu, Y., DeAngelis, P.L., Liu, J., Dordick, J.S. & Linhardt, R.J. (2014) 'Fibroblast growth factor-based signaling through synthetic heparan sulfate blocks copolymers studied using high cell density three-dimensional cell printing', *J Biol Chem.*, vol. 289, no. 14, pp. 9754-9765.

Sugaya, N., Habuchi, H., Nagai, N., Ashikari-Hada, S. & Kimata, K. (2008) '6-O-sulfation of heparan sulfate differentially regulates various fibroblast growth factor-dependent signalings in culture', *J Biol Chem.*, vol. 283, no. 16, pp. 10366-10376.

Takahashi, H. & Shibuya, M. (2005) 'The vascular endothelial growth factor (VEGF)/VEGF receptor system and its role under physiological and pathological conditions', *Clin Sci (Lond).* vol. 109, no. 3, pp. 227-241.

Tallquist, M. & Kazlauskas, A. (2004) 'PDGF signaling in cells and mice', *Cytokine Growth Factor Rev.*, vol. 15, no. 4, pp. 205-213.

Thompson, L.D., Pantoliano, M.W. & Springer, B.A. (1994) 'Energetic characterization of the basic fibroblast growth factor-heparin interaction: identification of the heparin binding domain', *Biochemistry.*, vol. 33, no. 13, pp. 3831-3840.

Thunberg, L., Backstrom, G., Grundberg, H., Riesenfeld, J. & Lindahl, U. (1980) 'The molecular size of the antithrombin-binding sequence in heparin', *FEBS Lett.*, vol. 117, no. 1, pp. 203-206.

Thunberg, L., Backstrom, G. & Lindahl, U. (1982) 'Further characterization of the antithrombin-binding sequence in heparin', *Carbohydr Res.*, vol. 100, pp. 393-410.

Thunberg, L., Backstrom, G., Wasteson, A., Robinson, H.C., Ogren, S. & Lindahl, U. (1982) 'Enzymatic depolymerization of heparin-related polysaccharides. Substrate specificities of mouse mastocytoma and human platelet endo-beta-D-glucuronidases', *J Biol Chem.*, vol. 257, no. 17, pp. 10278-10282.

Tissot, B., Ceroni, A., Powell, A.K., Morris, H.R., Yates, E.A., Turnbull, J.E., Gallagher, J.T., Dell, A. & Haslam, S.M. (2008) 'Software tool for the structural determination of glycosaminoglycans by mass spectrometry', *Anal Chem.*, vol. 80, no. 23, pp. 9204-9212.

Tone, Y., Pedersen, L.C., Yamamoto, T., Izumikawa, T., Kitagawa, H., Nishihara, J., Tamura, J., Negishi, M. & Sugahara, K. (2008) '2-o-phosphorylation of xylose and 6-o-sulfation of galactose in the protein linkage region of glycosaminoglycans influence the glucuronyltransferase-I activity involved in the linkage region synthesis', *J Biol Chem.*, vol. 283, no. 24, pp. 16801-16807.

Tracy, L.E., Minasian, R.A. & Caterson, E.J. (2016) 'Extracellular Matrix and Dermal Fibroblast Function in the Healing Wound', *Adv Wound Care (New Rochelle).* vol. 5, no. 3, pp. 119-136.

Trowbridge, J.M. & Gallo, R.L. (2002) 'Dermatan sulfate: new functions from an old glycosaminoglycan', *Glycobiology.*, vol. 12, no. 9, pp. 117R-125R.

Tsang, M. & Dawid, I.B. (2004) 'Promotion and attenuation of FGF signaling through the Ras-MAPK pathway', *Sci STKE.*, vol. 2004, no. 228, p. pe17.

Turnbull, J.E., Fernig, D.G., Ke, Y., Wilkinson, M.C. & Gallagher, J.T. (1992) 'Identification of the basic fibroblast growth factor binding sequence in fibroblast heparan sulfate', *J Biol Chem.*, vol. 267, no. 15, pp. 10337-10341.

Turnbull, J.E. & Gallagher, J.T. (1988) 'Oligosaccharide mapping of heparan sulphate by polyacrylamide-gradient-gel electrophoresis and electrotransfer to nylon membrane', *Biochem J.*, vol. 251, no. 2, pp. 597-608.

Turnbull, J.E., Hopwood, J.J. & Gallagher, J.T. (1999) 'A strategy for rapid sequencing of heparan sulfate and heparin saccharides', *Proc Natl Acad Sci U S A.*, vol. 96, no. 6, pp. 2698-2703.

Turner, N. & Grose, R. (2010) 'Fibroblast growth factor signalling: from development to cancer', *Nat Rev Cancer.*, vol. 10, no. 2, pp. 116-129.

Unemori, E.N., Ferrara, N., Bauer, E.A. & Amento, E.P. (1992) 'Vascular endothelial growth factor induces interstitial collagenase expression in human endothelial cells', *J Cell Physiol.*, vol. 153, no. 3, pp. 557-562.

van Wijk, X.M. & van Kuppevelt, T.H. (2014) 'Heparan sulfate in angiogenesis: a target for therapy', *Angiogenesis.*, vol. 17, no. 3, pp. 443-462.

Veikkola, T., Karkkainen, M., Claesson-Welsh, L. & Alitalo, K. (2000) 'Regulation of angiogenesis via vascular endothelial growth factor receptors', *Cancer Res.*, vol. 60, no. 2, pp. 203-212.

Venkataraman, G., Shriver, Z., Davis, J.C. & Sasisekharan, R. (1999) 'Fibroblast growth factors 1 and 2 are distinct in oligomerization in the presence of heparin-like glycosaminoglycans', *Proc Natl Acad Sci U S A.*, vol. 96, no. 5, pp. 1892-1897.

Vorup-Jensen, T., Chi, L., Gjelstrup, L.C., Jensen, U.B., Jewett, C.A., Xie, C., Shimaoka, M., Linhardt, R.J. & Springer, T.A. (2007) 'Binding between the integrin alphaXbeta2 (CD11c/CD18) and heparin', *J Biol Chem.*, vol. 282, no. 42, pp. 30869-30877.

Walenga, J.M., Jeske, W.P., Bara, L., Samama, M.M. & Fareed, J. (1997) 'Biochemical and pharmacologic rationale for the development of a synthetic heparin pentasaccharide', *Thromb Res.*, vol. 86, no. 1, pp. 1-36.

Walker, A., Turnbull, J.E. & Gallagher, J.T. (1994) 'Specific heparan sulfate saccharides mediate the activity of basic fibroblast growth factor', *J Biol Chem.*, vol. 269, no. 2, pp. 931-935.

Watanabe, Y. & Dvorak, H.F. (1997) 'Vascular permeability factor/vascular endothelial growth factor inhibits anchorage-disruption-induced apoptosis in microvessel endothelial cells by inducing scaffold formation', *Exp Cell Res.*, vol. 233, no. 2, pp. 340-349.

Wei, G., Bai, X., Gabb, M.M., Bame, K.J., Koshy, T.I., Spear, P.G. & Esko, J.D. (2000) 'Location of the glucuronosyltransferase domain in the heparan sulfate copolymerase EXT1 by analysis of Chinese hamster ovary cell mutants', *J Biol Chem.*, vol. 275, no. 36, pp. 27733-27740.

Weishaupt, M., Eller, S. & Seeberger, P.H. (2010) 'Solid phase synthesis of oligosaccharides', *Methods Enzymol*, vol. 478:463-84., no.

Weitz, J.I. & Harenberg, J. (2017) 'New developments in anticoagulants: Past, present and future', *Thromb Haemost.*, vol. 117, no. 7, pp. 1283-1288.

Wolberg, A.S., Rosendaal, F.R., Weitz, J.I., Jaffer, I.H., Agnelli, G., Baglin, T. & Mackman, N. (2015) 'Venous thrombosis', *Nat Rev Dis Primers.*, vol. 1:15006., no.

Wu, E., Palmer, N., Tian, Z., Moseman, A.P., Galdzicki, M., Wang, X., Berger, B., Zhang, H. & Kohane, I.S. (2008) 'Comprehensive dissection of PDGF-PDGFR signaling pathways in PDGFR genetically defined cells', *PLoS One*, vol. 3, no. 11, p. e3794.

Xu, R., Ori, A., Rudd, T.R., Uniewicz, K.A., Ahmed, Y.A., Guimond, S.E., Skidmore, M.A., Siligardi, G., Yates, E.A. & Fernig, D.G. (2012) 'Diversification of the structural determinants of fibroblast growth factor-heparin interactions: implications for binding specificity', *J Biol Chem.*, vol. 287, no. 47, pp. 40061-40073.

Xu, Y., Chandarajoti, K., Zhang, X., Pagadala, V., Dou, W., Hoppensteadt, D.M., Sparkenbaugh, E.M., Cooley, B., Daily, S., Key, N.S., Severynse-Stevens, D., Fareed, J., Linhardt, R.J., Pawlinski, R. & Liu, J. (2017) 'Synthetic oligosaccharides can replace animal-sourced low-molecular weight heparins', Sci Transl Med., vol. 9(406). no. pii, p. 9/406/eaan5954.

Yamada, S., Okada, Y., Ueno, M., Iwata, S., Deepa, S.S., Nishimura, S., Fujita, M., Van Die, I., Hirabayashi, Y. & Sugahara, K. (2002) 'Determination of the glycosaminoglycan-protein linkage region oligosaccharide structures of proteoglycans from Drosophila melanogaster and Caenorhabditis elegans', *J Biol Chem.*, vol. 277, no. 35, pp. 31877-31886.

Yamada, S., Yoshida, K., Sugiura, M. & Sugahara, K. (1992a) 'One- and two-dimensional 1H-NMR characterization of two series of sulfated disaccharides prepared from chondroitin sulfate and heparan sulfate/heparin by bacterial eliminase digestion', *J Biochem.*, vol. 112, no. 4, pp. 440-447.

Yamada, S., Yoshida, K., Sugiura, M. & Sugahara, K. (1992b) 'One- and two-dimensional 1H-NMR characterization of two series of sulfated disaccharides prepared from chondroitin sulfate and heparan sulfate/heparin by bacterial eliminase digestion', *J Biochem.*, vol. 112, no. 4, pp. 440-447.

Yates, E.A., Santini, F., Guerrini, M., Naggi, A., Torri, G. & Casu, B. (1996) '1H and 13C NMR spectral assignments of the major sequences of twelve systematically modified heparin derivatives', *Carbohydr Res.*, vol. 294, pp. 15-27.

Zhang, J.D., Cousens, L.S., Barr, P.J. & Sprang, S.R. (1991) 'Three-dimensional structure of human basic fibroblast growth factor, a structural homolog of interleukin 1 beta', *Proc Natl Acad Sci U S A.*, vol. 88, no. 8, pp. 3446-3450.

Zhang, X., Bao, L., Yang, L., Wu, Q. & Li, S. (2012) 'Roles of intracellular fibroblast growth factors in neural development and functions', *Sci China Life Sci.*, vol. 55, no. 12, pp. 1038-1044.

Zhang, X., Pagadala V., Jester, HM., Lim, AM., Pham, TQ., Goulas, AMP., Liu. J. and Linhardt, RJ. (2017) 'Chemoenzymatic synthesis of heparan sulfate and heparin oligosaccharides and NMR analysis: paving the way to a diverse library for glycobiologists', *Chemical Sci.*, vol. 8, pp. 7932-7940.

Zhou, H., Roy, S., Cochran, E., Zouaoui, R., Chu, C.L., Duffner, J., Zhao, G., Smith, S., Galcheva-Gargova, Z., Karlgren, J., Dussault, N., Kwan, R.Y., Moy, E., Barnes, M., Long, A., Honan, C., Qi, Y.W., Shriver, Z., Ganguly, T., Schultes, B., Venkataraman, G. & Kishimoto, T.K. (2011) 'M402, a novel heparan sulfate mimetic, targets multiple pathways implicated in tumor progression and metastasis', *PLoS One*, vol. 6, no. 6, p. e21106.

Ziegler, A. & Zaia, J. (2006) 'Size-exclusion chromatography of heparin oligosaccharides at high and low pressure', *J Chromatogr B Analyt Technol Biomed Life Sci.*, vol. 837, no. 1-2, pp. 76-86.

Appendix

Appendix 1

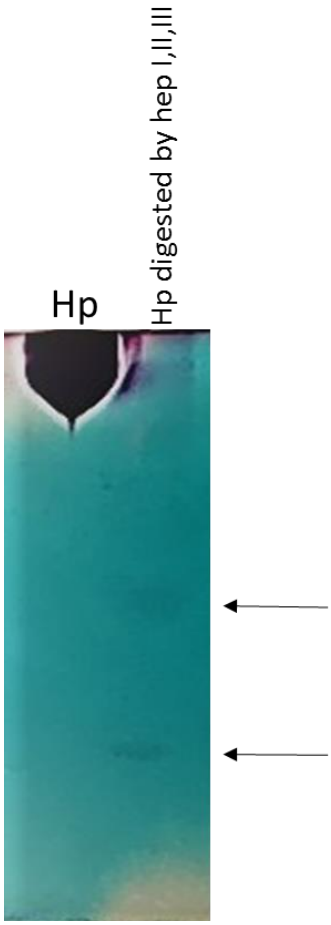

Figure A – Acrylamide gel of heparinase I, II and II digestion of Hp. 200µg of Hp was digested with 2.5mU of heparinase III, I and II (IBEX, Canada) added sequentially at 2 hour intervals, with heparinase II left incubating overnight at 37˚C, with an addition of all 3 enzymes the following day with a further 2 hour incubation.

Appendix 2

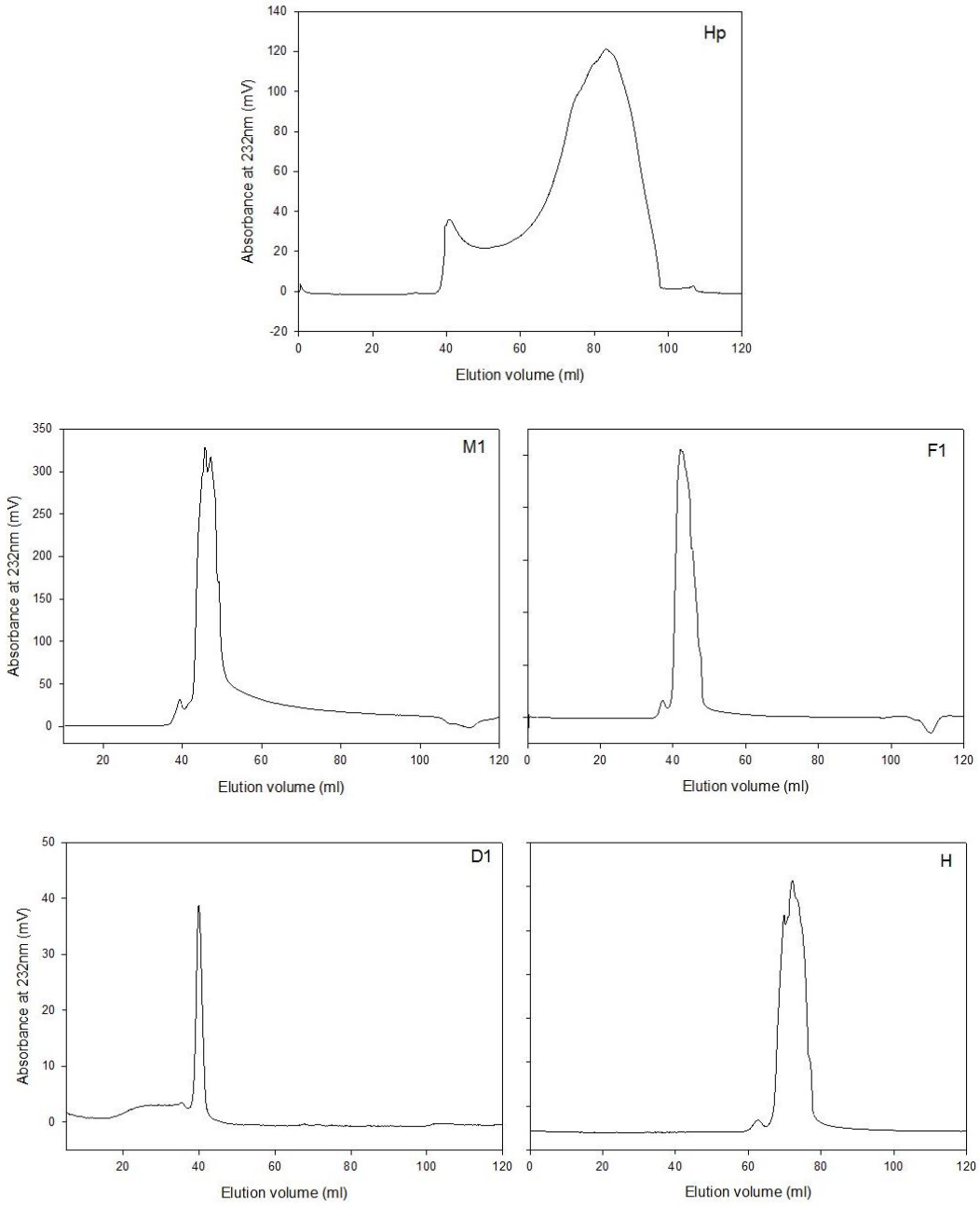

Figure B- Chromatographs of intact material separated by Superdex 30 beads. Intact material was separated as described in Chapter 3.2.3 by Superdex 30 beads on a 16/60 column at 0.5ml/min.

Appendix 3

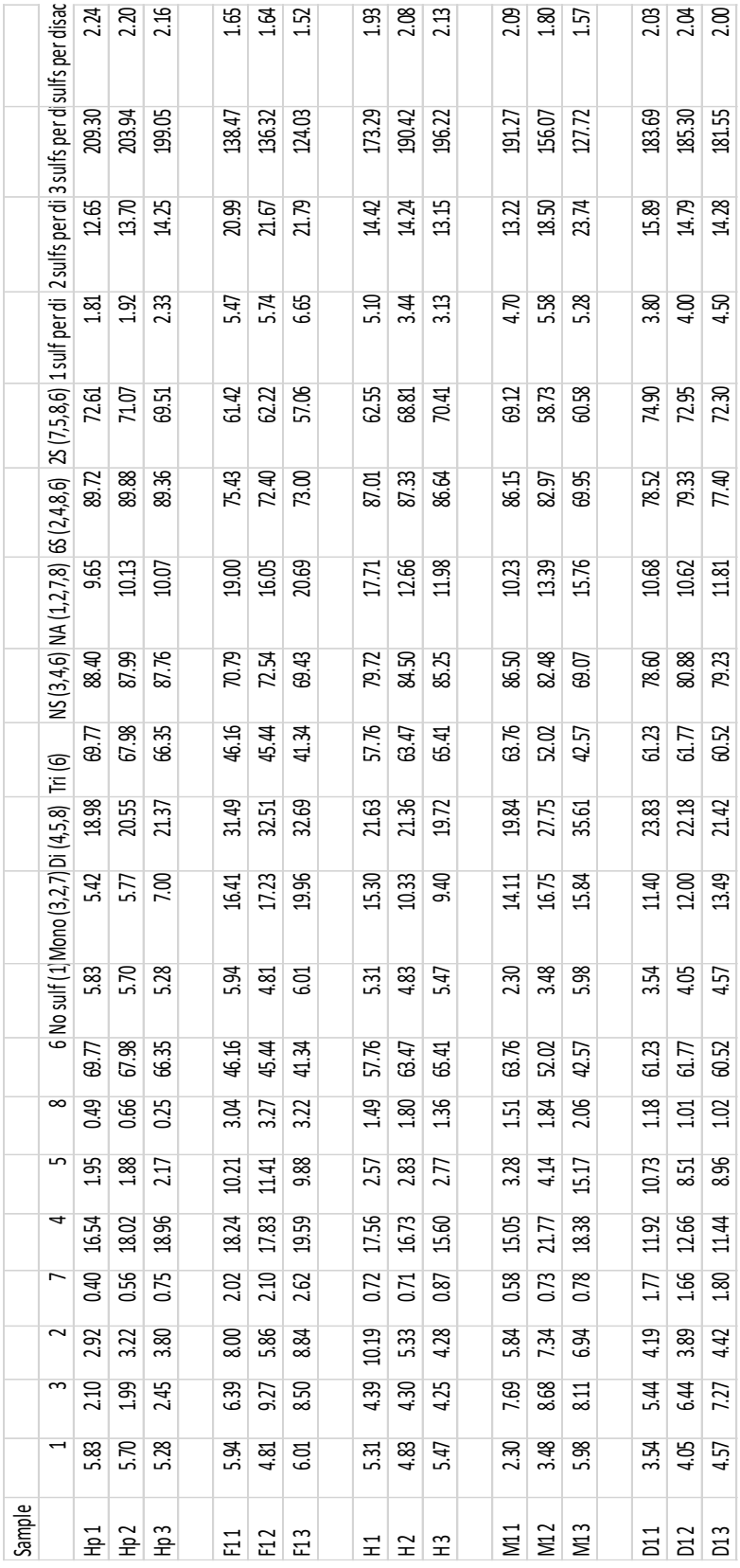

Sample	1	3	2	7	4	5	8	6	No sulf (1)	Mono (3,2,7)	Di (4,5,8)	Tri (6)	NS (3,4,6)	NA (1,2,7,8)	6S (2,4,8,6)	2S (7,5,8,6)	1 sulf per di	2 sulfs per di	3 sulfs per di	sulfs per disac
Hp 1	5.83	2.10	2.92	0.40	16.54	1.95	0.49	69.77	5.83	5.42	18.98	69.77	88.40	9.65	89.72	72.61	1.81	12.65	209.30	2.24
Hp 2	5.70	1.99	3.22	0.56	18.02	1.88	0.66	67.98	5.70	5.77	20.55	67.98	87.99	10.13	89.88	71.07	1.92	13.70	203.94	2.20
Hp 3	5.28	2.45	3.80	0.75	18.96	2.17	0.25	66.35	5.28	7.00	21.37	66.35	87.76	10.07	89.36	69.51	2.33	14.25	199.05	2.16
F1 1	5.94	6.39	8.00	2.02	18.24	10.21	3.04	46.16	5.94	16.41	31.49	46.16	70.79	19.00	75.43	61.42	5.47	20.99	138.47	1.65
F1 2	4.81	9.27	5.86	2.10	17.83	11.41	3.27	45.44	4.81	17.23	32.51	45.44	72.54	16.05	72.40	62.22	5.74	21.67	136.32	1.64
F1 3	6.01	8.50	8.84	2.62	19.59	9.88	3.22	41.34	6.01	19.96	32.69	41.34	69.43	20.69	73.00	57.06	6.65	21.79	124.03	1.52
H 1	5.31	4.39	10.19	0.72	17.56	2.57	1.49	57.76	5.31	15.30	21.63	57.76	79.72	17.71	87.01	62.55	5.10	14.42	173.29	1.93
H 2	4.83	4.30	5.33	0.71	16.73	2.83	1.80	63.47	4.83	10.33	21.36	63.47	84.50	12.66	87.33	68.81	3.44	14.24	190.42	2.08
H 3	5.47	4.25	4.28	0.87	15.60	2.77	1.36	65.41	5.47	9.40	19.72	65.41	85.25	11.98	86.64	70.41	3.13	13.15	196.22	2.13
M1 1	2.30	7.69	5.84	0.58	15.05	3.28	1.51	63.76	2.30	14.11	19.84	63.76	86.50	10.23	86.15	69.12	4.70	13.22	191.27	2.09
M1 2	3.48	8.68	7.34	0.73	21.77	4.14	1.84	52.02	3.48	16.75	27.75	52.02	82.48	13.39	82.97	58.73	5.58	18.50	156.07	1.80
M1 3	5.98	8.11	6.94	0.78	18.38	15.17	2.06	42.57	5.98	15.84	35.61	42.57	69.07	15.76	69.95	60.58	5.28	23.74	127.72	1.57
D1 1	3.54	5.44	4.19	1.77	11.92	10.73	1.18	61.23	3.54	11.40	23.83	61.23	78.60	10.68	78.52	74.90	3.80	15.89	183.69	2.03
D1 2	4.05	6.44	3.89	1.66	12.66	8.51	1.01	61.77	4.05	12.00	22.18	61.77	80.88	10.62	79.33	72.95	4.00	14.79	185.30	2.04
D1 3	4.57	7.27	4.42	1.80	11.44	8.96	1.02	60.52	4.57	13.49	21.42	60.52	79.23	11.81	77.40	72.30	4.50	14.28	181.55	2.00

Figure C.1 – Percentage peak areas of compositional analysis of by-products. After digestion of by-products with heparinase enzymes and separated by charge on a Propac PA-1 column.

Appendix 4

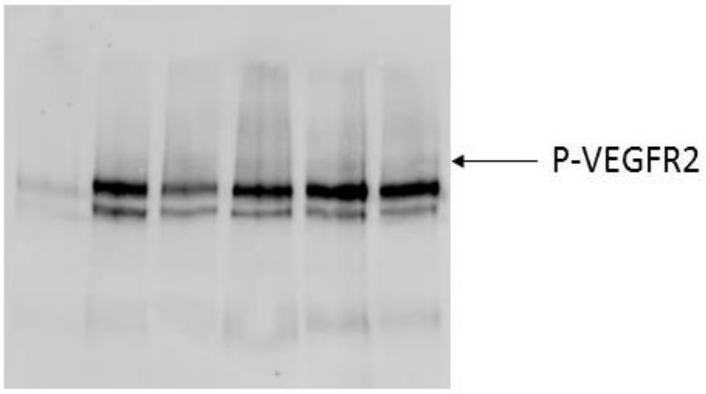

Figure D.1- Phospho-VEGFR2 signalling by induction with VEGF-A_{165} . 4x10^5 HUVECs per well were plated and 10ng of VEGF-A_{165} added. 30µg of protein, established by BCA assay, was ran on a gel. P-VEGFR2 (Try1175) primary antibody at 1:1000 was incubated overnight at 4°C.

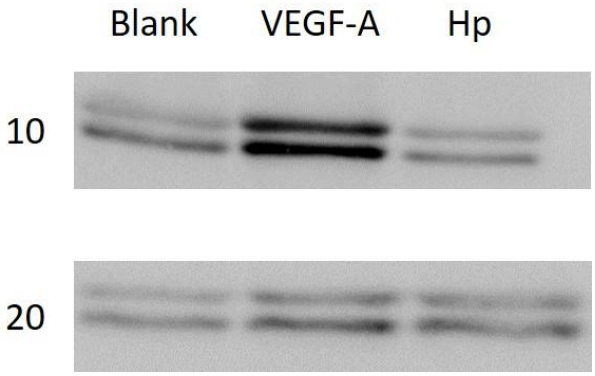

Figure D.2 – Phospho-ERK 1/2 signalling at 10 and 20 mins by induction with VEGF-A_{165} and Hp. 3x10^5 cells per well were plated and 10ng of VEGF-A_{165} and 10µg Hp were added and a time course was carried out for 10 and 20 mins. 15µg of protein, established by BCA assay was ran on a gel. P-ERK1/2 primary antibody at 1:1000 was incubated overnight at 4°C